



**University of
Zurich**^{UZH}

Using tree rings to assess the air quality in Klosters, Switzerland

GEO 511 Master's Thesis

Author

Davide Bernasconi
15-932-007

Supervised by

Prof. Dr. Paolo Cherubini (paolo.cherubini@wsl.ch)
Mrs. Paula Ballikaya (paula.ballikaya@wsl.ch)

Faculty representative

Prof. Dr. Markus Egli

30.09.2021

Department of Geography, University of Zurich



**University of
Zurich^{UZH}**

Using tree rings to assess the air quality in Klosters, Switzerland

GEO 511 Master's Thesis

Author

Davide Bernasconi

15-932-007

Supervised by

Prof. Dr. Paolo Cherubini

Mrs. Paula Ballikaya

Faculty representative

Prof. Dr. Markus Egli

30.09.2021

Department of Geography, University of Zurich

Table of contents

List of Figures	4
List of Tables	6
Abstract	8
1 Introduction	9
1.1 Emissions from anthropogenic burning of fossil fuels.....	9
1.1.1 Polluting emissions of road traffic	9
1.1.1.1 Emission of heavy metals	9
1.1.1.2 Emission differences between gasoline- and diesel-powered engines.....	9
1.1.1.3 Role of Catalysts	10
1.2 Implications of traffic pollution on human health.....	11
1.2.1 Detrimental effects of Particulate matter	11
1.2.2 Effects of traffic-related pollution on human health.....	11
1.3 Implications of traffic pollution on environmental health.....	12
1.4 Trees' role as passive pollutants archives	13
1.4.1 Pollutants deposition in forest ecosystems.....	13
1.4.2 Tree absorption of pollutants	13
1.4.3 Monitoring of heavy metals in tree rings	14
1.4.4 Investigation of stable isotopes in tree rings.....	15
1.4.5 Limitations of tree rings in atmospheric pollution studies.....	15
1.5 Case study: The village of Klosters.....	16
1.5.1 Description of Klosters and its characteristics	16
1.5.2 Klosters' traffic burden	17
1.5.3 Construction of the bypass road (A28)	19
1.6 Project description, aims, and research question.....	22
2 Material and methods	24
2.1 Study area	24
2.2 Samples collection.....	25
2.3 Dendro lab analyses.....	25
2.3.1 Measuring.....	25
2.3.2 Cross-dating and Gleichläufigkeit (GLK).....	27
2.3.3 Tree-ring width analysis.....	27
2.4 Chemical analyses	28
2.4.1 Nitrogen isotope ($\delta^{15}\text{N}$).....	28
2.4.1.1 $\delta^{15}\text{N}$ analysis procedure	30

2.4.2	Radiocarbon (^{14}C)	31
2.4.2.1	^{14}C analysis procedure	33
2.4.3	Laser Ablation-Inductively Coupled Plasma-Mass Spectrometry (LA-ICP-MS)	34
2.4.3.1	LA-ICP-MS analysis procedure	35
2.4.3.2	LA-ICP-MS Data normalisation	36
2.4.3.3	LA-ICP-MS Statistical analyses	36
3	Results	37
3.1	Nitrogen results	37
3.1.1	$\delta^{15}\text{N}$ signal	37
3.1.2	N-concentration	38
3.1.3	Reconstructed $\delta^{15}\text{N-NO}_x$ signal	38
3.2	Radiocarbon results (^{14}C)	41
3.2.1	Measured F^{14}C values and local dilution effect	41
3.2.2	Fossil fuel CO_2 component	43
3.3	LA-ICP-MS results	45
3.3.1	Measured heavy metals	45
3.3.2	Statistical analyses performed	50
3.3.2.1	Mann-Kendall test (M-K)	50
3.3.2.2	Pettitt test	50
3.4	Tree-ring width results	51
3.4.1	Comparison of tree-ring width with nitrogen isotope analysis	51
3.4.2	Comparison of tree-ring width with radiocarbon analysis	52
4	Discussion	53
4.1	Nitrogen isotope analysis ($\delta^{15}\text{N}$)	53
4.1.1	Nitrogen uptake and $\delta^{15}\text{N}$ signal in tree rings	53
4.1.2	Reconstructed $\delta^{15}\text{N-NO}_x$ signal	54
4.1.3	Alternative sources affecting the $\delta^{15}\text{N}$ value of tree rings	55
4.1.4	Nitrogen concentration in tree rings	55
4.1.5	Limitations of nitrogen isotope analysis in this investigation	56
4.2	Radiocarbon analysis (^{14}C)	56
4.2.1	Trees' uptake of carbon and ^{14}C signal	57
4.2.2	Radiocarbon concentration in tree rings	57
4.2.3	External variables radiocarbon concentration	58
4.2.4	Limitations of radiocarbon analysis in this investigation	58
4.3	LA-ICP-MS analysis	58

4.3.1	Heavy metal signal in tree rings.....	59
4.3.2	Pb	60
4.3.3	Hg.....	61
4.3.4	Cr.....	61
4.3.5	Ca and Mn.....	61
4.3.6	Limitations of LA-ICP-MS analysis in this investigation	62
4.4	Tree-ring width analysis	62
4.4.1	Detrended tree-ring width compared with nitrogen isotope analysis results	62
4.4.2	Detrended tree-ring width compared with radiocarbon analysis results.....	63
4.4.3	Limitations of nitrogen isotope and radiocarbon analyses in this investigation	64
5	Conclusion	65
	References	66
	Appendix	77
	Personal declaration	86

List of Figures

Figure 1: Panorama of Klosters (source: ETH-Bibliothek Zürich, Bildarchiv / Photographer: Krebs, H.).	17
Figure 2: Number of vehicles transported through the Vereinatunnel from its inauguration in 1999 until 2019 (own representation, data source: Rohner, S., 2020).....	19
Figure 3: Traffic comparison between weekdays and weekend in 1987 and the predicted values for 2005 (own representation, data source: Tiefbauamt des Kantons Graubünden, 1991).	19
Figure 4: Sketch of the project for the Klosters' bypass road (source: Kägi 1998).	20
Figure 5: The “Sunnibergbrücke” a section of the new bypass road (photographer: Paula Ballikaya).	20
Figure 6: Traffic development comparison of different scenarios, between the measured values in 1987 and the ones predicted for 2005 (own representation, data source: Tiefbauamt des Kantons Graubünden, 1991).....	21
Figure 7: Traffic volumes' comparison between predictions and measured values (own representation, data source: Tiefbauamt des Kantons Graubünden, 1991 and FEDRO 2020).....	22
Figure 8: Map of the village of Klosters showing the sampling sites and the main communication routes (own representation, background map from: swisstopo - Federal Topographic Office).	24
Figure 9: Visual difference between an unprocessed (a) and a processed core (b) – two different samples are represented (own picture).	26
Figure 10: Measured tree ring width in mm ⁻² for the samples of site ON, with the site average highlighted (software: TSAPwin, RINNTECH, Heidelberg, Germany).	26
Figure 11: $\Delta^{14}\text{C}$ (‰) in the atmosphere for both North and South hemisphere showing the “bomb spike” of the 1960s’ (source: Hua et al., 2013).....	32
Figure 12: $\delta^{15}\text{N}$ value of 5-years clusters for sites OU (a), ON (b), CT (c), and the comparison of average values between sites (d) – \pm SE.	37

Figure 13: Nitrogen concentration [% N] of 5-years clusters for sites OU (a), ON (b), CT (c), and the comparison of average values between sites (d) – \pm SE.	38
Figure 14: The relationship between $\delta^{15}\text{N}$ value and N-concentration measured in the tree rings (a), and the relationship between $\delta^{15}\text{N}$ value with 1/N concentration (b).	39
Figure 15: Reconstructed average $\delta^{15}\text{N}$ - NO_x signal per site.....	40
Figure 16: Average F^{14}C concentrations for sites OU, ON and CT are represented and overlaid on the Jungfraujoeh data gathered by Levin and Kromer (2004).	42
Figure 17: Dilution effect in % at site OU, ON and CT (\pm SE).....	43
Figure 18: Estimation of fossil fuel CO_2 component per site (\pm SE).....	44
Figure 19: Comparison between site OU and site ON of the average normalised signal of all the considered elements (Ca, Cr, Cu, Hg, Mn, Mo, Pb, Ti and Zn – \pm SE).	45
Figure 20: Normalised average signal per site for the elements Pb (a) and Hg (b) (\pm SE).	47
Figure 21: Raw average signal per site for the element Cr (\pm SE).	48
Figure 22: Normalised average signal per site for the elements Mn (a) and Ca (b) (\pm SE).....	49
Figure 23: Comparison between the % N (\pm SE) with the 5-year average tree-ring width (\pm SE) of site OU (a) and site CT (b).	51
Figure 24: Comparison between $\delta^{15}\text{N}$ - NO_x and the 5-year average tree-ring width (\pm SE) of the trees investigated through $\delta^{15}\text{N}$ analysis for site OU.....	51
Figure 25: Comparison between the radiocarbon dilution per site (\pm SE) with the tree-ring growth of the equivalent year (\pm SE).....	52
Figure 26: Raw average signal per site for the element Ca (\pm SE).	77
Figure 27: Normalised average signal per site for the element Ca (\pm SE).....	77
Figure 28: Raw average signal per site for the element Cr (\pm SE).	78
Figure 29: Normalised average signal per site for the element Cr (\pm SE).	78
Figure 30: Raw average signal per site for the element Cu (\pm SE).....	79
Figure 31: Normalised average signal per site for the element Cu (\pm SE).	79
Figure 32: Raw average signal per site for the element Hg (\pm SE).	80
Figure 33: Normalised average signal per site for the element Hg (\pm SE).	80
Figure 34: Raw average signal per site for the element Mn (\pm SE), with the concentration of tree 3.2 OU on the secondary y-axis.	81
Figure 35: Normalised average signal per site for the element Mn (\pm SE).	81
Figure 36: Raw average signal per site for the element Mo (\pm SE).....	82
Figure 37: Normalised average signal per site for the element Mo (\pm SE).	82
Figure 38: Raw average signal per site for the element Pb (\pm SE), with the concentration of tree 3.2 OU on the secondary y-axis.	83
Figure 39: Normalised average signal per site for the element Pb (\pm SE).....	83
Figure 40: Raw average signal per site for the element Ti (\pm SE).....	84
Figure 41: Normalised average signal per site for the element Ti (\pm SE).	84
Figure 42: Raw average signal per site for the element Zn (\pm SE).	85
Figure 43: Normalised average signal per site for the element Zn (\pm SE).....	85

List of Tables

Table 1: M-K test between site averages concentration of heavy metals	50
Table 2: result of the M-K test for each element	50
Table 3: average $\delta^{15}\text{N}$ [‰] values recorder per site.....	53
Table 4: Emissions of the transportation sector in Switzerland in tonnes (data from Bass et al., 2021).	59

Acknowledgments

I would like to thank in the first place my supervisor Prof. Dr. Paolo Cherubini for the opportunity to pursue this stimulating and endearing project, as well as for the support and guidance provided throughout the master thesis. I would also like to extend my sincere thanks to Paula Ballikaya for her insightful suggestions, advice, and continuous support.

Special thanks also to Fritz Eichenberger, of the Forstbetrieb Madrisa (Kloster's forestry office), who helped with the search for the suitable sampling locations and allowed the collection of the samples.

I am extremely grateful to the team of scientists and experts that made the analysis possible and offered fundamental help with the interpretation and elaboration of the results, in particular to Prof. Dr. Olivier Bachmann and Dr. Marcel Guillong, of the Institute of Geochemistry and Petrology, for the opportunity to use sophisticated analytical instrumentations, such as the LA-ICP-MS. To Dr. Lukas Wacker of the department of Earth Science of the ETH, who performed the radiocarbon measurements. And to Dr. Matthias Saurer, member of the forest dynamics department of the WSL, who conducted the nitrogen isotope analysis, and offered precious contributions to the project.

I would also like to thank the WSL staff, in particular Loïc Schneider and Anne Verstege who offered valuable help and advice during the preparation of the tree samples in the laboratory.

Finally, I am grateful for the practical support during field work and the motivating suggestions provided by Sergio Bazzurri, Nicola Paltenghi, Enkh-Uchral Batkhuyag, Nadja Studer and Alberto Bernasconi.

Abstract

Tree rings are widely recognised as passive environmental archives able to record the atmospheric composition and reflect the signal of the major pollutants with yearly resolution. This characteristic of trees and its efficacy has been tested in the current investigation. The case study of the village of Klosters was chosen to check the hypothesis that two groups of Norway spruce trees growing in relatively similar environmental conditions but exposed to two different quantities of atmospheric pollution from traffic exhausts, will store a dissimilar amount of pollutants within their tree rings. In order to verify this hypothesis, a combination of multiple analytical techniques was implemented to identify the signal of specific elements and isotopes usually associated with road traffic pollution. The Laser Ablation Inductively Coupled Plasma Mass Spectrometry (LA-ICP-MS) was performed to verify the presence and signal of several heavy metals, often found in vehicles exhausts or released by the wear of the engines. The nitrogen isotope analysis gave insights into the concentration of the $\delta^{15}\text{N}$ isotope, which depending on the emitting sources can be more or less depleted. Finally, the ^{14}C analysis depicted the sites' dilution effects generated by the emissions of radioactively dead CO_2 . However, the radiocarbon analysis revealed that in the site exposed to lower quantities of traffic pollution the growth of Norway spruces is limited by the availability of CO_2 rather than nitrogen, which is very often the case for most of the forested ecosystems. The results of the three analyses did not reflect the expectations of the initial hypothesis, since changes and differences in traffic volumes do not seem to produce major discrepancies in the recorded data of tree rings. Such lack of response in tree rings is possibly ascribable to the various limitation encountered in the current research for each of the applied method.

1 Introduction

1.1 Emissions from anthropogenic burning of fossil fuels

Anthropogenic activities revolving around the burning of fossil fuels are the major drivers for atmospheric pollution, and among those, road traffic has been proven to be the most prominent one, especially in urban environments (Al-Thani and Koç, 2018; Cheung et al., 2010; Coufalík et al., 2019; Sawidis et al., 2011). The exhausts emitted by the combustion of fossil fuels within the engine of vehicles usually consist of a mixture of different substances, including carbon (C), nitrogen and sulphur oxides (NO_x, SO_x), hydrocarbon, aldehydes, organic acids, and heavy metals (Krzyżanowski et al., 2005). Parts of these are emitted under the form of particulate matter (PM). The repercussions of this type of emission are often manifested mainly at the local level, showing an elevated level of environmental toxicity (Krzyżanowski et al., 2005). Moreover, the emitted components have the potential to develop into secondary and more deleterious substances (Sassýkova et al., 2019).

1.1.1 Polluting emissions of road traffic

1.1.1.1 Emission of heavy metals

Usually, in the exhaust of engines, traces of lead (Pb), copper (Cu), manganese (Mn), zinc (Zn), cadmium (Cd), chromium (Cr) and nickel (Ni) are to be expected; however, their concentration is highly dependent on the type of fuel used (Agarwal et al., 2011; Coufalík et al., 2019). For example, Cd, Ni, Pb, and vanadium (V) are mainly contained into the raw oil – such as mineral diesel (Coufalík et al., 2019). Other heavy metals, as in the case of Cu, might be increased during the refining process, whereas, if the fuel is stored in metal tanks there is a chance of increasing the amount of iron (Fe) and Zn (Coufalík et al., 2019). Mercury (Hg) is another element that is often part of road dust sediments (Huber et al., 2016), due to the fact that it can be contained in petroleum-derived products, such as fuels – sometimes even in relevant quantities (Brandão et al., 2005; García et al., 2017). The type of fuel has also an influence over the emitted elements and their proportions; titanium (Ti) has been reported to be mainly present in the exhaust of diesel originated fuels, whereas Cu and calcium (Ca) are predominantly bounded to the exhaust from gasoline powered engines (Wang et al., 2021). Nevertheless, the quantity of heavy metals released in the atmosphere from the exhaust's gases of the engine is not only dependent on their presence and concentration into the fuel itself. Relevant amounts of heavy metals that are also emitted through the tailpipe, e.g., Ca, Mn and Zn, come from the lubricating oils of the engine, in which they are usually employed as additives (Cheung et al. 2010; Coufalík et al., 2019). Zn in this context also serves the purpose of reducing the wear of metallic components (Coufalík et al., 2019). As a matter of fact, the wear of all the metallic parts of the engine, in particular pistons and pistons rings, as well as friction bearings and cylinder liners, represent another important source for the emission of heavy metals (Coufalík et al., 2019). In this case Cu, Fe, Pb are mainly released; Cr, Mn and Zn might also be emitted but in smaller quantities (Coufalík et al., 2019).

1.1.1.2 Emission differences between gasoline- and diesel-powered engines

The international market is mainly dominated by two different types of engines, which are powered either by diesel fuel or petrol/gasoline. In Switzerland, according to the most recent estimates provided by the Swiss Federal Statistical Office (n.d.), 29.6% of the vehicles that circulate on the national road network is powered by diesel, whereas the majority (around 66.3%) is petrol powered.

1. Introduction

The combustion of the former type of fuel within vehicles' engines results in the emission of a higher percentage of particles released in the atmosphere (Slezakova et al., 2013). The largest portion of PM emitted by the activity of diesel fuelled engine, up to 90%, consists of fine and ultrafine particles, with a strong preponderance of the latter (Coufalík et al., 2019). The reason diesel powered engines are more polluting while driving depends on the specific features of the engine itself; the fuel droplets in the combustion chamber tend to combust only partially (Sawidis et al., 2011), in particular during cold start and transient phases (Myung and Park, 2012). As a matter of fact, the catalytic converters need to reach a temperature of at least 300°C, in order to attain 97% of efficiency in filtering pollutants emissions (Walters et al., 2015). Therefore, in these phases, during which the target temperature is not reached yet, the emission of particles remains particularly high, accounting for 60-80% of the total emissions (Walters et al., 2015). Nonetheless, gasoline powered engines tend to also have irregular levels of particle emissions depending on the situation under which the engine is performing – in specific conditions petrol powered engines can potentially be more polluting than diesel-powered ones; e.g., when a gasoline-powered vehicle travels at more than 120 km/h or during acceleration phases the two types of engines appear to have the same level of impact in terms of particles emission (Slezakova et al., 2013).

1.1.1.3 Role of Catalysts

Exhaust fumes from vehicle engines are particularly polluting for the environment, and thus, in order to curb the number of toxic particles emitted, catalysts were developed. However, studies from the last decades highlighted that despite the aim of their design, catalysts could also be actively releasing harmful compounds (Liu et al., 2015; Rauch et al., 2005). Liu et al. (2015) demonstrated that this is the case for vanadium-based catalysts, since while operating, particles of their coating materials (which include V) are released in the atmosphere. An analogue situation was found for the platinum-group elements (PGE) catalysts (Rauch et al., 2005). Although originally PGE catalysts were believed to be harmless for the environment, Rauch et al. (2005) proposed in their study that the main active elements of the catalyst, i.e., palladium (Pd), platinum (Pt) and rhodium (Rh), were infiltrating into the vegetation located along the roadside and threatening the local ecosystems. In addition, it has been proven that a high presence of metallic elements within fuels, such as Hg (Brandão et al., 2005; García et al., 2017), can lead to a decreased efficiency of the catalyst, resulting in decreased number of filtered pollutants and in higher emission of heavy metals (Santos et al., 2011).

External factors can also have an influence on the volume of pollutants emitted – including heavy metals and PM. The type and age of the vehicle, as well as the style of driving, coupled with engine load speed seems to be the most impactful factors for what concerns the quantity of the exhaust (Coufalík et al., 2019). Moreover, Rönkkö et al. (2014), proved that there are some driving conditions that can also affect the dimension of the emitted particles. In fact, the situations in which the speed of a vehicle is adjusted by the so-called “motor brake” are responsible for 20 to 30% of all the emitted particles bigger than 3nm, even though in that moment the engine is not powered by fuel (Rönkkö et al., 2014).

In terms of air quality, in Switzerland, in the 40-year timespan from 1980 to 2020, several major progresses have been made in the reduction of pollution levels. For example, thanks to the introduction of the 3-way catalysts in the 1980s, the emissions of NO_x decreased by 62%; CO dropped by 86%; and non-methane volatile organic compounds declined by 74% (Bass et al., 2021). Diminishing the legally permitted content of sulphur in fuels strongly contributed to the abatement of the atmospheric emissions of SO₂, which since 1980 plummeted by 96%; For the same time period, improvements in agricultural practices helped to reduce the emissions of NH₃ by 34% (Bass et al., 2021).

1.2 Implications of traffic pollution on human health

1.2.1 Detrimental effects of Particulate matter

The definition of PM is based neither on their chemical composition or their structure, nor on the emitting source; but rather on the dimension of the particles, more specifically, their diameter (Grantz et al., 2003). As a result, PM is a mixture of different molecules having high variability in terms of chemical composition and size (Grantz et al., 2003). PM are particles having an aerodynamic diameter (AD) of less than 10 μm . Therefore, every molecule fulfilling the latter definition can be classified as PM.

Particles can be categorised as follows:

- 1) The particles that have an AD bigger than 10 μm are not considered PM. Although not being harmless, they have been reported to not be as dangerous as PM, possibly because bigger particles are stopped and trapped by the upper respiratory apparatus, and later expelled (Rabl and Spadaro, 2000);
- 2) PM_{10} have an AD ranging from 10 μm to 2.5 μm , and unlike the larger ones, these are able to infiltrate deeper into the human body, possibly reaching bronchi and bronchiole (Rabl and Spadaro, 2000), when not stopped in the upper airways – i.e., nasal cavities (Lee et al., 2014);
- 3) Fine particles ($\text{PM}_{2.5}$), have an AD ranging from 2.5 μm to 0.1 μm (Rabl and Spadaro, 2000) and, thanks to their smaller size, they can reach the alveoli within the lungs and consequently spread to the cardiovascular system (Lee et al., 2014);
- 4) Lastly there are the ultrafine particles ($\text{PM}_{0.1}$), also known as nanoparticles, which have an AD smaller than 0.1 μm (Lee et al., 2014; Slezakova et al., 2013). As is the case with $\text{PM}_{2.5}$, nanoparticles are able to reach the surface of the alveoli and from there they can spread within the body through the bloodstream, reaching extrapulmonary organs and the lymphatic system (Slezakova et al., 2013). Brain, hearth, liver, reproductive organs, and intestine might be targeted by ultrafine particles (Zhang et al., 2015).

Within the wide array of particles that are encompassed under the definition of PM, several chemical compounds can be found – including elemental carbon and organic carbon (Zhang et al., 2015). The chemical constitution of PM is often solidly correlated with the particle size – even though, as previously mentioned, they are not discriminated by their chemical properties (Grantz et al., 2003). As a matter of fact, trace elements and heavy metals, such as Pb, fall often under the category of PM_{10} (Grantz et al., 2003). NO_x and sulphur oxide (SO_x) are classified into the category of fine particles (Grantz et al., 2003). $\text{PM}_{0.1}$ are usually composed of trace metals, ammonium, sulphates, nitrates, and organic compounds (Slezakova et al., 2013).

1.2.2 Effects of traffic-related pollution on human health

The atmospheric pollution caused by the combustion of fossil fuels has become a concerning problem for public health. According to the most recent data collected by the World Health Organisation (WHO), in 2016, the premature death of roughly 4.2 million individuals could be reconducted to air pollution (WHO, 2018). It has been reported that an increase in PM concentration similar or above 10 mg/m^3 could have a significant impact on the level of mortality, with a growth of 0.8% (Ibald-Mulli et al., 2002). This means that high levels of exposure to fine particles can lead, in the worst cases, to higher mortality rates (Rabl and Spadaro, 2000), thus decreasing the overall life expectancy (Di et al., 2017). PM is responsible for cardiovascular and heart diseases, cellular DNA damage (Zhang et al., 2015), strokes, blood pressure problems (Ibald-Mulli et al., 2002; Lee et al., 2014) in

1. Introduction

addition to the aggravation of pre-existing diseases. Their adverse effects appear to intensify and worsen in individuals which are already struggling with respiratory diseases, such as asthma (Ibald-Mulli et al., 2002). The reason for the negative effects of PM could be reconducted to its chemical constituents (Zhang et al., 2015). If the PM is formed by a combustive process (Slezakova et al., 2013), it often contains polycyclic aromatic hydrocarbons, polychlorinated biphenyls, and heavy metals (Zhang et al., 2015). In the latter case, the presence of specific metallic elements such as Fe and Cu, can also induce the development of lungs cancer (Coufalík et al., 2019).

Moreover, a link has been found between the surface area of particle and its incidence on human health (Ibald-Mulli et al., 2002; Slezakova et al., 2013; Zhang et al., 2015). The gravity of the consequences for the health seems to be indirectly proportional to the dimension of the particle (Slezakova et al., 2013), the smaller the particle, the greater is the severity of the repercussions in terms of health.

1.3 Implications of traffic pollution on environmental health

Road traffic, and especially the engine's exhausts, exert important health damages to the whole surrounding environment (Bernhardt-Römermann et al., 2006; Bignal et al., 2007) independently from size or shape of the leaves; all trees seem to be affected likewise. Vehicular traffic can affect the nearby vegetation in direct ways, such as through the exhausts of the engines which are then absorbed by foliar uptake; or indirectly, by the construction and maintenance of road which alters the biogeochemistry of the soil and its hydrology (Lee et al., 2012). Motorway traffic is often the cause of increases in heavy metal concentrations, environmental enrichment of nitrogen (N) as well as higher levels of soil moisture and pH (Lee et al., 2012).

Nitrogen is one of the major drivers in forest and vegetation changes, since the more N is available, the more trees will tend to accumulate biomass and will colonize soil patches more intensively (Bernhardt-Römermann et al., 2007). Abrams (2011) reported that in Austria, in the last 60 years most of the growth increase of forest is to be reconducted not to climate change and the related global warming, but rather to the eutrophication caused by the increased rates in N deposition over the environment. Each deposited kilogram of N promotes an increase of stem wood between 20 and 40 kilograms (Abrams, 2011). The growth surplus is reflected in the overall increased width of the tree rings, making the analysis of growth patterns based on tree rings less intuitive and more complicated to implement (Ferretti et al., 2002). This is due to the fact that the fertilisation effect caused by N results in a homogenisation of the tree ring width, thus partially burying the growth pattern of the tree. Species with higher tolerance for N levels are more favoured by this type of condition and will therefore outcompete the other plants species (Lee et al., 2012). Shifts in species dominance has been reported as a consequence of the loss in species richness (Lee et al., 2012; Bernhardt-Römermann et al., 2006). In addition, N was proved to have phytotoxic effects over the environment (Stewart et al., 2002), to induce acidification and to increase the vulnerability to droughts (Clark and Tilman, 2008; Paoletti et al., 2010). Clark and Tilman (2008) discovered that, if the N depositions are constant throughout multiple years, their negative effects will occur with acute symptoms even at slightly higher deposition rates than the natural ones. A decrease in species richness is also caused the use of salt for de-icing the roads (Truscott et al., 2005), which by increasing the soil pH, it favours the settling of species that are more tolerant towards such environmental conditions (Lee et al., 2012). Thus, traffic roads exert a relevant stressing effect over the environment, which leads to a more homogenised composition of both the surrounding vegetation – i.e., by decreasing the species richness – as well as the internal composition – i.e., by smoothing the width variations of tree rings.

1. Introduction

The effects and the quantity of the pollutants infiltrating into the biosphere has been proven to decrease exponentially according to the distance of the emitting source (Bignal et al., 2007; Saurer et al., 2004). Effects over the vegetation are more pronounced in proximity of the highly trafficked roads – i.e., motorways –, particularly within 50-100 m (Bignal et al., 2007), and up to 200 m (Bernhardt-Römermann et al., 2006; Truscott et al., 2005). Going further away from the emitting source the effects are much more mellowed due to the filtering protection offered by canopies of the trees (Bernhardt-Römermann et al., 2007). As a matter of fact, Bignal et al. (2007), assessed that the damages presented by oak (*Quercus petraea*) and European beech (*Fagus Sylvatica* L.) depend on the plant distance from the motorway. The authors observed that trees closer to the traffic source were more prone to show severe foliage damage – both in terms of leaf decolouration and crown defoliation, as well as insects' perpetrated damages.

1.4 Trees' role as passive pollutants archives

1.4.1 Pollutants deposition in forest ecosystems

In comparison to biomes with low vegetation structures, such as grasslands, forests tend to have a higher deposition rate of pollutants due to their irregular shape, which acts as a remarkably effective filter (Bobbink et al., 2010). It is not by chance that trees are widely recognised as potentially very efficient barriers able to stop the spreading of PM (Gomez Moreno et al., 2019; Lee et al., 2012; Yin et al., 2011). Thanks to their elevated level of surface roughness, trees are particularly suited to increase dry and turbulent deposition of particulate matter, mostly PM₁₀ and PM_{2.5} with a strong preponderance of the former (Gomez Moreno et al., 2019).

When located near a polluting source and protected from precipitation events, trees tend to accumulate the highest rate of pollutants. During rainfall events, the majority of PM laying on the foliage surface can be washed away and more likely become immobile in the soil; thus, new PM can deposit on the leaves again. If the PM that was trapped by the foliage is resuspended, e.g., due to strong winds, the capturing effect of the plant will result to be marginal (Przybysz et al., 2014). Interestingly, these atmospheric conditions seem to not have an effect over the accumulation on the bark of the tree. The bark in fact has a porous structure which allows for elevated accumulation of PM, without having to cope with wind and rainfall events. Furthermore, the bark appears to not be affected by the potential health threats posed by the polluting agents (Sawidis et al, 2011).

Coniferous species (and *Pinus sylvestris* L. in particular) are better suited for air mitigation purposes than broadleaf species, because the former can still be effective even during the winter months, when the concentration of PM is often peaking. Furthermore, the aerodynamic properties of coniferous trees, having complex shoot structures and needles, are also considered to be important factors for their higher capture efficacy. The elevated efficiency of *P. sylvestris* however comes with a cost, resulting in increased amount and severity of physiological damages, which might be linked to their higher susceptibility to heavy metals, such as Fe (Przybysz et al., 2014).

1.4.2 Tree absorption of pollutants

In the last few decades, trees have aroused the interest of researchers due to their potentially unique role as environmental archives, which could be useful for the reconstruction of local pollution chronologies (Cherubini et al., 2021; Ferretti et al., 2002; Mihaljevič et al., 2011). First of all, it is important to mention the key distinctive characteristic of trees. In temperate regions, as a matter of fact, they do grow by one tree-ring every year, a so-called annual ring. The ring is usually split into two areas having a different colour; the first one is the earlywood which is characterised by a light

1. Introduction

colouration due to its cells having a large diameter and small cellular wall (Fritts 1971). Normally, the earlywood grows in spring, at a relatively fast pace. During the summer months and autumn, a darker and slower growing type of wood forms, i.e., the latewood, which as opposed to earlywood, consists of cells having small diameter and thick cell walls (Fritts, 1971; Higuchi, 1997). There are exceptional occasions however, of severe stress for the plant – due to diseases, competition or adverse climatic conditions – in which the ring only grows in parts of the stem, a so-called phenomenon of missing ring verifies (Novak et al., 2016). Based on their growing characteristics, there are various aspects of trees that could reveal noteworthy information. These are divided into two distinct categories: the physical properties of the tree ring, such as the width, the anatomical features of the wood or the wood density, and the chemical properties, which include the elemental composition of the tree rings (i.e., dendrochemistry) and the study of stable isotopes and their translocation within the rings (Ferretti et al., 2002; Turkyilmaz et al., 2019).

Several studies have confirmed the ability of trees to absorb the pollutants present in the atmosphere, as well as the soil, and store them within their tree rings, respecting the proportions of the chemical composition of soil and atmosphere (Bindler et al., 2004; Locosselli et al., 2018; Mihaljevič et al., 2011; Perone et al., 2018; Sawidis et al., 2011; Turkyilmaz et al., 2019; Watmough 1996).

Thus, considering that trees can reflect the atmospheric elemental composition with yearly resolution, they do have the potential to be a particularly good proxy for atmospheric pollution trend (Mihaljevič et al., 2011; Turkyilmaz et al., 2019; Watmough et al., 1996). Different investigations have shown that using trees for long-term exposure studies to reconstruct the environmental pollution levels – depending on the situation – can be easier (e.g., sampling) and cheaper than using other archives, such as sediments, ice, or peat (Bindler et al., 2004; Locosselli et al., 2018). Moreover, trees have two other practical advantages. Firstly, they have a remarkably high spatial resolution, due to the fact of being widespread all over the globe and across a multitude of different biomes (Bindler et al., 2004; Sawidis et al., 2011). Secondly, trees tend to be long lived species, which in some cases can live up to thousands of years (Turkyilmaz et al., 2019). This feature can be useful when investigating polluting events having an important impact over the environment, even a few decades after its conclusion (Sawidis et al., 2011).

1.4.3 Monitoring of heavy metals in tree rings

Dendrochemistry offers the possibility to study the presence of isotopes and trace elements, such as heavy metals, in tree rings. It has been often confirmed that heavy metals tend to leave tangible and specific signatures behind, making them easily detectable (Ferretti et al., 2002).

Trees have the ability to take up elements from the surrounding environment, and therefore heavy metals too (Binda et al., 2021). Trace elements are primarily absorbed from the soil by the root system of the tree; however, the uptake can also take place at the level of the crown (from the atmosphere and through the leaves), or even through the bark (Binda et al., 2021).

Nonetheless, if the atmospheric concentration of pollutants emitted by the source is particularly dense and abundant in a relatively small area, e.g., of highly trafficked roads (Turkyilmaz et al., 2019), the uptake of heavy metals may involve upper parts of the trees (e.g., leaves) rather than the roots (Mihaljevič et al., 2011). In these circumstances, trees have the potential to be used as a monitoring tool for heavy metal concentrations in the atmosphere of a specific geographic location (Mihaljevič et al., 2011; Turkyilmaz et al., 2019).

1.4.4 Investigation of stable isotopes in tree rings

In addition to the tracing of heavy metals, several stable isotope ratios can be investigated through dendrochemistry, such as carbon, nitrogen, oxygen, or hydrogen (Savard, 2010). For this type of investigation an Isotope Mass Ratio Spectrometry (IRMS) is utilised (Binda et al., 2021). This technique requires usually a pre-treatment of the samples, in which they are also separated in individual annual rings (Binda et al., 2021). Carbon isotopes are often analysed in studies focused on investigating the atmospheric pollution, since the CO₂ taken up by trees is directly absorbed from the atmosphere through the leaves (Savard, 2010). Similarly, there is potential in this field for the use of N isotopes as well, as it has been documented by Amman et al. (1999) and Saurer et al. (2004). However, due to the fact that N is taken up by both the leaves from the atmosphere and by the roots through absorption from the soil, this aspect might affect the interpretation of the results. The elements stored in the soil in fact do not always reflect the respective concentration in the atmosphere (Savard, 2010). Moreover, the concentrations of chemical compounds from anthropogenic pollution have to be discriminated from the natural fluctuations of the element in the atmosphere and the pedosphere (Savard, 2010).

1.4.5 Limitations of tree rings in atmospheric pollution studies

Trees have the potential to be considered as environmental archives. However, since they are living organisms, they are not passive (Binda et al., 2021; Watmough, 1997). Physiologic interactions of biological and chemical nature take place within trees (Binda et al. 2021).

Tree rings, despite having a concrete array of advantages, are not always a perfect method of choice to study the historical trends of air pollution (Ferretti et al., 2002; Mihaljevič et al., 2011; Sawidis et al., 2011). Bindler et al. (2004) concluded that the use of dendrochemistry to investigate the presence of trace elements is not a suitable tool for monitoring the variation of environmental pollution. The authors stated that the application of dendrochemistry on trace elements has poor potential for the investigation of historic atmospheric pollution, although it must be considered that the chosen sampling location for their study do not appear to have locally important sources emitting Pb isotope (the trace element chosen for their investigation). Many studies confirmed that relevant local sources of air pollutions, having high resilience to various environmental conditions and the presence of plants with sufficient tissue to be analysed are necessary factors (e.g., Beramendi-Orosco et al., 2013; Ferretti et al., 2002; Mihaljevič et al., 2011).

Nonetheless, the situation is not always straightforward to assess; there are some elements, such as N and oxygen that can be taken up by both the root and the foliar system (Binda et al., 2021). This complicates the matter, since the response of trees that absorb the element of interest through a deep root system is delayed in respect to the environmental changes taking place in the atmosphere (Binda et al., 2021; Watmough, 1999). Furthermore, in such circumstances of absorption from a deep root system, there is a subsequent sap transport of the chemical element within the vessels (Mihaljevič et al., 2011), which could lead to the radial translocation of the particle within the sapwood (Locosselli et al., 2018; Mihaljevič et al., 2011). Radial translocation implies that the pollutant may cross tree-ring boundaries and move to the adjacent ring of the one formed in the current year of the pollutant uptake. Cutter and Guyette (1993) highlighted six factors that are responsible for the movement of elements within the xylem: i) ion solubility, ii) sapwood-heartwood equilibrium concentrations, iii) charge/ionic radius ratio, iv) essential nature, v) sap pH, and vi) bonding in the xylem matrix. According to Locosselli et al. (2018), owing to the fact that radial translocation is a required process for the development of heartwood, trees showing a visible section of heartwood are also more susceptible to radial translocation. Interestingly, the transition from heartwood to sapwood can

1. Introduction

potentially arise at different time along the same circumference (Cutter and Guyette, 1993). The thickness of the sapwood in fact varies between and within species, since it depends on different stresses (such as hormonal or hydric), as well as genetic and environmental factors (Cutter and Guyette, 1993).

Some heavy metals – defined as essential elements – such as Cu and Zn have the tendency to accumulate in the sapwood, while other – nonessential – such as Cd and Pb do not show this pattern of accumulation in the sapwood (Watmough, 1999). Coniferous species appears to be less affected by translocation issues, due to the physiology of this wood type, which present a fewer number of parenchymal rays – which are responsible for the radial translocation (Binda et al., 2021). Additionally, Watmough (1999) reported that the concentration of trace metals could also be dependent on at least two more factors: the age of the tree and the presence of wounds. As a matter of fact, the presence of a damage causes the tree to react and thus in the interested region of the plant the concentration of essential metals (i.e., Cu and Zn) might result particularly high (Watmough, 1999).

On the one hand, it is true that some tree species are better than others for dendrochemical analyses, depending on the scope of the research, however one must adapt to the resources present in-situ (Cutter and Guyette, 1993). The choice of the tree species might be restricted by the singular characteristics of the study area, thus, there is the possibility that the most suitable species for the task might not be locally available for the study (Cutter and Guyette, 1993). On the other hand, as highlighted by Watmough (1997) sometimes the element concentration within a tree differs for every individual even in the same site. The reason is that there are many variables that come into play when using trees as environmental proxies, such as the soil characteristics (Beramendi-Orosco et al., 2013), the hydrology and the canopy structure (Watmough, 1997). All these can influence the fitness for the task for a specific tree, and potentially affect the results of an investigation.

1.5 Case study: The village of Klosters

1.5.1 Description of Klosters and its characteristics

The municipality of Klosters (46°52'12.633" N 9°52'55.533" E) is located in the canton of Graubünden, Switzerland. It is an alpine community, which lays in the upper Landquart valley, at 1200 m a.s.l. of elevation (Gemeinde Klosters, n.d). With 219.8 km², the territory of the municipality is fairly vast, and it covers most of the upper catchment area of the Landquart river (Gemeinde Klosters, n.d). Klosters is surrounded by mountains whose peaks (often surpassing the 3'000 m a.s.l. threshold) mark its territorial the boundaries (Gemeinde Klosters, n.d). According to the Köppen classification of climate, Klosters belongs to the subtype "Cfb", Marine West Coast Climate, and is characterised by an average yearly temperature of 2.2 °C (12.8°C and -9.4 °C during the warmest and coolest month respectively) and a total average rainfall of 840 mm per year (Weatherbase, n.d.).

With roughly 4'600 inhabitants, it is the second biggest community in the region of Prättigau/Davos after the municipality of Davos itself. Klosters, along with the neighbouring town of Davos, is best known for being an attractive location for tourists. According to a recent report of the private firm BAK Economics AG (2018), published on behalf of Canton Graubünden, the region of Davos – Klosters was included in the top ten's most attractive destinations for the winter season in the whole alpine region – therefore including not only Swiss resorts but also the ones of every alpine country. During summer, the touristic attractiveness of Davos – Klosters is not as strong as in the winter months, however it still ranks far above average compared to the other locations in the alpine region (BAK Economics AG, 2018). As a matter of fact, Davos – Klosters has been regarded as an international holiday destination for more than a century (Davos-Klosters, n.d.). In the 1950's there

1. Introduction

were already more than 1.5 million overnight stays in the region (Davos-Klosters, n.d.). The destination was, and still is, particularly popular among American celebrities of the cinematographic industry, as well as the British Royal Family (Davos-Klosters, n.d.).

In the relatively small context of the Canton Graubünden, the region of Davos – Klosters is considered to be a major hub for tourism (BAK Economics AG, 2018). In the season of 2016/2017 (which includes summer 2016 and winter 2016/2017) the total number of overnight stays surpassed 2.5 million with a growth of 1.75% in comparison to the previous season (Klosters Tourismus, 2016-2017). Almost half million of these tourists chose to spend their holidays in the accommodations offered by the municipality of Klosters (Klosters Tourismus, 2016-2017). The tourism industry is crucial for the region. For the public sector, in the business season of 2016/2017, tourism related activities generated around 3 million CHF of income for the public finances of Klosters – this number does not consider the revenue for the private sector, only the public gains (Klosters Tourismus, 2016-2017).

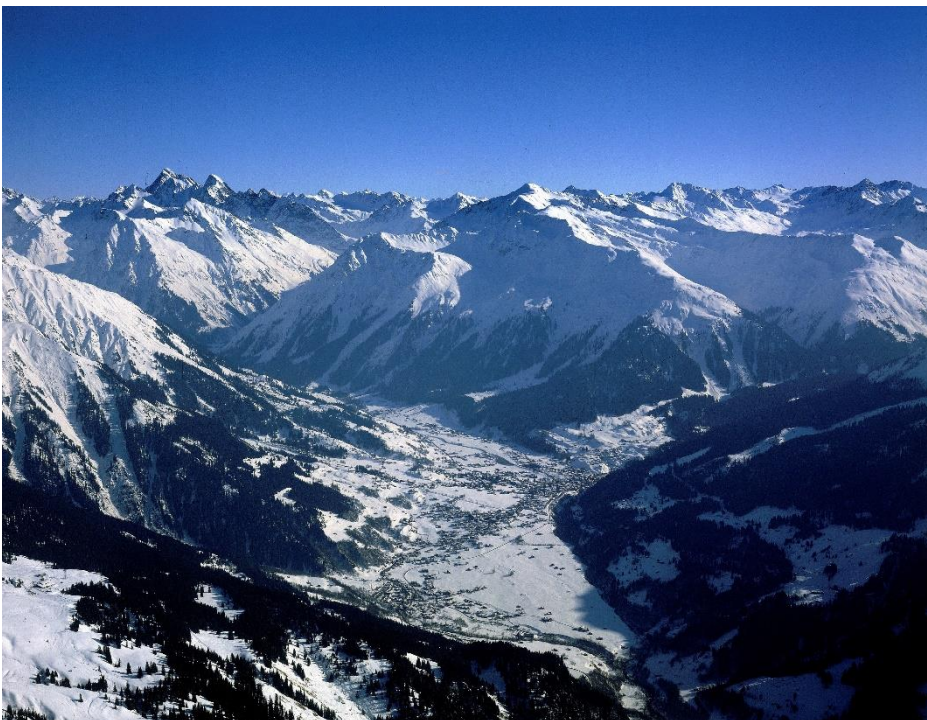


Figure 1: Panorama of Klosters (source: ETH-Bibliothek Zürich, Bildarchiv / Photographer: Krebs, H.).

The village possesses various point of strength, which are attractive for tourists. Remarkable is the elegance of the old village's buildings, the recreational activities offered and the peaceful character of the surrounding nature (Davos-Klosters, n.d.), displayed in Figure 1.

1.5.2 Klosters' traffic burden

The fact that Klosters and Davos are both located along Prättigauerstrasse (the national road A28), represents an issue for the former village, as many of the tourist that aim to spend their vacation in Davos, often come from the north, (i.e., the Swiss plateau) and travel with private vehicles. Therefore, they have to pass through Klosters in order to reach their destination, creating a condition, which, due to the important growth of the tourism industry in the 20th century, became progressively more and more problematic for the local community.

1. Introduction

As a matter of fact, in the second half of the 20th century, the communities of Küblis, Saas and Klosters – all located along the national road A28 – were indeed concerned that the growing popularity among tourists of the Prättigau/Davos region could backfire and ruin the touristic attractiveness of their villages. This potential backlash was especially noticeable during the peaks of traffic in the winter weekends, situations in which the road, that for the most part was at least a century old (Tiefbauamt des Kantons Graubünden, 1991), could count up to 17'000 transits (Engler, 2005). Thus, the emission thresholds for toxic engine exhausts were often reached and, occasionally, exceeded. The situation was deemed problematic firstly because it posed numerous challenges for the livelihood of the local population, such as the overloading of the ways of communication, the negative effects of engine exhausts for both human beings and the surrounding environment, the noise pollution from traffic, a higher chance of being involved in an accident, and the increased difficulty for rescue vehicles to circulate freely (Tiefbauamt des Kantons Graubünden, 1991). Secondly, the development goals for the regional touristic industry decided by the Federal Government, the Canton, and the local authorities aimed to a different direction (Tiefbauamt des Kantons Graubünden, 1991). The main idea was to encourage the growth of a “sanfter tourismus” (sustainable tourism) based on weeklong stays rather than daily ones – which is focused on using a private mean of transportation instead of a public one (Tiefbauamt des Kantons Graubünden, 1991). However, the recent trend showed a situation in contrast with the one envisioned by the regional plans, the resorts of Davos-Kloster were attracting primarily tourists coming with a private vehicle who would not stay overnight in a touristic accommodation nearby (Tiefbauamt des Kantons Graubünden, 1991).

To further worsen the traffic situation, in November 1999, the Vereina Tunnel was inaugurated. The Vereina line is a 20 km long railway, known as “Vereina Autoverlad” (Vereina car transporter), which connects Klosters-Selfranga, in the Prättigau region, with Sagliains in the Engadin Valley. The opening of this new connection shortens the travel time from Zürich to the Lower Engadin (Dünser, n.d.). Moreover, it grants an all-year-round connection between the two regions, which is especially important when the Flüela and the Julier Pass are closed for the winter season (Dünser, n.d.). The line itself has been particularly successful. As it is visible from Figure 2, it transported 306'000 vehicles during its first year of operation and grew considerably, up to 529'000 in 2019. Nonetheless, this important result does come with a price, which is expressed with a pronounced growth of road traffic volumes for the Prättigau region.

Already during the 1980s the outlook of the traffic situation appeared grim, and with the perspective given by the evolutions of the touristic trend as well as the opening of the Vereina line, the condition in the future could only worsen. In Figure 3 the forecasts for the traffic development on the Prättigauerstrasse, made in 1990, are displayed. The estimations show that in 2005 traffic for both weekdays and weekend would increase as much as 60%, for an average total growth of 70%, and one fifth of this amount was to be directly attributed to the opening of the Vereina Tunnel (Tiefbauamt des Kantons Graubünden, 1991). For this reason, the affected communities were highly incentivised to find a long-lasting solution, without undermining the regional touristic vocation.

1. Introduction

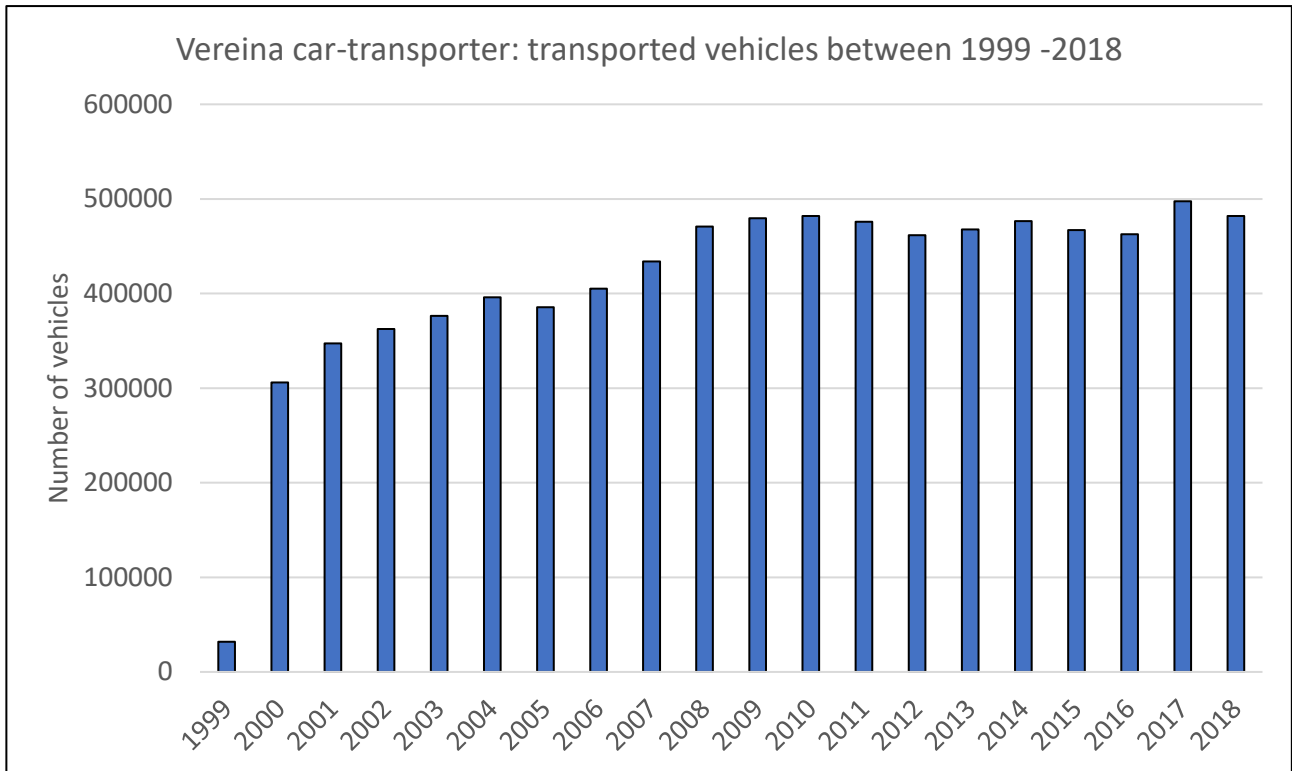


Figure 2: Number of vehicles transported through the Vereinatunnel from its inauguration in 1999 until 2019 (own representation, data source: Rohner, S., 2020).

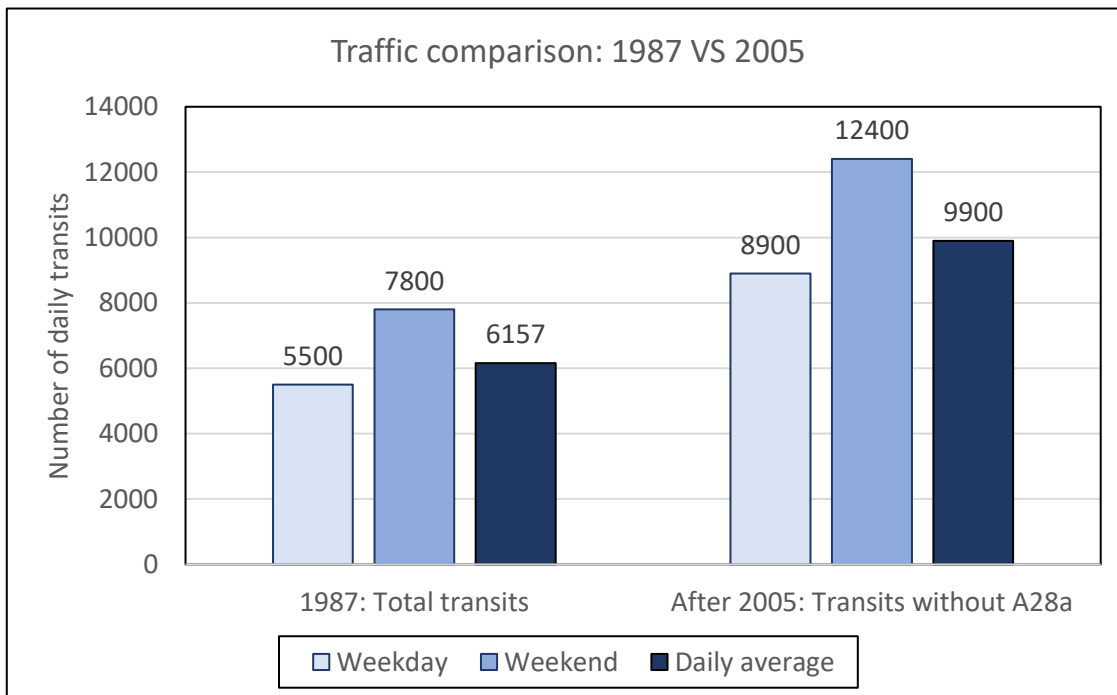


Figure 3: Traffic comparison between weekdays and weekend in 1987 and the predicted values for 2005 (own representation, data source: Tiefbauamt des Kantons Graubünden, 1991).

1.5.3 Construction of the bypass road (A28)

At the beginning of the 1960s, the local authorities started to develop a plan that would mitigate the adverse effects of traffic in the Prättigau region (Gemeinde Klosters, n.d. b). The conceived idea was to build a new road (A28) that would divert the traffic flow from passing through the villages of

1. Introduction

Kloster, Saas and Küblis (Tiefbauamt des Kantons Graubünden, 1991) – The bypass road (A28), in the planning phase was referred to as A28a, since there were multiple variants but eventually the A28a was built. Considering the important dimension of the project, it was cut into three different sections, one for each village. Here, the focus is on the segment that is related to this study, namely the sector spanning from Büel to Selfranga, which includes the municipality of Klosters. The section of the project is shown in Figure 4 (the bypass road is highlighted in bold), and this part alone, spanning from Büel to Selfranga costed more than half a billion CHF (Kägi, 1998). The central piece of the bypass road is represented by the Sunnibergbrücke (Figure 5), a 525 m long bridge which, due to its peculiar architecture is considered having a relevant aesthetic quality (Kägi, 1998).

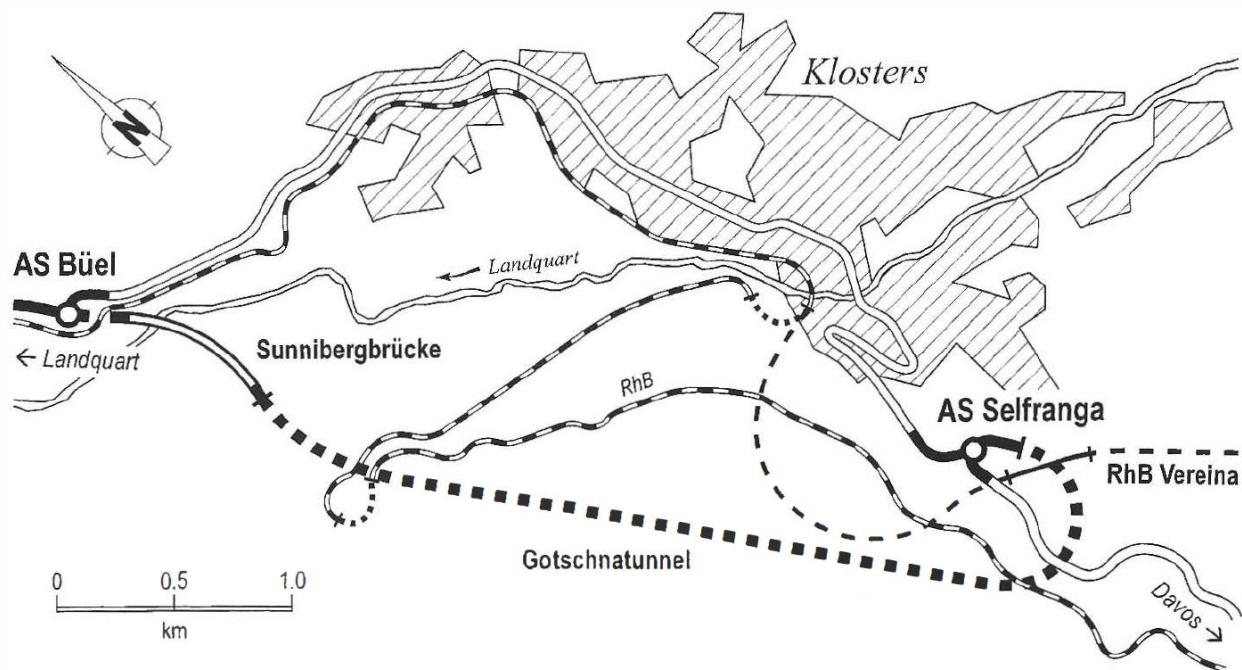


Figure 4: Sketch of the project for the Klosters' bypass road (source: Kägi 1998).



Figure 5: The "Sunnibergbrücke" a section of the new bypass road (photographer: Paula Ballikaya).

1. Introduction

The project aimed at minimising the excessive traffic volumes on the local road, while simultaneously decreasing the quantity of pollutants emitted by the vehicles in the village.

On the one hand, according to the predictions made before the construction of the A28 by the team in charge of the delivery of the environmental impact assessment report, it was expected that 78% of the future traffic flow would avoid passing through the village using the new bypass road (Figure 6), whereas the average amount of vehicles travelling along the old road would have decreased by at least 35% in comparison with the current situation – i.e., in 1987 (Engler, 2005). On the other hand, the gains in terms of time by using the A28a would have resulted in an increased attractiveness of the route as a collateral damage (Tiefbauamt des Kantons Graubünden, 1991). However, this growth was estimated to be 1-2% of the overall traffic using the A28a in 2005 – i.e., adding only 100-200 vehicles per day to the total (Tiefbauamt des Kantons Graubünden, 1991).

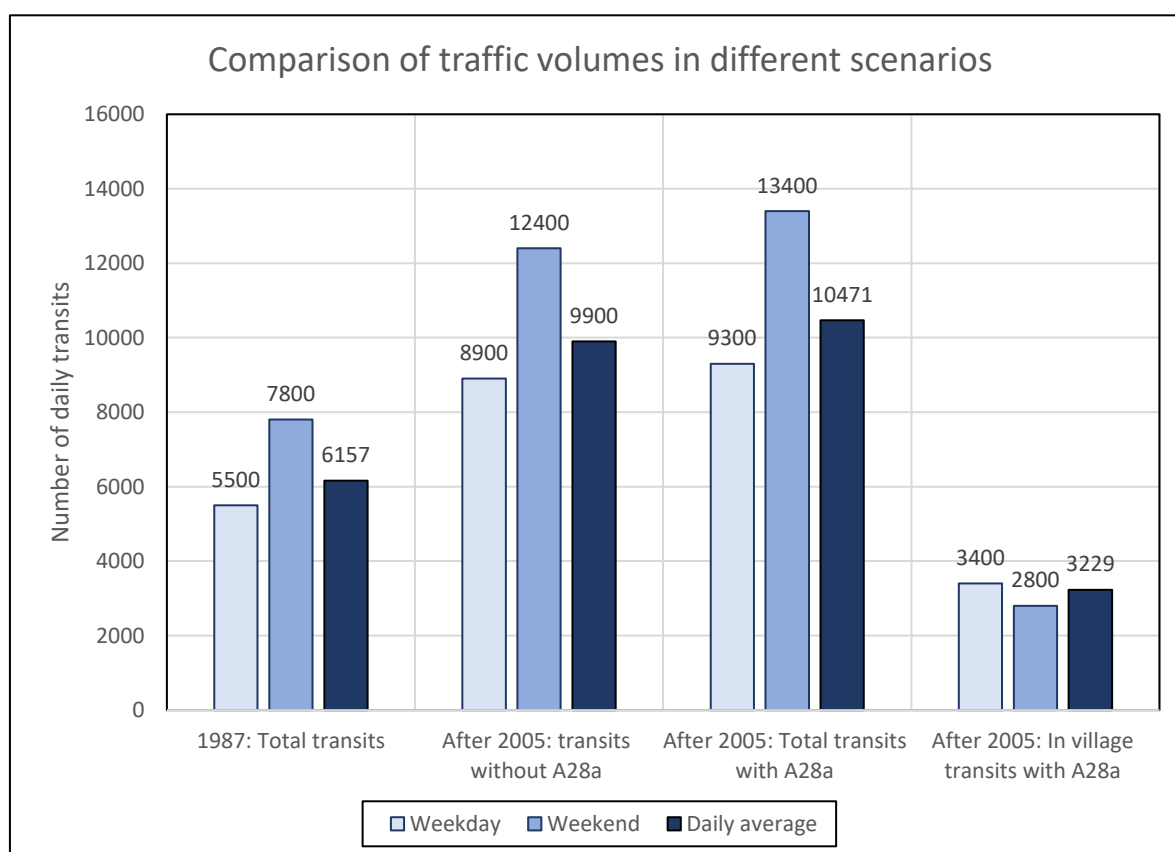


Figure 6: Traffic development comparison of different scenarios, between the measured values in 1987 and the ones predicted for 2005 (own representation, data source: Tiefbauamt des Kantons Graubünden, 1991).

Once the projecting phase was completed, in the mid-1990s the cantonal authorities gave the permission to begin with the construction works (Gemeinde Klosters, n.d. b), which started in 1995. After nine years of construction the bypass road was built, and it was inaugurated on the 9th of December 2005.

Figure 7 shows the difference in the development of the average daily traffic fluxes between 1987, the prediction made for 2005 during the projecting phase in the 1990's, and the actual traffic volumes measured in 2014 and 2019. From the graph it is possible to see that the prediction estimated a total of 10'500 right after the opening of the bypass road. The forecasted volume for 2005 was presumably more dramatic than the actual value (unfortunately there are no data provided by the FEDRO before 2014), since as much as 10'500 vehicles, which represent a 70% growth, were not reached even after

1. Introduction

14 years. However, in comparison with the number of transits of 1987, the volume of traffic reached in 2019 shows that there has been a robust increase of 60%.

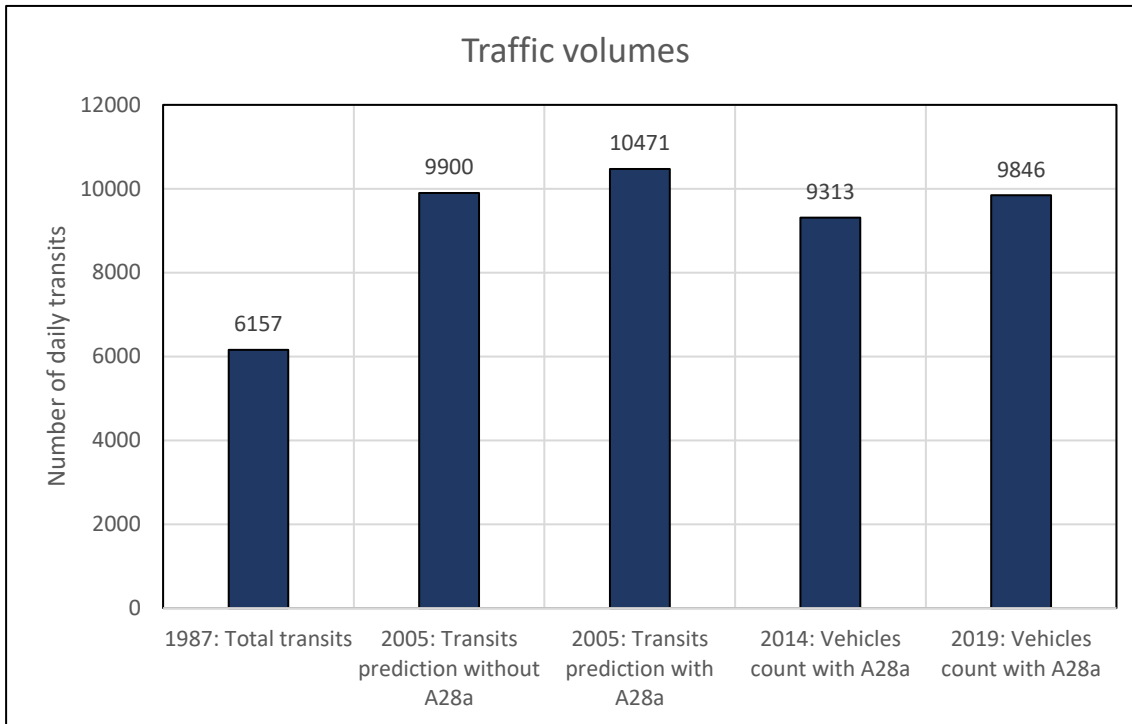


Figure 7: Traffic volumes' comparison between predictions and measured values (own representation, data source: Tiefbauamt des Kantons Graubünden, 1991 and FEDRO 2020).

1.6 Project description, aims, and research question

This study is a multi-approach research aiming to assess the capability of trees as a proxy for environmental pollution – the atmospheric one in particular. The main idea of the project is to determine the variations of the air quality in the village of Klosters by using evidence of major traffic fluctuations throughout time found within tree rings. The variations of traffic taken into consideration for this study are not night/day cycles (which indeed do show high excursion levels, but also have an extremely small temporal scale, less than 24 hours) but rather yearly changes. Trees, which form one growth ring each year, allow to study the fluctuations of vehicular emissions over an extended timescale (with yearly or decadal resolution) through the chemical analyses of the rings. The specific case of the village of Klosters appears to have all the required criteria to allow such investigation, as the changes in traffic flow have been important – after the 1980s there has been an overall increase of 60% vehicles – and the timescale is relatively large (more than 30 years). Furthermore, the construction of the bypass road created a unique situation. After its inauguration, trees that are located along both the previously heavily accessed road and the new A28 road are exposed to a considerably higher level of pollution from engine exhausts in comparison to the trees that are located in the centre of Klosters. Thus, for this Master thesis, tree cores of Norway spruce (*Picea abies* L.) were extracted at three sites. The first location is situated along the village road, the second one is adjacent to both the old village road and the new bypass road (A28), and the last one is in a distant area, far away from the two roads.

The research question is the following: How are recorded the effects of changes in traffic volumes in tree rings in terms of pollutants' signal?

The main hypothesis of the current research is that the signal of-pollutants from traffic exhaust present in tree rings reliably reflect the changes in traffic volumes at the study sites, with possibly low

1. Introduction

temporal delay. The hypothesis is based on the environmental archive characteristic of trees; therefore, this feature and its efficacy will also be investigated.

The objectives of this study were pursued by investigating the chemical concentration of pollutants stored within tree rings, and by depicting their variation in the atmosphere caused by vehicular traffic flows from 1970 to 2020. Several studies have already focused on the use of tree rings to monitor the changes in environmental pollution, with higher or lower success rate depending on various factors, including the methods applied. This research however will not rely only on the implementation of a single approach but rather on a combination of three different methods, namely:

1) the analysis of tree-ring stable nitrogen isotopes ratio ($^{15}\text{N}/^{14}\text{N}$), that highlights the variation in isotopic composition of N in the wood over time, i.e., showing whether there is a depletion or enrichment of ^{15}N over ^{14}N within tree rings.

2) the analysis of radiocarbon ($^{14}\text{C}/^{12}\text{C}$), which identifies the portion of radioactive ^{14}C in comparison to its decayed counterpart ^{12}C . This technique is applied to discover how much fossil fuel derived CO_2 is taken up by trees over time, and thus the magnitude of ^{14}C dilution due to traffic emissions.

3) The Laser Ablation Inductively Coupled Plasma Mass Spectrometry (LA-ICP MS), which in this case, is mainly used to detect the signal of trace/heavy metals within the tree rings of the samples.

Finally, based on the obtained results, the suitability of the different methods, for this project, will be evaluated by discussing strengths and weaknesses of each method, giving insights on their complementarity.

2 Material and methods

2.1 Study area



Figure 8: Map of the village of Klosters showing the sampling sites and the main communication routes (own representation, background map from: swisstopo - Federal Topographic Office).

In order to carry out the required analyses for the evaluation of the air quality in the village of Klosters, four sampling sites were selected in accordance with the local forestry office (Forstbetrieb Madrisa). The major limitation in the choice of the sampling locations was the fact that many terrain plots having trees in suitable position were owned by private citizens and were consequently not accessible for coring. The samples were extracted from a tree species that commonly grows in the region, Norway spruce; site OU, ON and CT were sampled (Figure 8), and display the following characteristics.

- 1) Site Old road Uphill (OU – $46^{\circ}51'N$, $9^{\circ}52'E$, 1265 m a.s.l.) is positioned on a slope having an eastward exposition, and it is located along the Landstrasse (old road), hence, it is subject to the vehicular traffic passing through the village of Klosters. The tree vegetation here consist of only Norway spruce. This site is particularly close to the village and could be affected by anthropogenic pollution unrelated to traffic exhausts, but rather routine activities from the settlement.
- 2) Site Old and New road (ON – $46^{\circ}53'N$, $9^{\circ}51'E$, 1065 m a.s.l.) is located on a slope exposed to southwest with a similar inclination to site OU. The vegetation here is mixed, Norway spruce and European beech (*Fagus Sylvatica*, L. 1753) are present. As shown in Figure 8, this location lays within a close range from both the new bypass road, the Prättigauerstrasse (A28), as well as the Landstrasse, therefore the hereby trees should be exposed to the engine exhausts of traffic flowing by either route. It is worth noting that a stone wall, of at least 2m in high, is separating the road from the trees, even though, the crowns of the sampled trees were all above the wall.

- 3) The last sampling location of the project is site Control (CT – 46°51'N, 9°56'E, 1394 m a.s.l.). It is located in a remote area far away, around 4.5 km from site OU so as to be unpolluted by the exhaust of vehicular traffic. In this area the samples of the control group were extracted, in order to measure the local (i.e., of Klosters) background concentration for the chemical analyses. Similar to the other sites, it is also located on a slope, with southwest exposition. The only tree species in the area is again Norway spruce. It is relevant to note that site CT, despite being located far away from important sources of fossil fuel emissions, might report unprecise background data (especially for nitrogen – Koerner et al., 1999), since there are a few runoff surface streams and the area is potentially used as a pasture for cattle.

2.2 Samples collection

In each site 7 trees were sampled and a total of 14 cores were extracted by means of an increment borer. All the cores were extracted at breast height (1.5m). Regarding the sampling strategy, all the trees found in the field that appeared having a diameter of less than 0.2m were excluded, because for this study a minimal age of 40 to 60 years is required. Notwithstanding the fact that a small diameter does not unequivocally correspond to a young tree, dendrochronological and dendrochemical analyses must be carried out on specific tree rings, and therefore it is needed that the rings of the selected trees do have enough material – which might not be the case for an old tree having a small diameter. An additional factor that must be taken into account is the influence of reaction wood, which should be minimised when possible. According to Achim et al. (2006) the sides of the trees exposed to the slope gradient tend to be more prone to the development of reaction wood. Hence, as target trees were identified those that were standing as straight as possible, and they were sampled perpendicularly to the slope gradient and parallelly to the soil. The effect of wind, in terms of direction and speed, was proven to be even more incisive than the slope gradient in terms of reaction wood production (Duncker and Spieker, 2008), however during the sampling this factor was not considered, due to the difficulties to implement wind speed and direction into the sampling equation. After every extraction all the components of the increment borers were sterilised in order to minimise the chances of sample contamination.

2.3 Dendro lab analyses

2.3.1 Measuring

Once the samples were collected, a series of cuts was performed with a microtome, in order to remove the first few millimetres of the surface so that the annual rings became easier to be detected. Figure 9 shows the visual difference between an unprocessed (Figure 9a) and a processed (Figure 9b) tree core of Norway spruce. During this operation it is important that the blade cuts the wood fibres perpendicularly, so as to obtain a transversal cut of the wood cells, otherwise detecting the tree rings might become harder. This is an issue especially for broadleaves, in which the distinction between earlywood and latewood is not as pronounced as in coniferous. Furthermore, to obtain rings that are more easily discernible, the last performed cut has to be clean, leaving a smooth surface. This can be achieved with a blade as sharp as possible. The cores that were used for the LA-ICP-MS analysis were firstly analysed with the instrument and afterwards cut and measured. The procedure was inverted for this case only, and the main reason behind it is that we wanted to avoid as much contamination as possible.

2. Material and methods



Figure 9: Visual difference between an unprocessed (a) and a processed core (b) – two different samples are represented (own picture).

The ring width measurement of all samples was performed at the WSL laboratory (Birmensdorf, Switzerland), with the software Time Series Analysis Program (TSAPwin, RINNTECH, Heidelberg, Germany) to the closest 0.01 mm. For example, Figure 10 depicts the measured ring width of the trees sampled in site ON. The tree-ring width of Norway spruce trees were identifiable with minor hassle, except for a few rings. There are ways in which the readability of tree rings can be improved, such as sanding the surface of the core or applying chalk and water. However, these are not suited for the subsequent chemical analyses that are planned to be carried out, because wood powder or other substances could contaminate the tree rings leading to an erroneous outcome.

Due to changes in the environmental conditions, trees sometimes might develop intra-annual density fluctuations (IADFs), which are oscillations in the density of the wood (Battipaglia et al., 2016). These can appear in the form of earlywood cells within latewood and vice versa (Battipaglia et al., 2016). IADFs are a potential issue since, they might influence the measuring of the tree-ring width and the cross-dating (Battipaglia et al., 2016). Similar effects can also be caused by missing rings – MR (Novak et al., 2016). Therefore, to improve the accuracy of the tree-ring measurements it is often relevant to have a scrupulous look at the second core of each tree and check for clues of the presence or absence of IADFs and MR. Nonetheless, for this study, only one sample for each tree was measured prior to the chemical analyses, therefore the tree-ring width and the cross-dating values are based only on one measurement. The reason for this approach is that for the LA-ICP-MS analysis the samples have to be the least contaminated as possible. Thus, we decided to only measure one core

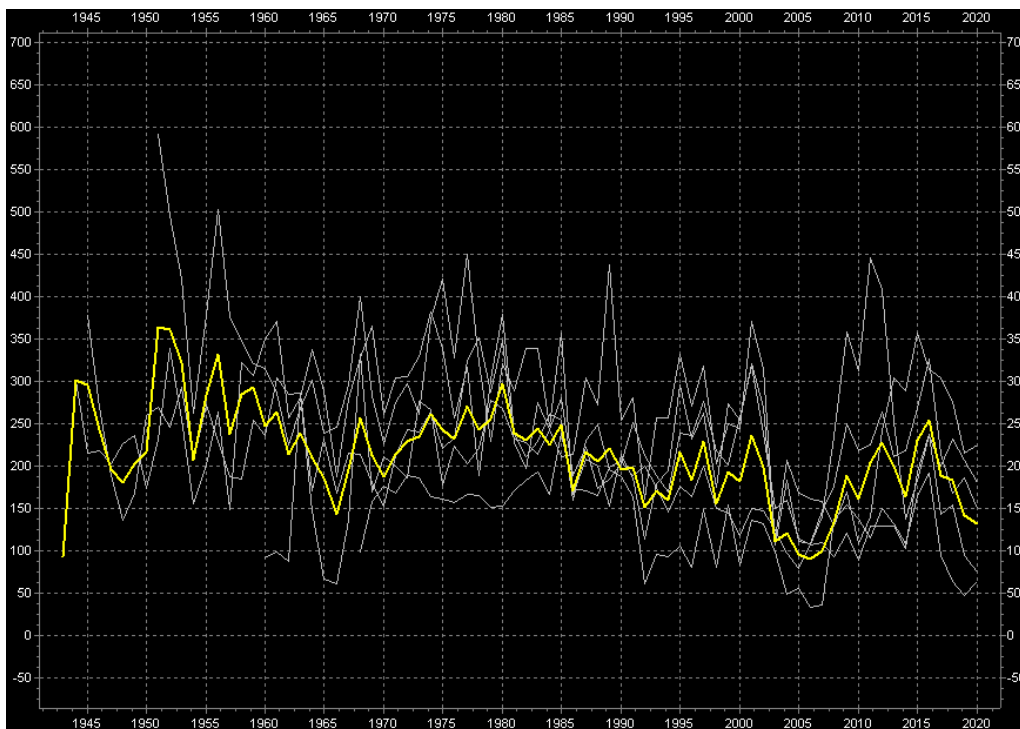


Figure 10: Measured tree ring width in mm^2 for the samples of site ON, with the site average highlighted (software: TSAPwin, RINNTECH, Heidelberg, Germany).

from each tree, so as to leave the other samples within their paper container and to avoid any possible contamination that could occur during the cutting and measuring phases.

2.3.2 Cross-dating and Gleichläufigkeit (GLK)

In order to be sure to have reliably dated the tree cores, these need to be cross-dated. Already in the first half of the 20th century Douglass (1941) stated that this method is aimed at the detection of identical patterns into different trees, so that the dates of the growth patterns can be determined. Tree rings have different widths, which are dependent on a multitude of external factors, spanning from the availability of nutrients to disturbances of various nature, such as wildfires, pollution or diseases. The width differences in consecutive tree rings creates a pattern which is often present in many other individuals laying in the proximity of the studied subject (Maxwell et al., 2011). However, in order to correctly identify and interpret the environmental features leading to a specific tree-ring width pattern, it is important to have a cross-date measure of high quality (Maxwell et al., 2011). If this is not the case, the investigators might face serious constraints in applying a time series approach, because it is not possible to reliably establish that the rings of the different trees under inspection originated in the same years. As stressed by Cutter and Guyette (1993), having a reliable cross-date is crucial for dendrochronological studies.

Given the aforementioned reasons, cross-dating has been defined as the fundamental principle of dendrochronology (Maxwell et al., 2011). Therefore, it is equally important to assess the quality of a cross-date. For this purpose, the so-called Gleichläufigkeit (GLK) technique has been developed. The GLK checks the level of coherence between the different tree-ring width chronologies and reports their level of concert between each other (Esper et al., 2008). The higher is the percentage of GLK, the more accurate the cross-dating is. The significance of the cross-dating can be afterwards statistically checked by means of a t-test.

2.3.3 Tree-ring width analysis

The tree-ring width can be influenced by the input of additional nitrogen into an ecosystem, since the vegetation is often limited by the quantity of N that is available (Evans, 2001). In contrast, when in an ecosystem N is readily available, the limiting factor is often identified in other substances, such as atmospheric carbon, i.e., CO₂ (Vallano and Sparks, 2007). The nitrogen that is absorbed by foliar uptake enters directly into the metabolism of the plant, making it thus readily available for the plants (Vallano and Sparks, 2004). Therefore, the abundance of NO_x for either short- or long-term promotes the increase of photosynthetic rates through the activation of carboxylation enzymes, which leads to a NO_x-induced fertilisation effect (Cherubini et al., 2021). Consequently, if the surplus of nitrogen is coupled also with higher quantities of CO₂, which allows for an increment of carbon sequestration rates, the plant is able to sustain its higher growth rates (Vallano and Sparks, 2007). This fertilisation phenomenon induced by pollution can potentially be witnessed in this investigation, given that nitrogen and carbon are both main by-products of the combustion of fossil fuels from vehicles engines (Saurer et al., 2004). For this reason, the tree-ring width curves of each site will be compared with the results of the nitrogen analysis, as well as the radiocarbon dilution, of the respective site.

The study of tree-ring growth, however, presents two main age-related issues (Sullivan et al., 2016). The first one is a geometric effect that is linked to the increase of the circumference of the stem. The produced biomass has to be distributed over a bigger area, and therefore the bigger the circumference becomes, the thinner the growth rings become. Secondly, there are physiological effects for which the trees tend to grow less as the age increases (Sullivan et al., 2016). Both of these aspects influence the radial dimension of the tree rings; thus, the most recent rings have a smaller diameter even if all the external factors affecting tree growth stay constant. Consequently, when comparing external effects with the growth of tree rings, it is important to remove the decreasing trend related to the growth of the tree (Sullivan et al., 2016). One of the most widely used method for detrending the age-related growth pattern, which is also used in this investigation, is the negative linear, or negative

exponential. It operates by fitting the raw measured individual ring width series (determined with TSAPwin, RINNTECH, Heidelberg, Germany) with either a horizontal line, a line with a negative slope or a negative exponential model, depending on the presence and form of the trend in the data (Sullivan et al., 2016). The values obtained after detrending are indexed and not absolute anymore. The negative exponential curve fits a model with the formula reported in Eq. (1), which is explained in detail by Bunn (2008):

$$G_t = ae^{-bt} + k \quad (1)$$

Where: G_t represent the growth trend and it is estimated as a function of time (t), with coefficients a , b and k (Bunn, 2008). The calculation was performed by using the R software (R core team, 2020), with the “d1pR” package and using the “detrend” function (Bunn et al., 2021).

Consequently, in order to avoid the influence on growth of age-related patterns, the results of nitrogen and radiocarbon analysis will be compared with the detrended growth curves.

2.4 Chemical analyses

Once the tree cores have been measured and cross-dated it is possible to proceed with the chemical analyses. The impact of air pollution at different sites, was assessed by measuring the tree-ring content of nitrogen isotope ($\delta^{15}\text{N}$), radiocarbon (^{14}C) trace/heavy metals.

2.4.1 Nitrogen isotope ($\delta^{15}\text{N}$)

The isotopic ratio of nitrogen ($\delta^{15}\text{N}/\delta^{14}\text{N}$) stored within tree rings can be used to track both the local climatic conditions (in terms of precipitation and temperature), as well as the past rates of fossil fuel's burning due to anthropogenic activities (Bukata and Kyser, 2007; Savard et al., 2007). The former will be represented in the results by short term fluctuations, as opposed to the latter which will be represented by long term ones (Bukata and Kyser, 2007; Savard et al., 2007). Typically, the use of nitrogen isotope in tree ring studies is a rather tricky technique to work with, because there are several issues that have to be overcome:

- 1) The distinction between the variations caused by natural fluctuations and the ones induced by anthropogenic activities is not straightforward, and it often represents a challenge for field studies (Savard, 2010). For this reason, Savard (2010) purposes the implementation of at least one out of four of the following techniques, in order to tell natural and anthropogenic fluctuations apart: i) Comparing the results obtained from trees in a control site with polluted trees – which is what was applied also for this project. ii) Applying statistical relationships and/or spatial trends to link case and effects of pollution levels with the variation of the isotopic ratio. iii) Comparing segments of the tree cores in which the rings were not affected by pollution with tree-rings exposed to pollution. iv) Implement a model to compare the natural isotopic changes on the base of pre-industrial times, with the measured values affected by anthropogenic forcing.
- 2) Trees do absorb nitrogen by both the roots as well as the foliar system (Binda et al., 2021; Saurer et al., 2004). The absorption of chemical elements from the soil tends to be problematic for dendrochronological studies focusing on the assessment of atmospheric conditions based on those elements (Binda et al., 2021). As a matter of fact, on the one hand, the signature of $\delta^{15}\text{N}$ in the soil is subject to the phenomenon of isotopic fractionation – i.e., the separation between lighter and heavier isotopes in a natural system (Tiwari et al., 2015), such as ^{14}N and

2. Material and methods

^{15}N –, which occurs during the processes of nitrification, denitrification and mineralisation (Guerrieri et al., 2009).

On the other hand, the year of deposition in the soil is not the same as the one in which the element is taken up by the roots, hence when nitrogen is absorbed in this way there is a possible dissonance of several years between the concentration shown in the tree rings and the atmospheric one (Binda et al., 2021).

- 3) In addition of the issues created by the bimodal absorption of nitrogen, a relevant problem for most trace elements, and nitrogen as well, is represented by the lateral transport of nitrogen within stem wood (Bukata and Kyser, 2007). It has been proven that when the converting process of sapwood to heartwood is taking place, trees are able to retrieve the nitrogen from the dying cells (Saurer et al., 2004). This mechanism shifts the concentration of nitrogen between neighbouring rings, and therefore it does not allow to use the $\delta^{15}\text{N}$ isotope ratio method for studies aiming at results having an annual resolution (Savard, 2010; Saurer et al., 2004). However, if annual resolution is not required, and consequently adjacent years can be merged for the sake of the analysis, the technique is applicable (Saurer et al., 2004).
- 4) The $\delta^{15}\text{N}$ value of emission produced by anthropogenic activities can show considerable variations depending on the source from which it has been emitted (Amman et al., 1999). In addition, according to Savard (2010), the depletion or enrichment of $\delta^{15}\text{N}$ is usually dependent on the isotopic fractionation and the signature of the anthropogenic nitrogen stored in the soil. For these reasons, the influence of anthropogenic N can usually be detected by either an increase or decrease of the $\delta^{15}\text{N}$ ratio within the tree rings (Savard, 2010; Stewart et al., 2002).

A general consensus among the researchers, suggesting that $\delta^{15}\text{N}$ can have the potential to be a relevant indicator for local pollution studies using tree rings, seems to be prevalent (Amman et al., 1999; Bukata and Kyser, 2007; Saurer et al., 2004; Savard et al., 2009; Savard, 2010; Stewart et al., 2002). However, issues have been encountered in its application as evidenced by the study of Battipaglia et al. (2010), where the method was employed to track traffic pollution in an urban area. In fact, they inferred that the results were too complicated to interpret, because the measured nitrogen isotope value varied greatly between trees and even over time (Battipaglia et al., 2010). Thus, in those circumstances $\delta^{15}\text{N}$ was not suitable to draw any sort of conclusions. Instead, the nitrogen isotope analysis was successfully employed in two studies aiming to reconstruct the local pollution history near a motorway in Switzerland using tree rings of Norway spruce (Amman et al., 1999; Saurer et al., 2004). According to Amman et al. (1999) the $\delta^{15}\text{N}$ value contained in fossil fuel is close to 0. The positive $\delta^{15}\text{N}$ value that they have found (+5.7‰) in their study near a motorway is to be reconnected to local conditions – i.e., traffic density, engine types (light versus heavy duty), and the combustion regimes that these engines have in average (Amman et al., 1999).

Saurer et al. (2004) affirmed in their study that despite the high $\delta^{15}\text{N}$ level of variation of both the natural background concentration as well as the once produced by traffic, the positive signature found, in terms of ‰, can be unequivocally linked to the nitrogen dioxide (NO_2) emitted by engine vehicles. In the case of Norway spruce, when nitrogen is absorbed through the foliar system, the process of metabolization of $\text{NO}_2 - \text{N}$ takes place in the needles, and afterwards nitrogen migrates to the stem in form of amino acids or nitrate (Saurer et al., 2004). There, the living cells use it as a storage compound or for structural purposes in order to create lignin polymers (Saurer et al., 2004). However, the nitrogen taken up by the needles in form of NO_2 cannot be consistently found throughout the tree core, its detection is rather intermittent (Saurer et al., 2004). Thus, it is possible that this behaviour is to be reconnected to a regulation mechanism of the tree, which depending on the availability of nitrogen in the environment, it either uses the element, or stores it in reserves (Saurer et al., 2004). The results obtained by Amman et al. (1999) and Saurer et al. (2004) show that, by investigating the nitrogen

2. Material and methods

isotope signal, it is possible, at least for Norway spruce, to track the local history of pollution emitted by engine exhausts.

Stewart et al. (2002) and Bukata and Kyser (2007) successfully implemented the technique in the Americas, in the south as well as in the north, Brazil and Canada, respectively. In both studies however, they reported that the nitrogen isotope ratio had constantly decreased over the years (Stewart et al., 2002; Bukata and Kyser, 2007). This difference with the other studies conducted by Amman et al. (1999) and Sarurer et al. (2004) might be to be reconduct to the fact that the studies in Switzerland were carried out in close proximity with a motorway. In contrast, Stewart et al. (2002) conducted the study in the extremely polluted industrial area of Cubatão in São Paulo State (Brazil), and Bukata and Kyser (2007) in seven Canadian cities (Burlington, Kingston, L. Opinicon, Murray Brook, North Bay, Peterborough). Thus, the four studies have different sources of N, vehicular traffic versus industrial plants (Guerrieri et al., 2009).

2.4.1.1 $\delta^{15}\text{N}$ analysis procedure

Once the tree cores were measured and cross-dated, the preparation of the samples began. A total of 9 cores were selected, 3 for each site (OU, ON and CT). For the $\delta^{15}\text{N}$ analysis, substances that might interfere with the analysis have to be separated from the tree cores by means of the Soxhlet Extraction technique, which is a common pre-treatment method for analysis in the environmental field (de Castro and Ayuso, 2000). In this case it was employed in order to discard the N-compounds that could be extracted (Saurer et al., 2004). During the process the samples were placed in a permeable holder that was then inserted into the chamber of the Soxhlet apparatus which was afterwards filled with solvent and water. Once the chamber was full, and the overflow level was reached, the liquid, containing the removed material, was drained through a syphon that led the liquid to a round-bottom distillation flask. The liquid in the distillation flask was then heated and started start to slowly fill the chamber once again, repeating the whole process until the extraction was finished (de Castro and Ayuso, 2000). After the cleaning process with the Soxhlet apparatus, the rings were cut vertically into very thin slices (up to 1 mm thick) with a scalpel. All the slices were separated into groups of 5 years adjacent to each other, such as 2020 to 2016, 2015 to 2011 and so on, until 1971 included. In the case of $\delta^{15}\text{N}$ analysis, there are multiple reasons for which it is useful to not only analyse a single year but rather a cluster of them. Firstly, the amount of material required in order for the analysis to work is 10 mg, which for a single annual ring might be difficult to reach. Secondly, the signal of nitrogen tends to translocate over the adjacent year rings, therefore by measuring multiple years it is possible to tackle signal dilution and still retrieve information about the temporal variation of the $\delta^{15}\text{N}$ signal (Saurer et al., 2004).

The chosen clusters of years for the analysis are:

- 1) 1976 to 1980 is located at the beginning of the temporal scale of this research and it should represent the conditions in which the local government started to seriously take in consideration the idea of constructing the new Prättigauerstrasse.
- 2) 1990 to 1995 is the period before the construction work started, and it should also represent the last moment in which the pollution levels between site OU and site ON are similar.
- 3) 1995 to 2000 is in the middle of the temporal scale of the study and it is also placed during the first section of the construction work of the bypass road. Thus, it is supposed to be representative for the concentration of the atmospheric pollutants during the roadworks.
- 4) 2006 to 2010 represent the period after the opening of the Prättigauerstrasse – which took place in December 2005 –, therefore the traffic volumes are expected to have adjusted with the new option as before the beginning of the construction works.

- 5) 2016 to 2020 is located at the end of the study's temporal scale and is supposed to represent the current situation in terms of atmospheric pollution.

The thin sliced-core sections arranged in period of 5 years were grinded and milled into a very fine powder and collected again in their respective vials. From the vials, 10mg of wood powder were measured and tightly enclosed into a tin capsule, which were finally sent into the Stable Isotope Laboratory at the WSL Birmensdorf, for the $\delta^{15}\text{N}$ analysis. The process for the analysis is similar to the one described by Saurer et al. (2004). The tin capsules containing the samples were combusted into an elemental analyser (Iso Earth, Secron, Crewe, UK) and consequently the amount of $\delta^{15}\text{N}$ was measured with an isotope ratio mass spectrometer (Iso Earth, Secron, Crewe, UK).

2.4.2 Radiocarbon (^{14}C)

From the year 1000 until 1880 the global concentration of carbon dioxide (CO_2) in the atmosphere remained at a constant level (Rakowsky et al., 2010). However, with the industrial revolution, more and more quantities of fossil fuel began to be combusted each year, leading to a steady and incremental growth of CO_2 in the atmosphere (Henrique and Borowiecki, 2017). Many conferences were held in an attempt to curb the emissions, however, despite the several pledges and promises by various world powers, the concentration of CO_2 in the atmosphere is still rising nowadays (Gupta, 2010). During the mid-20th century, the emissions of carbon dioxide were around 5 billion tons per year while by the end of the century the emission were seven times higher at about 35 billion tons (Lindsay, 2020). In 2019 the concentration of CO_2 in the atmosphere reached 409.8 parts per million, a number that in 800'000 years had never been reached (Lindsay, 2020).

All the CO_2 that has been released from its solid form (i.e., fossil fuel), represents the so-called radioactively "dead" carbon; namely carbon that does not contain the radioactive isotope (^{14}C) anymore (Battipaglia et al., 2010; Djuricin et al., 2012). The reason behind it is that the age of the deposits of fossil fuel is extremely high ($\gg 50'000$ years), especially in comparison to the decaying rate of radiocarbon (Battipaglia et al., 2010; Capano et al., 2010; Rakoswky et al., 2008), which is roughly 5'730 years (Djuricin et al., 2012). In contrast, the isotope ^{14}C is present in the natural carbon dioxide of the atmosphere – i.e., CO_2 that is not emitted by the combustion of fossil fuels (Djuricin et al., 2012; Rakowsky et al., 2010). Therefore, in locations where the emissions of CO_2 are extremely high, the presence of the radiocarbon isotope is low in comparison to its stable counterparts, or as Rakoswky et al. (2008) state, ^{14}C is missing. This effect in which the "clean," i.e., natural air (containing ^{14}C) is mixed with the polluted one (^{14}C -free) resulting in lower concentrations of radiocarbon is known as Suess effect (Rakowsky et al., 2008). Despite the fact that the vast majority of carbon dioxide (around 95%) is released in the northern hemisphere, the influence of the Suess effect is observable in both the hemispheres (Rakowsky et al., 2010), as it is shown in Figure 11. The reason for the ubiquitous presence of the Suess effect is that the air masses of north and south hemispheres are not physically separated and therefore are subject to mixing (Rakoswky et al., 2010). Hence, in every study area around the globe, there are usually two major factors affecting the ^{14}C concentration; i.e., the Suess effect and the local emissions of carbon dioxide (Rakoswky et al., 2010).

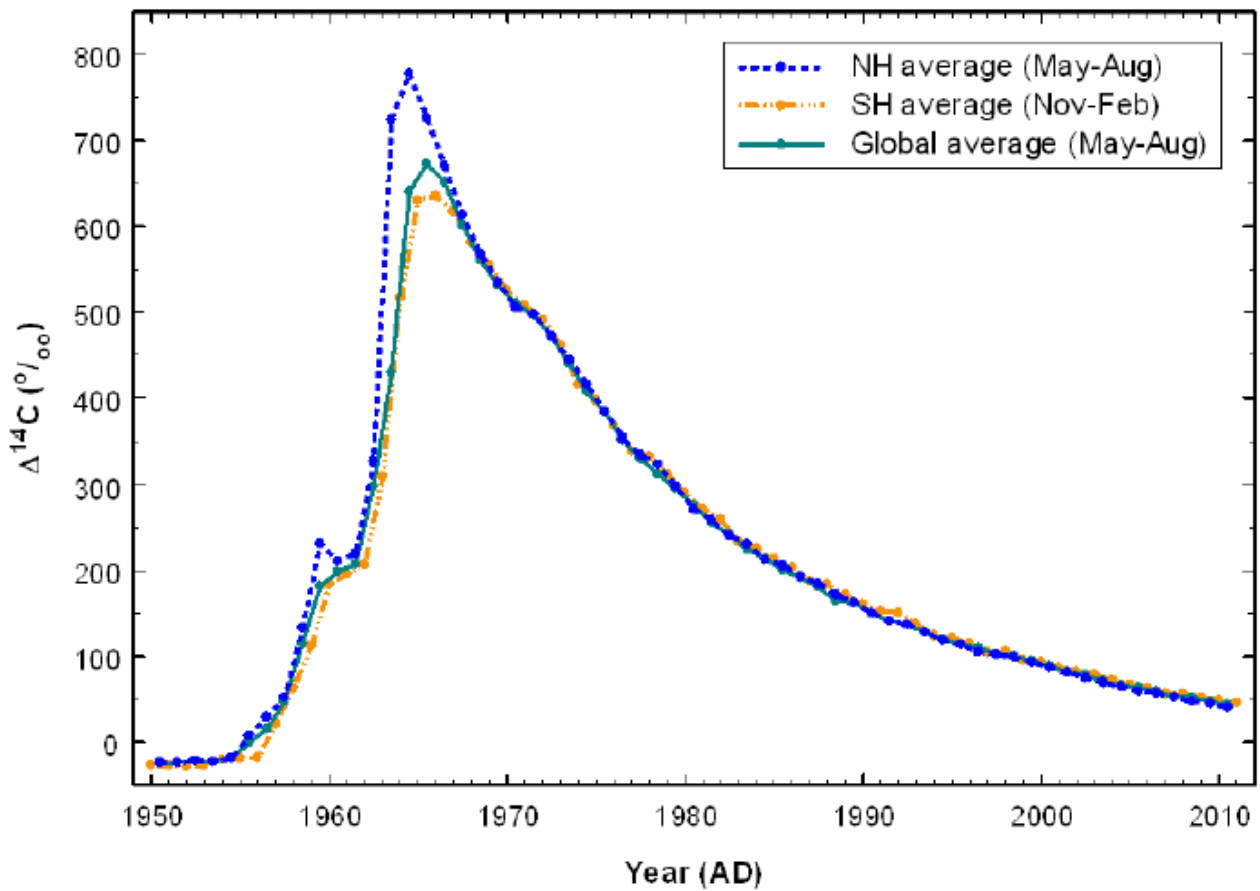


Figure 11: $\Delta^{14}\text{C}$ (‰) in the atmosphere for both North and South hemisphere showing the “bomb spike” of the 1960s’ (source: Hua et al., 2013).

The ^{14}C curve describing the concentration of the isotope in the atmosphere, does not present a regular decreasing pattern as it should be expected, due to the constantly increasing emissions of “dead” isotopes. In contrast, as it is shown in Figure 11, there is a sudden increase during the 1950s’ and 1960s’, with a subsequent exponential decrease. The reason for this behaviour is to reconduct to the several nuclear tests that took place during the mid-20th century, which involved the detonation of atomic bombs (Battipaglia et al., 2010; Rakowsky et al., 2008; Rakowsky et al., 2010). The explosions released neutrons having enough thermal energy in order to produce ^{14}C (Rakowsky et al., 2008). This resulted in a sudden and extremely marked growth of radiocarbon concentration in comparison to the periods previous of the tests (Battipaglia et al., 2010). The peak concentration was reached in the mid-60s’ (Rakowsky et al., 2008), and it started to decrease exponentially ever since (Battipaglia et al., 2010), creating the so-called “bomb spike” (Clarke et al., 2012) – the highest concentration peak. The rapid decrease of ^{14}C concentration following the pinnacle is to reconduct to both the Suess effect, as well as exchanges of carbon dioxide present in the atmosphere with the terrestrial and oceanic reservoirs (Battipaglia et al., 2010; Capano et al., 2010).

Like with trace metals and nitrogen, trees do absorb CO_2 from the atmosphere to sustain their metabolic functions (Sala et al., 2012) and thus, they store the current atmospheric ratio of $^{14}\text{CO}_2/^{12}\text{CO}_2$ for each year in the wood tissue of the respective annual ring (Battipaglia et al., 2010; Capano et al., 2010). Thanks to this behaviour, it is possible to estimate the emission generated by the combustion of fossil fuels by making a comparison of the annual radiocarbon concentration of the study site with the local background concentration of trees not influenced by polluting sources

2. Material and methods

(Battipaglia et al., 2010). According to Battipaglia et al. (2010), this technique is well suited to track the local pollution history of heavily polluted environments, since $\Delta^{14}\text{C}$ have shown to be particularly responsive to changes in emissions derived by fossil fuels. During the last decades, several investigations (Battipaglia et al., 2010; Capano et al., 2010; Djurcin et al., 2012; Pietrowska et al., 2019; Rakowsky et al., 2008; Rakowsky et al., 2010) successfully employed the $\Delta^{14}\text{C}$ method coupled with dendrochronology to assess the track of the presence of anthropogenic pollutants in the environment.

2.4.2.1 ^{14}C analysis procedure

For the ^{14}C analysis, similarly to the $\delta^{15}\text{N}$, nine tree cores were selected, six of these were extracted in sites OU and ON (i.e., 3 from each site), whereas the remaining 3 were collected in the control site (site CT). Upon discussion with the technician of the laboratory where the samples were measured – at the Laboratory of Ion Beam Physics, of the ETH Zurich – it was agreed to retrieve the concentration of radiocarbon from five meaningful years for the project. The selected years were: 1980, 1994, 2000, 2008 and 2018. The reasoning behind the decision was similar to the one explained for the $\delta^{15}\text{N}$ years clusters in the subchapter 2.4.1.1.

In the laboratory of the ETH the samples were prepared for the $\Delta^{14}\text{C}$ analysis similarly to the procedure reported in the paper of Sookdeo et al. (2020). In order to minimise the contamination during the measurements, blank, standards and reference material samples were added to the already present field samples (from site OU, ON and CT). Two types of blanks were added, the first one was a chemical blank, Phthalic Anhydride, while the second ones, processed blanks, were fossilised wood – which sometimes is also referred to as brown coal – as well as kauri wood (Sookdeo et al., 2020). Oxalic acid I and Oxalic acid II were used as standards (Sookdeo et al., 2020), whereas as a reference material a recent segment of wood, in terms of age, was used.

The cellulose was extracted from all the samples from the field, the reference material and the process blanks by means of a chemical treatment (Sookdeo et al., 2020) known as base-acid-base-acid-bleaching – BABAB (Němec et al., (2010)). Due to its property to not mutate over time, cellulose makes for a suitable candidate to retrieve an accurate measure of $\Delta^{14}\text{C}$ (Sookdeo et al., 2020). In order to accomplish this process, a BABAB technique similar to the one described by Němec et al. (2010) was followed. Firstly, the materials (field samples, reference material and processed blanks) were inserted into glass vials, soaked into 5ml of base (Sodium hydroxide – NaOH) and stored overnight at 60 °C. Secondly, the morning of the successive day the base was removed from all the vials which were subsequently washed using ultrapure water and filled with 3ml of acid (Hydrochloric Acid – HCl) for 1 hour at 65 to 70 °C. Afterwards, the vials were washed with ultrapure water and the first step was repeated, however the temperature was set between 65 and 70 °C and only for 1.5 hours. Right after, the solution was again removed and the vials cleaned with ultrapure water, so as to repeat the second step, but this time only for 15 minutes at the same temperature. Lastly, after the cleaning round with ultrapure water, the samples were bleached by means of a solution containing 5% of NaClO₂ (Sodium Chlorite) and 0.1 ml of HCl at 0.5 molar concentration, for 2 hours at 70 °C. Once the samples have been bleached the vials were emptied of the solution for the last time and were stored into a freeze dryer overnight. After the cellulose extraction process was over, 2.5-3 mg of material were weighted and separated from the wood samples, in order to be confined into aluminium capsules, that were moulded as spherically as possible. Samples, standards, reference material and blanks were then inserted into an elemental analyser, where with the help of O₂ gas the carbon present was combusted to CO₂ and trapped into a zeolite trap (Sookdeo et al., 2020). This process was repeated for each sample one at a time, and it is known as graphitisation (Sookdeo et al., 2020). Subsequently the graphitised material was pressed into aluminium cathodes (Ionplus) that were

correctly sorted and placed into a magazine so as to be analysed on a MICADAS (mini carbon dating system – Ionplus) located in the Laboratory of Ion Beam Physics at the ETH-Zürich. Once the latter analysis was completed the concentration of $\Delta^{14}\text{C}$ of the samples was finally measured.

2.4.3 Laser Ablation-Inductively Coupled Plasma-Mass Spectrometry (LA-ICP-MS)

The idea of the LA-ICP-MS as an analytical technique started to develop during the 1980's (Günther and Hattendorf, 2005; Kim et al., 2020). It was created by combining a direct sampling method, i.e., a laser beam, with the ICPMS – the most sensitive analyser for elements (Binda et al., 2021). Ever since its conception, the implementation of LA-ICP-MS investigations have been growing in a wide array of scientific fields (Günther and Hattendorf, 2005; Kim et al., 2020). Although in recent years the domain of geochemistry has seen the most extensive use of this technology (Günther and Hattendorf, 2005), already in the 1990's there had been a few studies which began to explore and apply the method also in the dendrochemical field, such as Garbe-Schönberg et al. (1997), Hoffmann et al. (1994) and Prohaska et al. (1998). As a matter of fact, the technique is highly versatile and allows to not only analyse rock samples, but biological tissues as well – trees included (Zyskowski et al., 2021). Owing to the fact that the LA-ICP-MS is able to detect almost every element present within the target sample, including heavy/trace metals, it is regarded as an extremely powerful instrument also in terms of reach (Binda et al., 2021). The only elements of the periodic table that cannot be analysed with this method are nitrogen, oxygen, phosphorus, sulphur, and fluorine (Binda et al., 2021). In addition to the wide range of components that can be investigated, the technique features several benefits also from an analytical perspective; i) In most cases no pre-treatment of the samples is required (Bardule et al., 2020; Prohaska et al., 1998; Zyskowski et al., 2021). ii) It is micro-destructive (Bardule et al., 2020; Zyskowski et al., 2021). iii) The risks of contamination during the analysis (Bardule et al., 2020; Prohaska et al., 1998; Zyskowski et al., 2021), as well as the loss of volatile elements, are minimal (Bardule et al., 2020). iv) It provides a two-dimensional map of the distribution of heavy metals throughout the samples (Bardule et al., 2020). v) Lastly, it yields high spatial resolution (Bardule et al., 2020; Perone et al., 2018; Prohaska et al., 1998; Zyskowski et al., 2021), even with low signal of pollutants within the tree material. The LA-ICP-MS is regarded in the scientific community as a viable and interesting option due not only to its analytical advantages, but also thanks to the fact that its functioning is relatively simple, making it a painless and efficient tool (Günther and Hattendorf, 2005).

The whole operating process is well explained in the scientific paper written by Günther and Hattendorf (2005). Firstly, the samples need to be fixed to the samples' holder so that all their surfaces are at the same height and cannot move; the aim here is to have them all equally distant from the laser extruder in the ablation process, so that the laser focus is the same for every measurement. Once the samples are immovable, the holder is inserted into the airtightly closed ablation chamber. Afterwards the chamber is filled with either helium or argon, which serves as main carrier for the ablated material. The laser beam, after being fired over the surface of the target, will start to ablate the material, creating a mixture of gas, agglomerates and particles that will be conducted to the plasma section of the instrument. In the ICP phase the ablated material is vapourised, atomised and ionised, so that in the next step it can be separated and analysed in the mass spectrometer (Günther and Hattendorf, 2005). The detecting process is regulated by the property of the laser used for the investigation. All the factors regarding the laser, such as the spot size (which directly correlates with the amount of material that gets ablated) duration of the ablation, as well as frequency, wavelength and energy of the light pulse have an influence in constraining the detection (Binda et al., 2021). By increasing the spot size, it is possible to relax these constraints. As a matter of fact, the resolution is directly dependent on it; the bigger the diameter of the pulse, the more mass will be ablated, and the more elements can be

2. Material and methods

analysed. Vice versa, by decreasing the spot size, in addition to the fewer detectable elements, the analysis time can become excessively longer. However, it seems that in the recent literature there is still no consensus on the maximal value. Binda et al. (2021) affirm that dimensions over 100 μm are never used in analysis concerning tree rings. Instead, Kim et al. (2020) state that recent studies have been carried out using spot sizes ranging from 1 to 200 μm .

One of the main drawbacks of the LA-ICP-MS is the presence of elemental fractionation (Günther and Hattendorf, 2005) which, in this case, it is caused by a thermal alteration on the surface of the ablated sample, induced by the laser (Pozebon et al., 2014). This phenomenon can occur if the large particles are not fully vaporised by the beam (Mokgalaka and Gardea-Torresdey, 2006) and it represents an obstacle when trying to acquire quantitative results about the signal of elements (Pozebon et al., 2014). The fractionation is influenced by the pulse of the laser, duration of the ablation, spot size and power used (Pozebon et al., 2014). The intensity of the effect depends on the target material, and it appears to be particularly pronounced for metals and geologic materials; nonetheless it can affect also biological tissues (Pozebon et al., 2014). The problem can be partially mitigated (especially for inorganic samples) by decreasing the thermal alteration of the sample through the employment of shorter wavelengths as well as shorter laser pulses (Mokgalaka and Gardea-Torresdey, 2006; Pozebon et al., 2014), and by using helium as a main carrier gas (Günther and Hattendorf, 2005).

2.4.3.1 LA-ICP-MS analysis procedure

Considering the high sensitivity level of this method, the tree cores require to be handled as carefully as possible in order to minimise the chances of contamination. Hence, the tree samples, once extracted with the increment borer, were immediately placed within their paper holder, where they rested until the day of the analysis at the at the laboratory of the Institute of Geochemistry and Petrology (ETH, Zürich, Switzerland). A total of 6 Norway spruce cores were measured. Three from site OU, three from site ON. Owing to the fact that the ablation chamber has a limited dimension of roughly 10 x 15 cm, in order to fit all the cores without having to split them into two pieces, the shortest ones were selected. Despite minor inconvenience, for which a few cores required to be cut, they were all able to fit into the holder of the ablation chamber. The 6 samples were analysed in one run of the instrument. For the purpose of the current research, the heavy metal signal of the tree rings at intervals of 5 years was measured. Starting from 2018, and going back 45 years, until 1973, a total of 10 measurements per each core was performed. A total of 20 elements (Bi, Ca, Cd, Co, Cr, Cu, Fe, Hg, Mn, Mo, Ni, Pb, Pd, Pt, Rh, Sn, Ti, Tl, V and Zn), which are mainly involved in the pollution caused by road traffic were analysed. The specification parameter of the laser used for this investigation are almost the same as the ones applied in the study of Perone et al. (2018). The differences between their and this investigation lay in the flow of the helium carrier gas transporting the ablated material to the next section of the instrument, and the crater size of the laser. In this study, the former was set at a rate of 0.5 l/m, and for the latter a crater spot size of 163 μm was used.

Before each measurement, a cleaning round with the laser was performed so as to have the surface of the samples as clean as possible from contamination. The latewood region of the tree ring was ablated, since during the dormancy phase of the tree, the translocation of the elements should be less prominent than in the earlywood (Hagemeyer et al., 1994), which is the stage of vegetative growth. The measuring process with the spruce samples was quite straightforward, although the cores were utterly unprocessed and left in the same condition as they were right after the extraction, the annual rings were easily detectable. This allowed for a precise aiming of the laser beam on the sample surface, directly at the latewood section of the desired year.

2.4.3.2 LA-ICP-MS Data normalisation

Due to the fact that trace metals are present in the environment at very different quantities and are not taken up in equal quantities by the trees, the elemental signal within different trees might display important fluctuations. Thus, the data needs to be normalised so that different elements coming from different trees can be compared. Consequently, the data obtained were normalised according to the process described by Bukata and Kyser (2008), which was also employed in more recent studies performed using the LA-ICP-MS technique over tree rings, such as Perone et al. (2018). Each element in each tree ring was normalised according to Eq. (2):

$$N_x = \frac{(S_x - S_l)}{(S_h - S_l)} \quad (2)$$

Where: S_x is the normalised value for the target year, S_x is the signal measured by the LA-ICP-MS for the target year, S_l is the lowest signal found in the tree core and S_h is the highest signal found in the tree core. The resulting values are comprised between 0 and 1, with the lowest and highest values at the extremes (0 and 1 respectively) and all the others in between (Bukata and Kyser, 2008).

2.4.3.3 LA-ICP-MS Statistical analyses

Two statistical analyses were performed over the average time series of each element:

- 1) The Mann-Kendall test (M-K test) is generally used to detect monotonic trends in the data, either increasing or decreasing. In this context, the M-K test was performed so as to check if the trace metal signal in the two sites do follow a similar pattern. If it is the case, then it may be possible to assume that the temporal evolution of the signal of that specific element is dependent on factors affecting both sites, and therefore not site specific.
- 2) The Pettitt test is often used in environmental sciences when working with time series analysis. Its main function is to locate change points, which can occur in the form of the beginning of a linear trend, the change of a trend or an abrupt change of the mean throughout the series (Rybski and Neumann, 2011).

3 Results

3.1 Nitrogen results

3.1.1 $\delta^{15}\text{N}$ signal

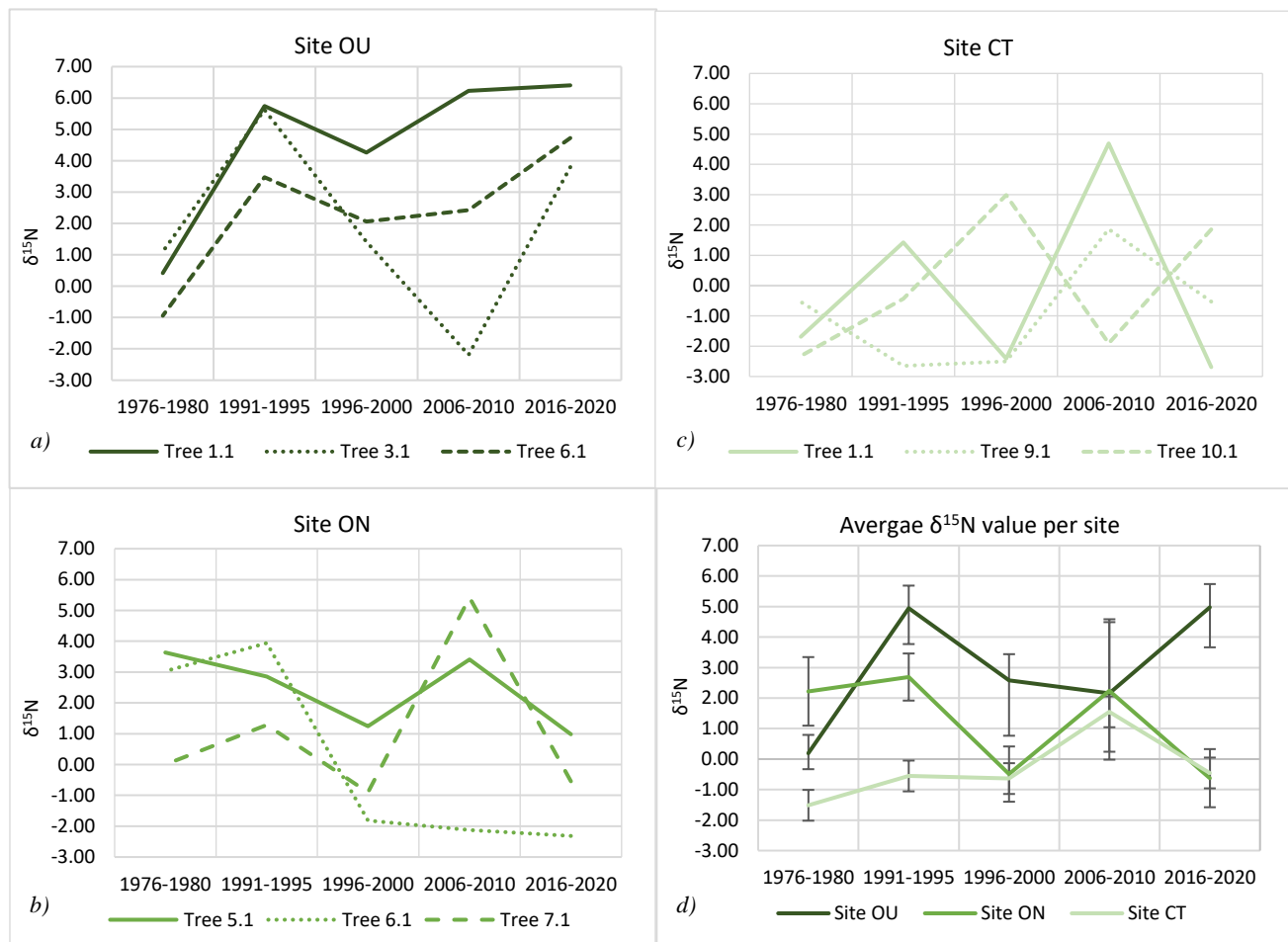


Figure 12: $\delta^{15}\text{N}$ value of 5-years clusters for sites OU (a), ON (b), CT (c), and the comparison of average values between sites (d) – \pm SE.

Figure 12 represents the concentration of $\delta^{15}\text{N}$ of 5-years clusters for sites OU (a), ON (b) and CT (c), as well as the comparison of the average $\delta^{15}\text{N}$ value of each site (d). The graphs show that there is no site having all the trees with exactly the same pattern. Site OU appears to be the one with the most coherence, however in the lustrum 2006-2010 there is a value substantially lower for the Tree 3.1 (Figure 12a). The results of site ON are similar, since, in the same period, Tree 6.1 displays a particularly low value when compared with the other samples (Figure 12b). The control site (CT) appears to be the one presenting the most confused signal with no easily identifiable pattern in the data (Figure 12c). By looking at the averages of the sites (Figure 12d), CT displays the lowest value of $\delta^{15}\text{N}$. Surprisingly, starting from the lustrum 1996-2000, the measured value for site ON becomes very similar to site CT, for all the most recent measurements. Nevertheless, a t-test performed to determine the statistical significance of the points' similarities, disproved the equality of the means ($P > 0.05$). Site OU seems generally to be the one with the highest $\delta^{15}\text{N}$ values. It is interesting to notice how in the period 2006-2010, the average $\delta^{15}\text{N}$ measured for site OU is similar to the ones of the other two sites, however in the most recent lustrum, the curves diverge considerably, the former reaches a $\delta^{15}\text{N}$ value of almost 5, while site ON and CT drop to -0.5.

3. Results

3.1.2 N-concentration

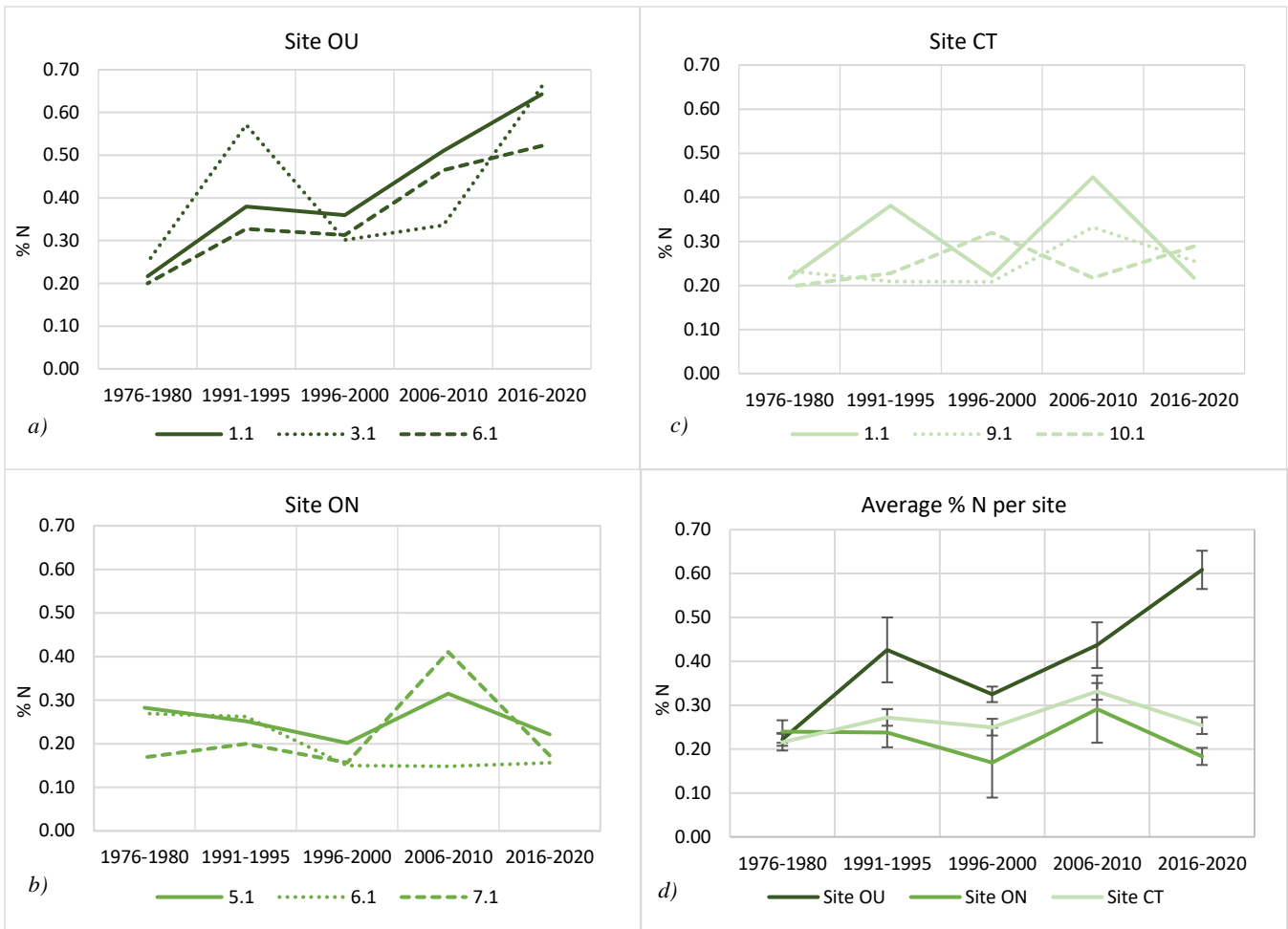


Figure 13: Nitrogen concentration [% N] of 5-years clusters for sites OU (a), ON (b), CT (c), and the comparison of average values between sites (d) – \pm SE.

Figure 13 shows the measured concentration of nitrogen [% N] within the tree rings of the 5-years clusters. The situation appears to be fairly similar to the one for $\delta^{15}\text{N}$, meaning that there is not exactly equal pattern among the measurements of the trees from the same site. The samples from site OU appears to have again a quite similar pattern, except for Tree 3.1, which on one occasion especially, the period 1991-1995, reports a higher measurement (0.57), almost the double compared to site Tree 6.1 (0.33) and Tree 1.1 (0.38) (Figure 13a). Fairly similar are also the measures reported for site ON (Figure 13b). Site CT exhibit again a quite confused signal without patterns (Figure 13c). Among the average measurements per site (Figure 13d) the lowest values are recorded mostly in site CT, whereas the highest ones in site OU. In this case however, there seems to be a more coherent average value between all the sites, except for the lustrum 2016-2020, where like in Figure 12d, a divergence is displayed, with site OU showing an increase while site ON and CT a decrease.

3.1.3 Reconstructed $\delta^{15}\text{N}$ - NO_x signal

With the available data from the nitrogen isotope analysis, it is possible to display the relationship between the $\delta^{15}\text{N}$ value with the N-concentration (Figure 14a). Figure 14a shows that for each site, there is a non-linear relationship between the concentration of nitrogen in the tree rings and the $\delta^{15}\text{N}$ value. The graph (Figure 14a) indicates that higher concentration of nitrogen often does also correspond to elevated $\delta^{15}\text{N}$ values. The relationship is particularly strong for site ON and CT, which

3. Results

have an elevated R^2 value of 0.93 and 0.88 respectively. As carefully explained in the study presented by Saurer et al. (2004), by assuming that the nitrogen taken up by the trees comes from only two sources (i.e., the soil, which is considered as the background concentration, and the one that is emitted from the exhausts of vehicles' engines) the two-members mixing model of Figure 14b can be created.

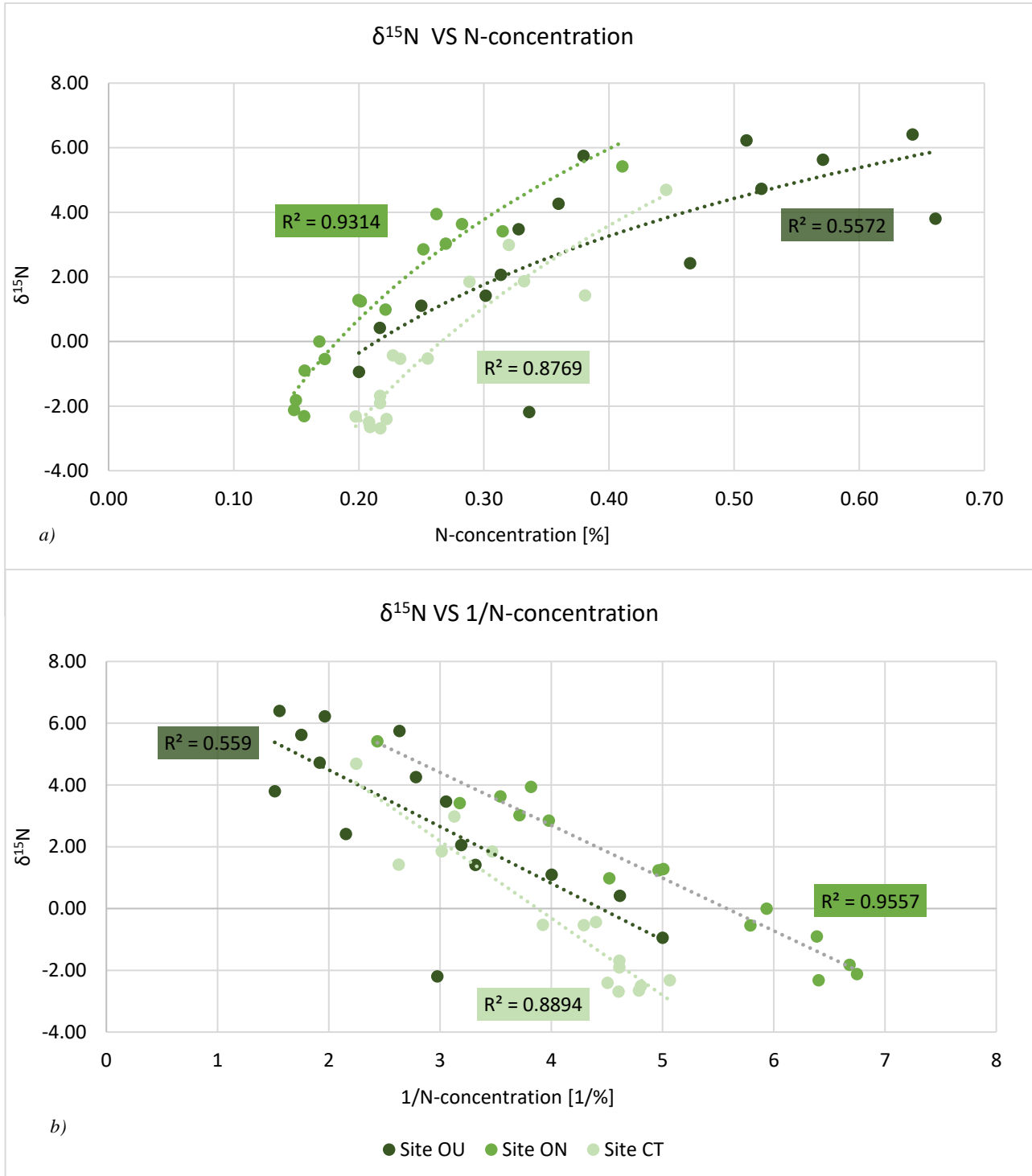


Figure 14: The relationship between $\delta^{15}\text{N}$ value and N-concentration measured in the tree rings (a), and the relationship between $\delta^{15}\text{N}$ value with 1/N concentration (b).

3. Results

For all the sites there is a strong linear relationship between $\delta^{15}\text{N}$ and the inverse of the N-concentration, showing an R^2 of 0.56 for site OU, 0.90 for site ON and 0.96 for site CT (Figure 14b). From the graph in Figure 14b it is possible to retrieve the average $\delta^{15}\text{N}$ value of the emissions that can be reconducted to nitrogen oxides (NO_x), since this value is represented by the y-intercept of the curves (Saurer et al., 2004). The method can then be extended and applied to each time period (1976-1980, 1991-1995, 1996-2000, 2006-2010, 2016-2020) of every site. Thus, every point shown in Figure 15, corresponds to the y-intercept value of the regression line created by the relationship between the $\delta^{15}\text{N}$ value and 1/N-concentration from 3 data point from the 3 measured trees per site. Figure 15 represents the $\delta^{15}\text{N}$ - NO_x value originating from emissions. The signal for site ON appears to be rather stable throughout the whole measured period, and it could suggest that here the polluting source is the same for each 5-year cluster, or that the polluting sources have different signatures of $\delta^{15}\text{N}$ - NO_x , but their proportions either do not change or the variations eventually balance out at a similar value. The frequent fluctuations in site CT instead could indicate that there are different polluting sources affecting the location, making the signal unstable, as opposed to site ON. The biggest excursions in terms of $\delta^{15}\text{N}$ - NO_x value are reported by site OU. The sharp drop between the clusters 2006-2010 and 2016-2020 where the $\delta^{15}\text{N}$ - NO_x value shifts from 19.9 to 5.6‰, is particularly striking. This fluctuation could be interpreted as a change in the major polluting sources in site OU.

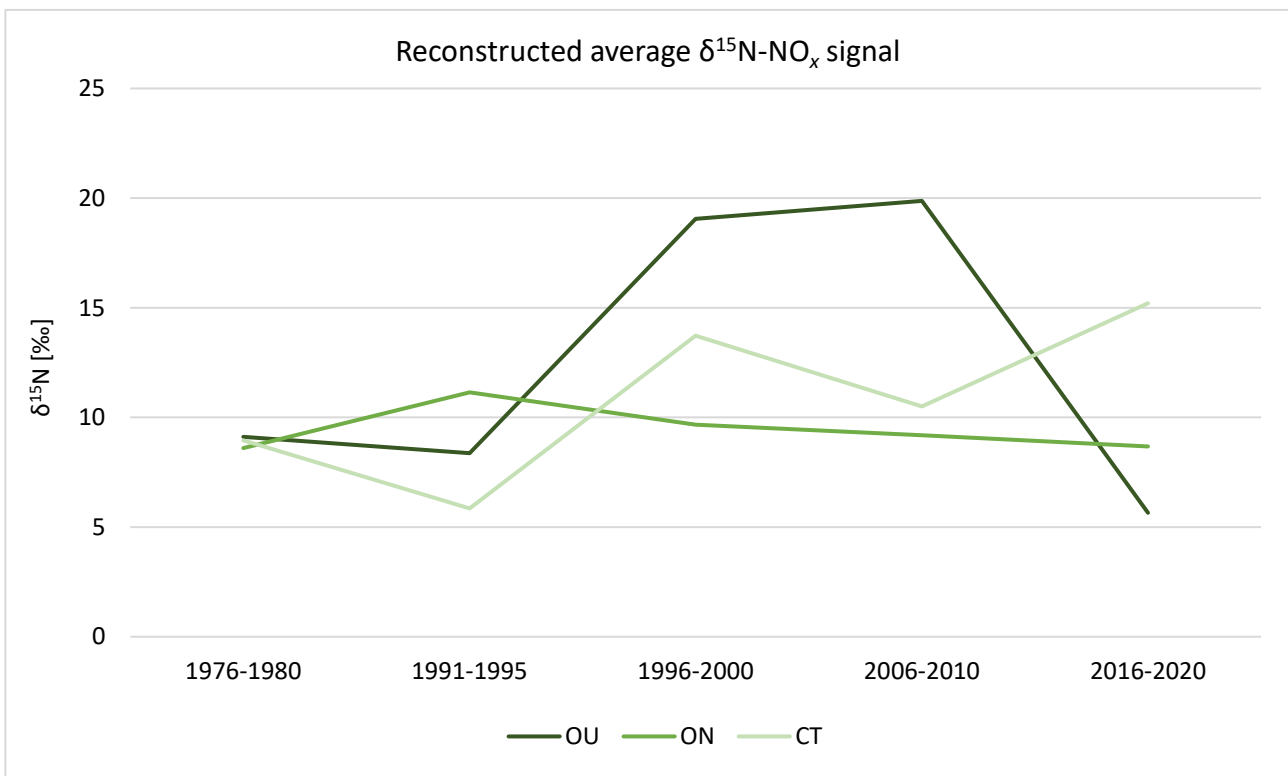


Figure 15: Reconstructed average $\delta^{15}\text{N}$ - NO_x signal per site.

3.2 Radiocarbon results (^{14}C)

3.2.1 Measured $F^{14}\text{C}$ values and local dilution effect

The data of the radiocarbon analysis are presented in the form of $F^{14}\text{C}$, which means that the ^{14}C activity was corrected for $\delta^{13}\text{C}$ and normalised to the standard of modern biosphere. Although $\Delta^{14}\text{C}$ is a very useful measure for geochemical studies and pre 1962 samples, for post-bomb samples the use of $F^{14}\text{C}$ (i.e., fraction modern) is advised (Reimer et al., 2004; Stenström et al., 2011). The main issue related with $\Delta^{14}\text{C}$ is that it will yield different results if a sample that was formed or grown in 1962, is measured today versus if it was measured in 1962 (Reimer et al., 2004). In contrast, $F^{14}\text{C}$ is not dependent on the measurement year and does not change over time (Stenström et al., 2011).

The $F^{14}\text{C}$ analysis was performed on 3 Norway spruce trees for each site, so as to obtain 3 measurements per year per location. Subsequently an average value for each year (1980, 1994, 2000, 2008 and 2018) at every site was calculated – the datapoint laying outside of the $\pm 2\sigma$ interval were not included in the average. The obtained results are visualised in Figure 16 – for the analysis the latewood was selected, therefore, the datapoints in the graphs are slightly shifted on the right, since they represent the summer months. The site averages were overlaid on the $F^{14}\text{C}$ curve from the data gathered by Levin and Kromer (2004) at 3450 m a.s.l. in the high-altitude research station located on the Jungfrauoch, in the Swiss Alps.

Figure 17 represents the dilution effect at the three sites. The dilution effect shows the difference, in %, in terms of radiocarbon concentration between the measured values at the three sites and the background (“clean air”) concentration, measured at the Jungfrauoch station.

3. Results

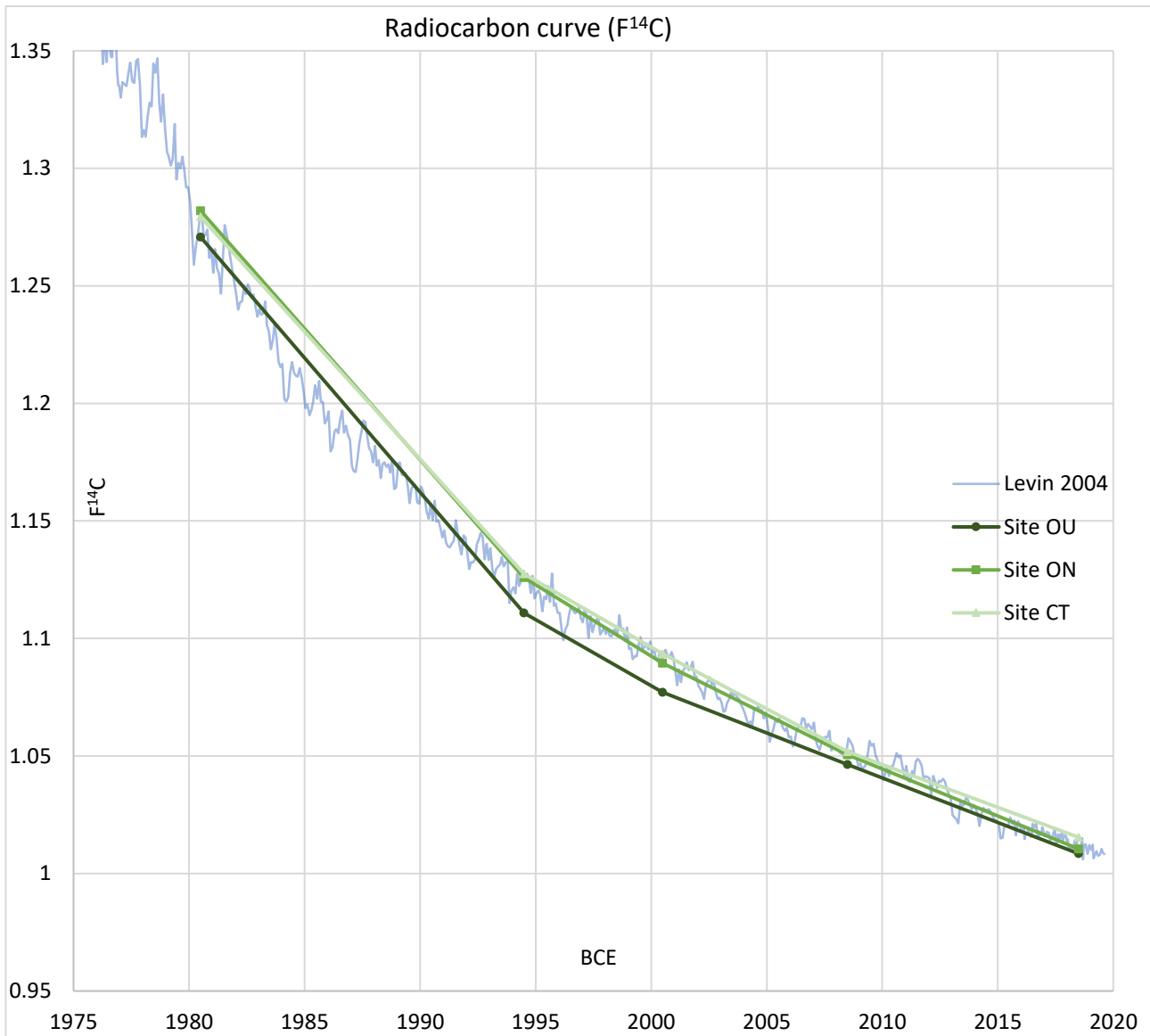


Figure 16: Average $F^{14}C$ concentrations for sites OU, ON and CT are represented and overlaid on the Jungfraujoch data gathered by Levin and Kromer (2004).

Lower $F^{14}C$ values, indicate that in the tree rings, and consequently in the atmosphere, there is a higher concentration of ^{12}C . Thus, where the $F^{14}C$ signal in the experimental sites is lower in Figure 16, which is also reflected by a higher dilution level in Figure 17, it can be concluded that a local Suess effect is taking place.

This in turn suggests that the effect is presumably promoted by the presence of one or more polluting sources emitting radioactively dead carbon, possibly from the combustion of fossil fuels. This condition seems to apply to site OU for every measured year, given that its $F^{14}C$ value is consistently lower than the reference level. Site ON instead, does not show any sign of local Suess effect, until the year 2000, in which it is possible to see the begin of a minor dilution effect. These signs could reflect the construction of the bypass road and its opening in late 2005. Site CT presents mostly small fluctuation around 0% and with a relatively high standard error, except for year 2008, where there seem to be a slight dilution in $F^{14}C$ concentration. Overall, the values for the control site are reasonable since it is located more than 4 km away from the two main roads. What is particularly surprising is the magnitude by which site OU is consistently more polluted than site ON.

3. Results

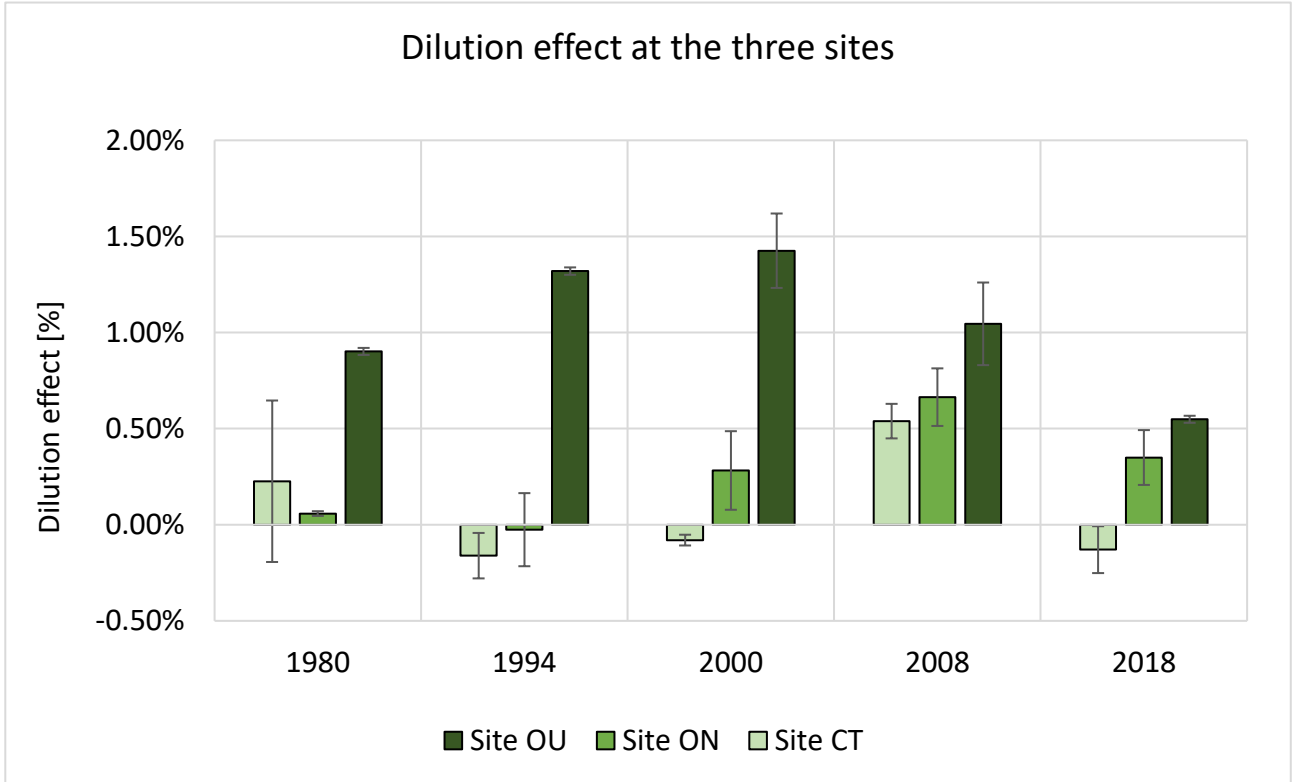


Figure 17: Dilution effect in % at site OU, ON and CT (\pm SE).

3.2.2 Fossil fuel CO₂ component

The quantification of the emissions produced by the burning of fossil fuels (CO_{2foss}) at a local scale is a relevant measure for assessing its impact on a local Suess effect (Battipaglia et al., 2010; Levin et al., 2008; Rakoswky et al., 2008). The calculation of CO_{2foss} is explained in detail by Levin et al. (2008) and can be estimated through Eq. (3):

$$CO_{2foss} = CO_{2meas} \frac{\Delta^{14}C_{bg} - \Delta^{14}C_{meas}}{\Delta^{14}C_{bg} + 1000\%} \quad (3)$$

Where: CO_{2meas} is the atmospheric CO₂ concentration in ppm, $\Delta^{14}C_{bg}$ is the background radiocarbon concentration from an unpolluted site, and $\Delta^{14}C_{meas}$ is the radiocarbon concentration measured at the experimental sites. Thus, in this investigation, for the atmospheric CO₂ concentration the corresponding data collected at Mauna Loa by Keeling et al. (2001) are used. Instead, for the $\Delta^{14}C_{bg}$ the Jungfraujoch data is used since it is the best radiocarbon reference for sites located in south/western Europe (Levin et al., 2008). The main reason is that the atmosphere at the Jungfraujoch measuring station is believed to not be influenced by any local Suess effects (Piotrowska et al., 2019). Consequently, it can best represent the global scale influences of ¹⁴CO₂ sources and sinks such as stratosphere–troposphere exchange at this latitude and release of bomb ¹⁴CO₂ from the terrestrial biosphere (Levin et al., 2008). The suitability of the data from the Jungfraujoch is also confirmed by the fact that all the collected samples at each site were checked with the Pearson correlation coefficient and all show a very high r value (> 0.99) with a high significance level (P << 0.01).

Eq. (3), however, requires the use of $\Delta^{14}C$ data, and not F¹⁴C, thus the measurements have to be transformed into $\Delta^{14}C$ via Eq. (4), which details are explained by Plicht and Hogg (2006):

3. Results

$$\Delta^{14}C = 1000 * [(F^{14}C * e^{-\lambda(Ti-1950)}) - 1] \quad (4)$$

Where: λ is the decay constant for the ^{14}C isotope, i.e., 8267 yr^{-1} ; and Ti is the calendar year in which the measured tree ring was formed.

By means of Eq. (3) and Eq. (4), it is possible to create Figure 18, which shows the fossil fuel CO_2 component emitted per site. Figure 18 shows that there is a clear influence of pollution from fossil sources in the last decades, predominantly in site OU, but also in site ON, although minorly. The CO_{2foss} results however do not describe the patterns that were hypothesised according to the development of the traffic situation in Klosters. As a matter of fact, by comparing year 2018 of Figure 18 with Figure 17 it appears that there is a discrepancy in the results, for the sites OU and ON. On the one hand, Figure 16 highlights a very strong increase in CO_{2foss} for 2018 compared to 2008 (+406.6% for site OU and +408.2% for site ON). On the other hand, Figure 17 shows that there is a decrease in $F^{14}C$ dilution for the same periods (-52.1% for site OU and -52.3% for site ON), suggesting a weakening of the locals Suess effects.

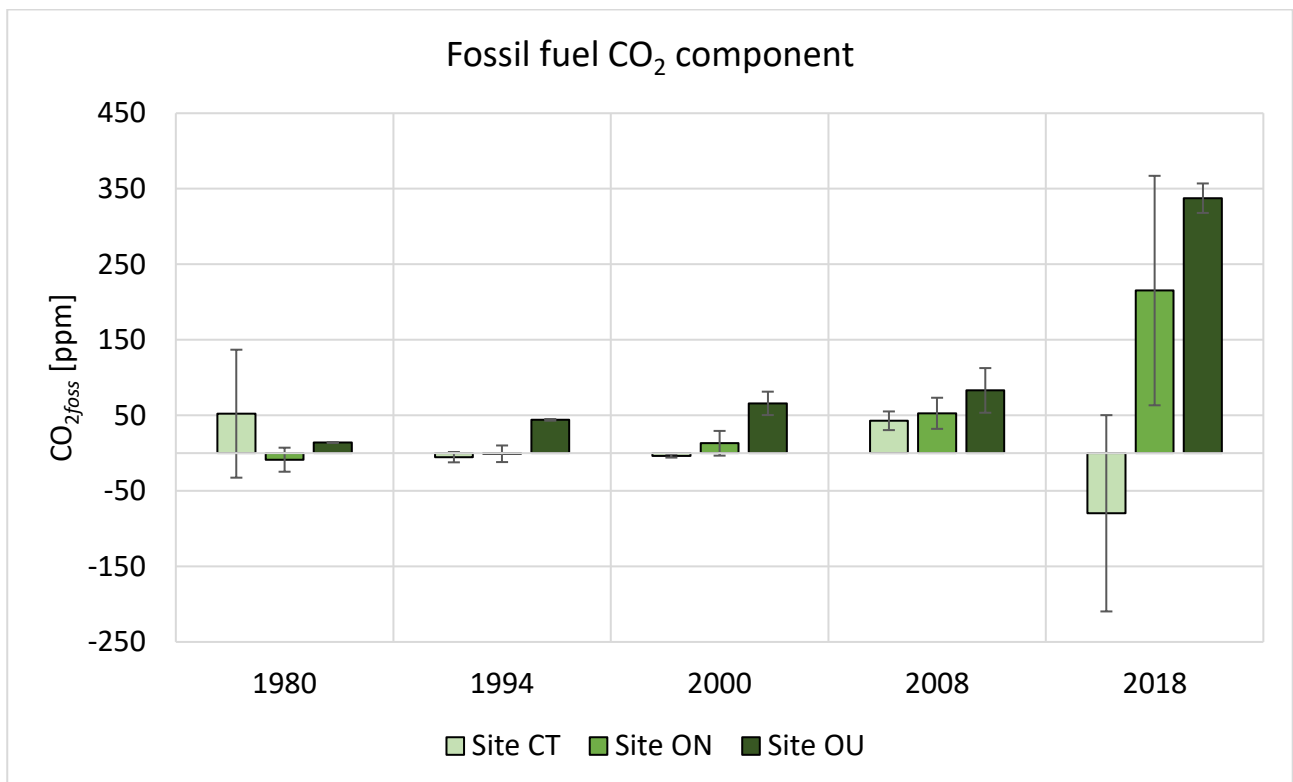


Figure 18: Estimation of fossil fuel CO_2 component per site ($\pm SE$).

3.3 LA-ICP-MS results

3.3.1 Measured heavy metals

Out of the 20 elements that were measured with the LA-ICP-MS, only 9 (Ca, Cr, Cu, Hg, Mn, Mo, Pb, Ti and Zn) were considered in the evaluation of the results. The signal of the elements that were excluded (Bi, Cd, Co, Fe, Ni, Rh, Sn, Th, Pd, Pt, V), was below their limit of detection (LOD). The results obtained from the LA-ICP-MS are intrinsically complicated and their signals are time-dependent (Longerich et al., 1996). The quantity of the material that is ablated from the sample is not constant between each analysis, but rather, it oscillates significantly. Therefore, it is required to calculate a new LOD for each analysis (Longerich et al., 1996). In this study, the LOD for each element was calculated according to the procedures illustrated by Longerich et al. (1996), and subsequently compared with the signal measured for each analysis. Thus, all the measurements whose elemental signal was lower than the LOD were discarded. The only elements kept are those that have a higher signal than the respective LOD for all 6 tree rings, for each of the 10 measurements. The majority of the elements discarded recorded a lower signal than their LOD for all the tree rings in every tree core. Fe and Cd have 2-3 measurements that were not admissible for each core, however the elements were discarded anyway so as to not further complicate the evaluation of the results.

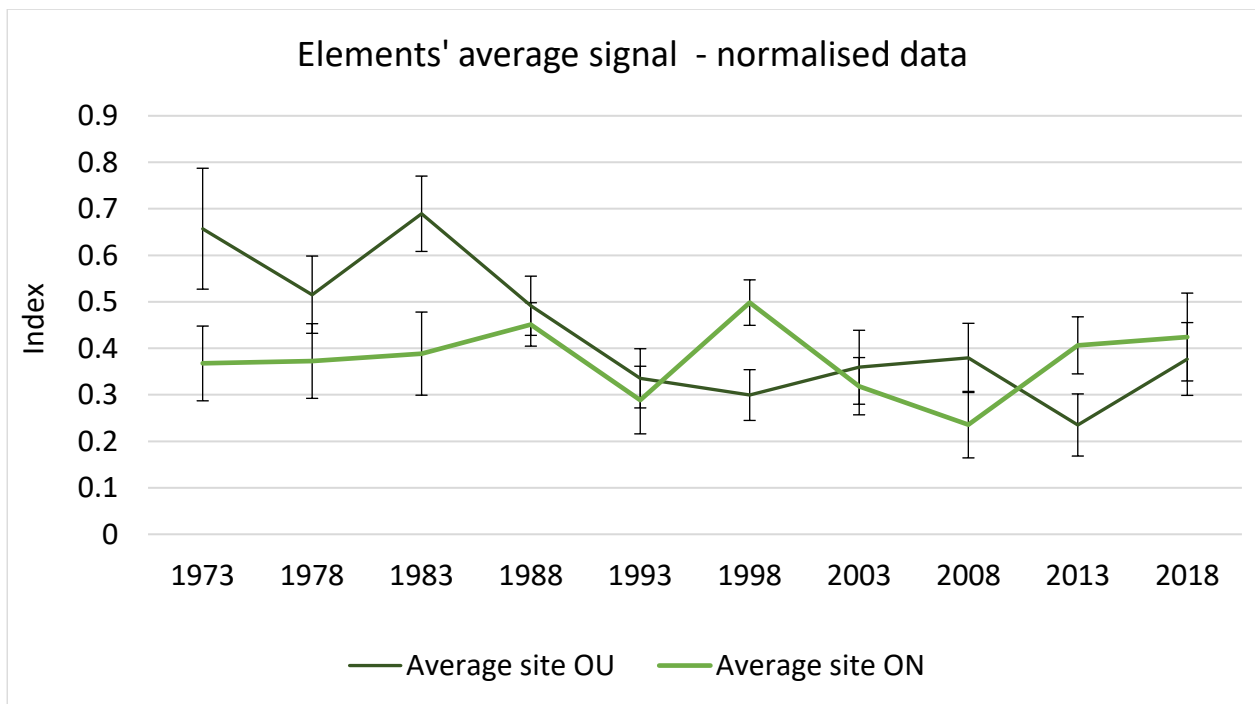


Figure 19: Comparison between site OU and site ON of the average normalised signal of all the considered elements (Ca, Cr, Cu, Hg, Mn, Mo, Pb, Ti and Zn – \pm SE).

Figure 19 depicts the average signal of all the elements in site OU and ON. The curve for site OU shows higher values until 1983 where a marked decrease is presented until 1993. From 1998 to 2008 there is a slight increase, followed by a drop in 2013. These findings are possible to be reconducted to the main events that took place in Klosters, i.e., the construction of the bypass road and its successive opening to the traffic. Even though there is a peak in 1998 which corresponds to the road work and higher pollution rates than site OU for 2013 and 2018, the curve for site ON appears to be more enigmatic to interpret. The lowest value is reached in 2008, when the area is supposedly polluted

3. Results

by the roadworks and the increased traffic rates. However, as the error bar show, there is an important quantity of uncertainty in the data, making the interpretation harder.

Cd, Cr, Hg, Pb and As (arsenic) are often considered as priority heavy metal, because of their accumulation in the environment and extremely toxic consequences for the living beings (Tilako et al., 2020). In Switzerland the monitoring of priority heavy metals is focused on Cd, Hg and Pb (Bass et al., 2021). Their indexed signals found with the LA-ICP-MS in site OU and ON are shown in Figure 18. The graph for Cd is not present because its detected signal is often lower than its LOD for the majority of the measurement. Thus, since such collected data are unreliable, Cd was omitted. In Figure 20a is represented the normalised average signal of Pb for sites OU and ON. The most peculiar behaviour is shown in site OU, where the Pb signal drastically drops from 1978 and stays on low levels for the whole period. In site ON instead the signal shows important oscillations with peaks in 1988, 1998 and 2013. It is important to notice that the average for site OU was calculated with only 2 datapoints per year, since the measures of Tree 3.2 were omitted. Tree 3.2 was excluded because it recorded extremely high values in comparison to the other trees, by several folds. This enrichment phenomenon was also recorded for Mn – the comparison with Tree 3.2 is visible in the graphs of Pb (Figure 38) and Mn (Figure 34) in the Appendix (the values for Tree 3.2 are recorded on the secondary y-axis, on the right side of the graph). Tree 3.2 is the only tree core for which all the measurements of Cd were higher than its LOD by a considerable amount – comparable to the other two anomalies in elemental signal in Tree 3.2 for Pb and Mn. Figure 20b depicts the normalised average signal of Hg, which in comparison with Pb is more similar among the sites. The main differences are to be found in year 1998, where the signal decreases for site OU and increases for site ON. Moreover, before 1998 the index is lower for site ON and higher for site OU. Instead, afterwards, site OU becomes the one the lower values and vice versa. Overall, the index value of Hg suggests that there is an increase of the element over time.

3. Results

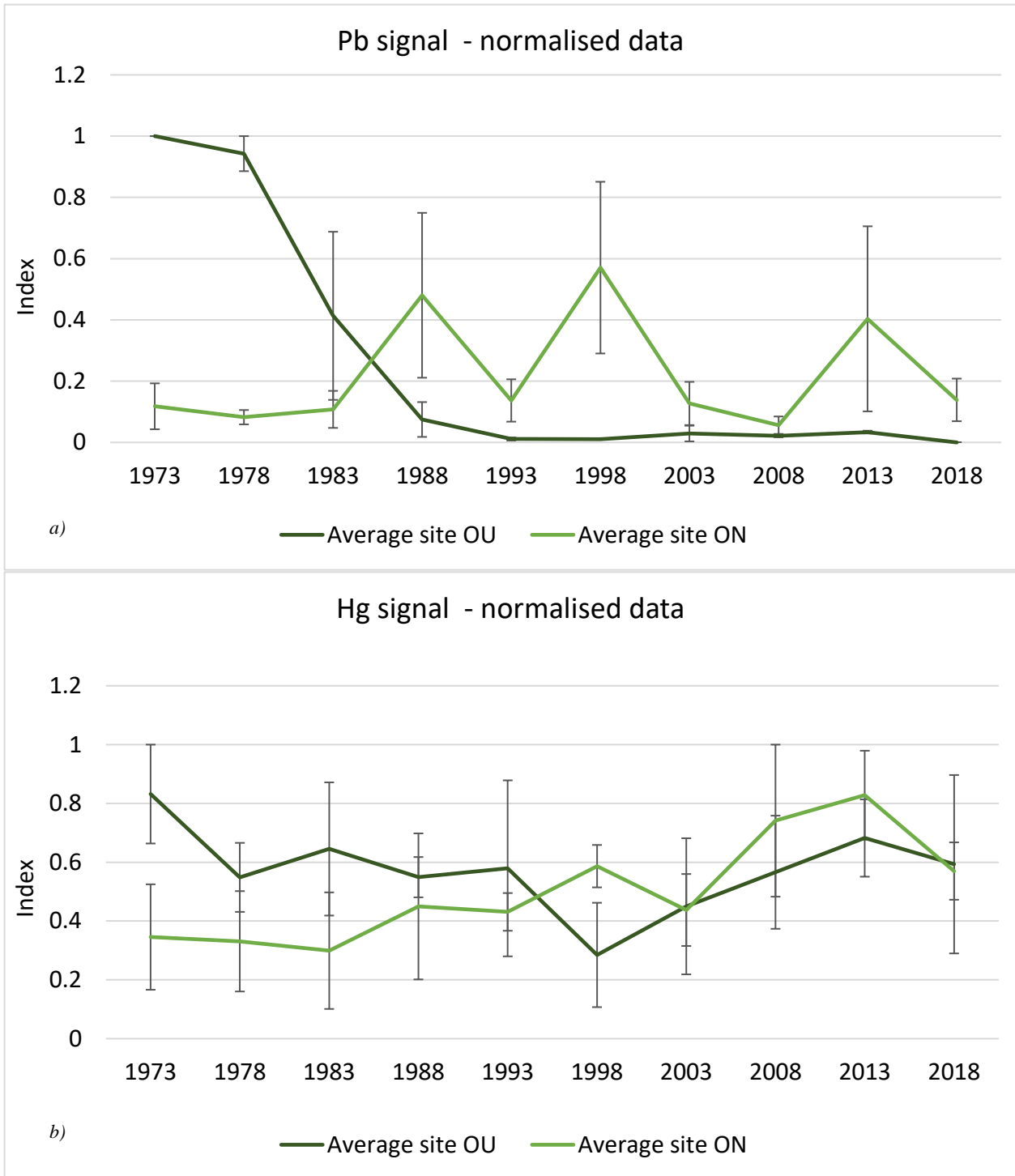


Figure 20: Normalised average signal per site for the elements Pb (a) and Hg (b) ($\pm SE$).

3. Results

Despite the practical advantage of normalisation, and the potential interpretation issue presented by the use of raw data (i.e., non-normalised), these can still be useful to compare the signals of the same elements that are found in the two sites, in order to see where higher pollution rates are found (all the graphs can be found in the Appendix, with normalised and raw values). A good example of the utility of raw data is the signal of Cr (Figure 21). The signal of Cr for the two sites appears to be relatively stable over time without showing any major fluctuation. In this case site ON records consistently higher values than site OU.

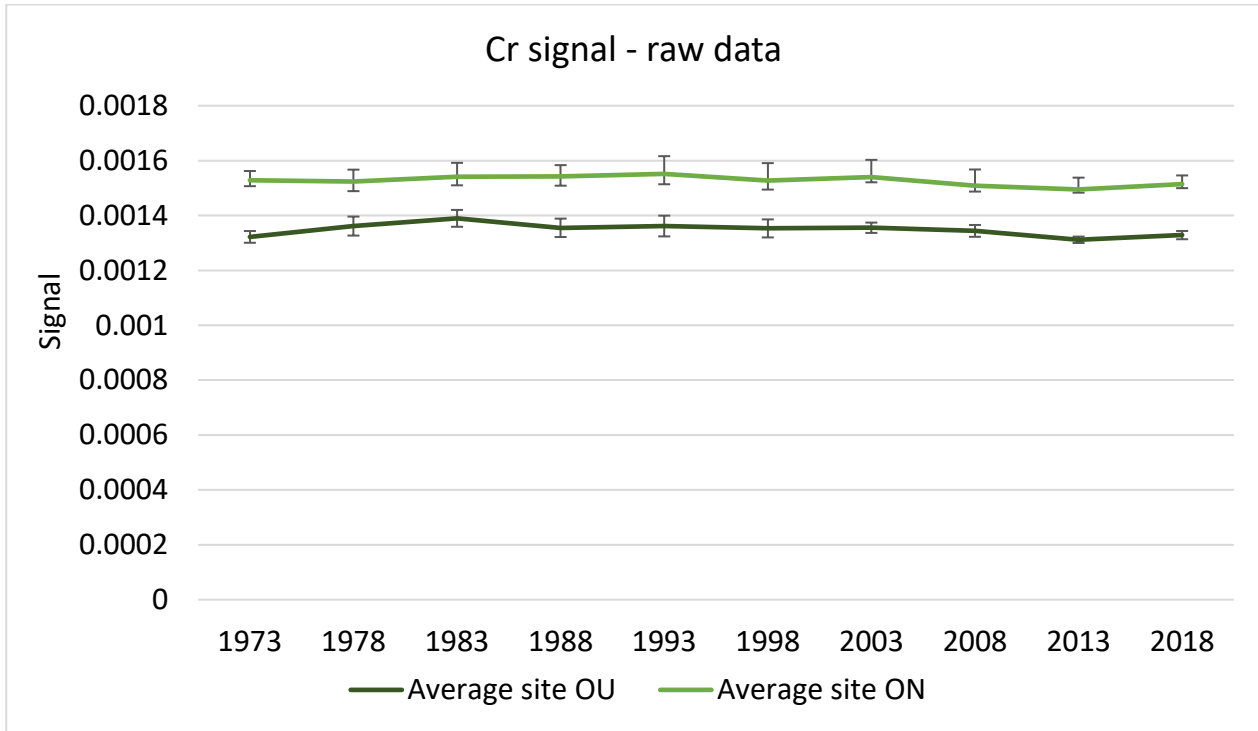


Figure 21: Raw average signal per site for the element Cr ($\pm SE$).

3. Results

Figure 22 depicts the normalised average signal of Mn (Figure 22a) and Ca (Figure 22b). Both the elements present an overall decreasing trend. For site ON the index value of Ca and Mn is particularly similar. The Mann-Kendall test confirmed that the two curves (for site ON) do have a similar monotonic trend with a Tau of 0.689 ($P < 0.01$). In contrast, the monotonic trend for site OU is not statistically significant as opposed to site ON, but it is present nonetheless, with a Tau value of 0.511 ($P > 0.05$).

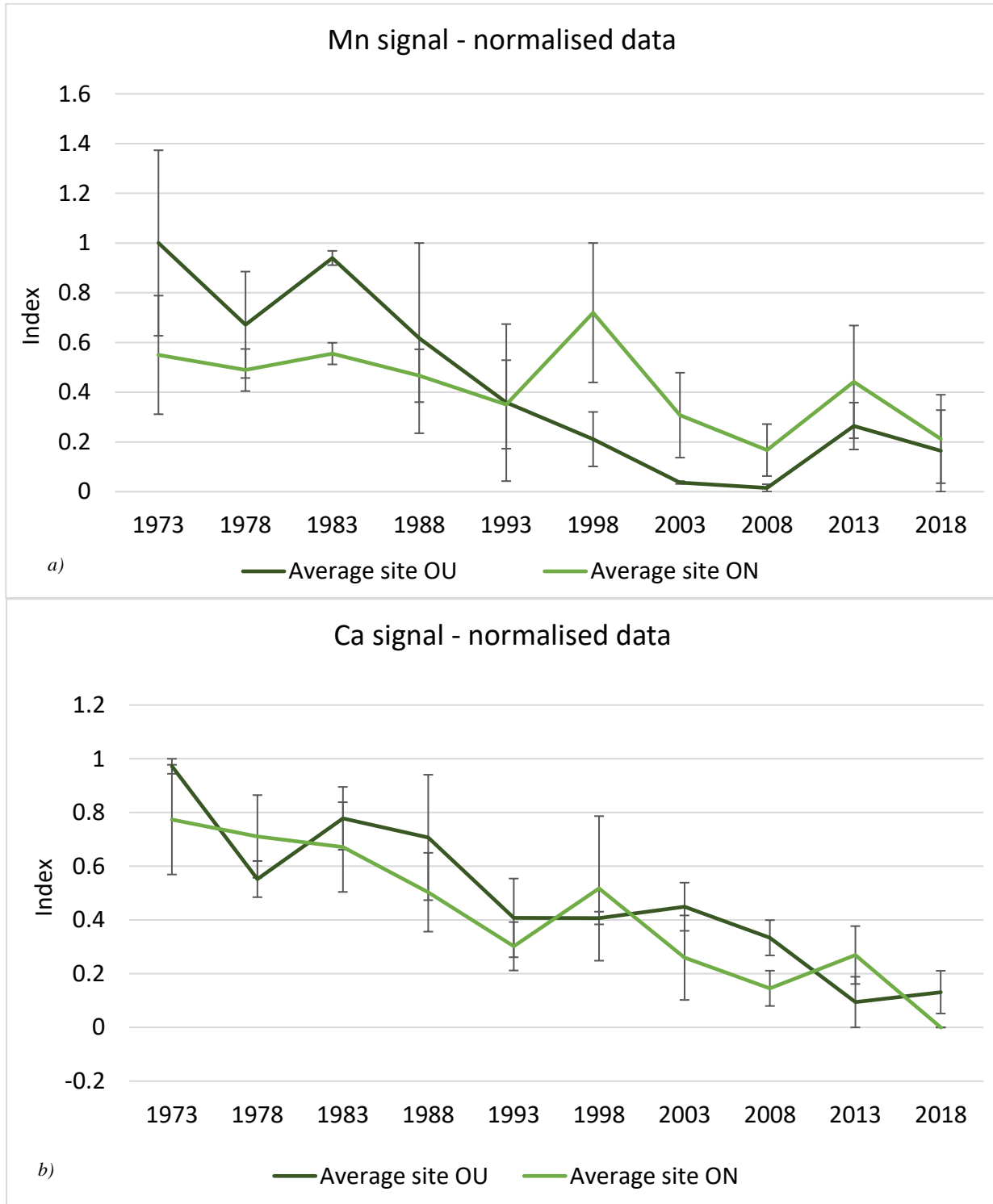


Figure 22: Normalised average signal per site for the elements Mn (a) and Ca (b) (\pm SE).

3. Results

3.3.2 Statistical analyses performed

3.3.2.1 Mann-Kendall test (M-K)

Table 2: result of the M-K test for each element

Mann-Kendall test		
Element	Tau	P-value
Ca	0.600	0.020
Cr	0.644	0.012
Cu	0.022	1.000
Hg	-0.067	0.858
Mn	0.600	0.020
Mo	0.556	0.032
Pb	-0.289	0.283
Ti	0.156	0.592
Zn	0.244	0.371

The results of the M-K tests are shown in Table 1, for the signal of single trace metals between sites, while Table 2 shows the result of the test for the average elemental signal per site (plotted in Figure 17). In the tables, the rows highlighted in grey correspond to the elements for which a monotonic trend has been confirmed, i.e., Ca, Cr, Mn and Mo. In contrast the result presented in Table 2 demonstrate that between the two sites' average signals there is no monotonic trend.

Table 1: M-K test between site averages concentration of heavy

Mann-Kendall test	
Tau	P-value
-0.0667	0.85803

3.3.2.2 Pettitt test

This test was applied to all the time series of each trace metal and of each site, separately, with the aim of finding a correspondence between the change points indicated by the Pettitt test, and the years having potential impactful events for the village of Klosters – e.g, the begin of the construction works or the opening of the bypass road. For the Pettitt test, the raw data are used, since the normalisation might heavily distort the values of the elemental signal. The test however did not identify any change point for any trace metal, in neither site.

3. Results

3.4 Tree-ring width results

3.4.1 Comparison of tree-ring width with nitrogen isotope analysis

Figure 23 represents the comparison between the concentration of nitrogen in the tree rings with the detrended tree-ring width for site OU (Figure 23a) and site CT (Figure 23b). In order to make the tree-ring width comparable with the 5-year cluster data of the N analysis, the average detrended tree-ring width was also calculated in 5-years clusters and only the clusters matching the analysed years for N are selected and presented in the graphs. This procedure is also applied for Figure 24.

In Figure 23a site OU presents a similar pattern for both variables. The main difference is that N concentration presents a negative peak in 1996-2000, which is reported in the successive measurement (2006-2010) for the tree-ring width. The Pearson correlation coefficient reports a weak correlation between the two variables, with an r value of 0.30 and a low level of significance ($P = 0.63$). Site CT does also show a similar pattern between N concentration in the tree rings and their detrended growth. In this case the fall of 2016-2020 of % N is not reported in the growth pattern. The Pearson

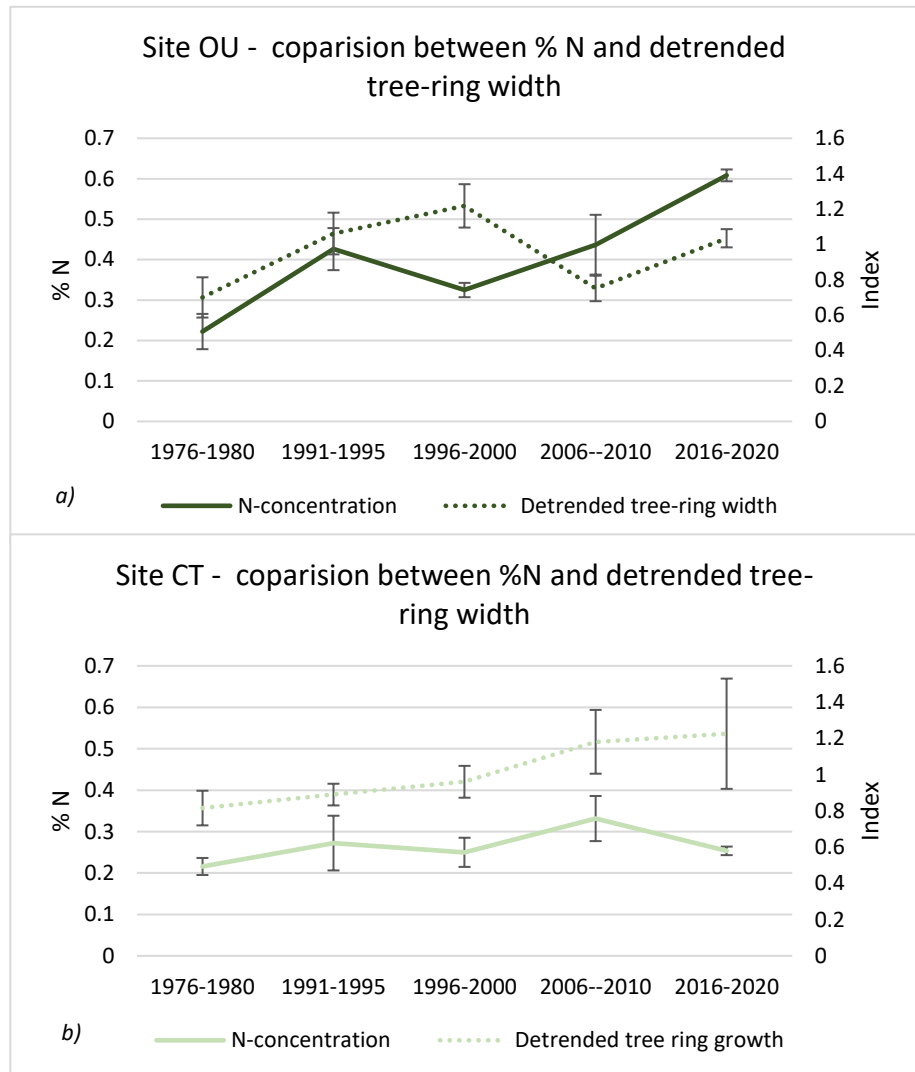


Figure 23: Comparison between the % N (\pm SE) with the 5-year average tree-ring width (\pm SE) of site OU (a) and site CT (b).

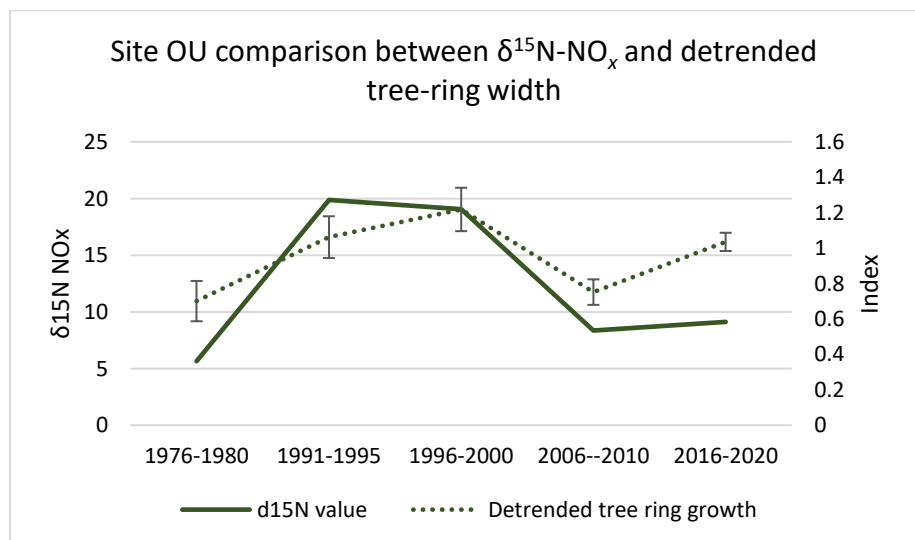


Figure 24: Comparison between $\delta^{15}N-NO_x$ and the 5-year average tree-ring with (\pm SE) of the trees investigated through $\delta^{15}N$ analysis for site OU.

3. Results

correlation coefficient is sturdier this time ($r = 0.60$), although it is still not significant ($P = 0.29$). The correlation between the $\delta^{15}\text{N}$ values and the detrended tree-ring growth was also checked with the Pearson correlation coefficient. Among these two variables however there is no correlations, since the r values are slightly negative for each site. A high correlation is shown instead in site OU by comparing the detrended tree-ring growth and the $\delta^{15}\text{N}\text{-NO}_x$ value (Figure 24). This correlation reports an r value of 0.84, despite not being statistically significant ($P = 0.08$).

3.4.2 Comparison of tree-ring width with radiocarbon analysis

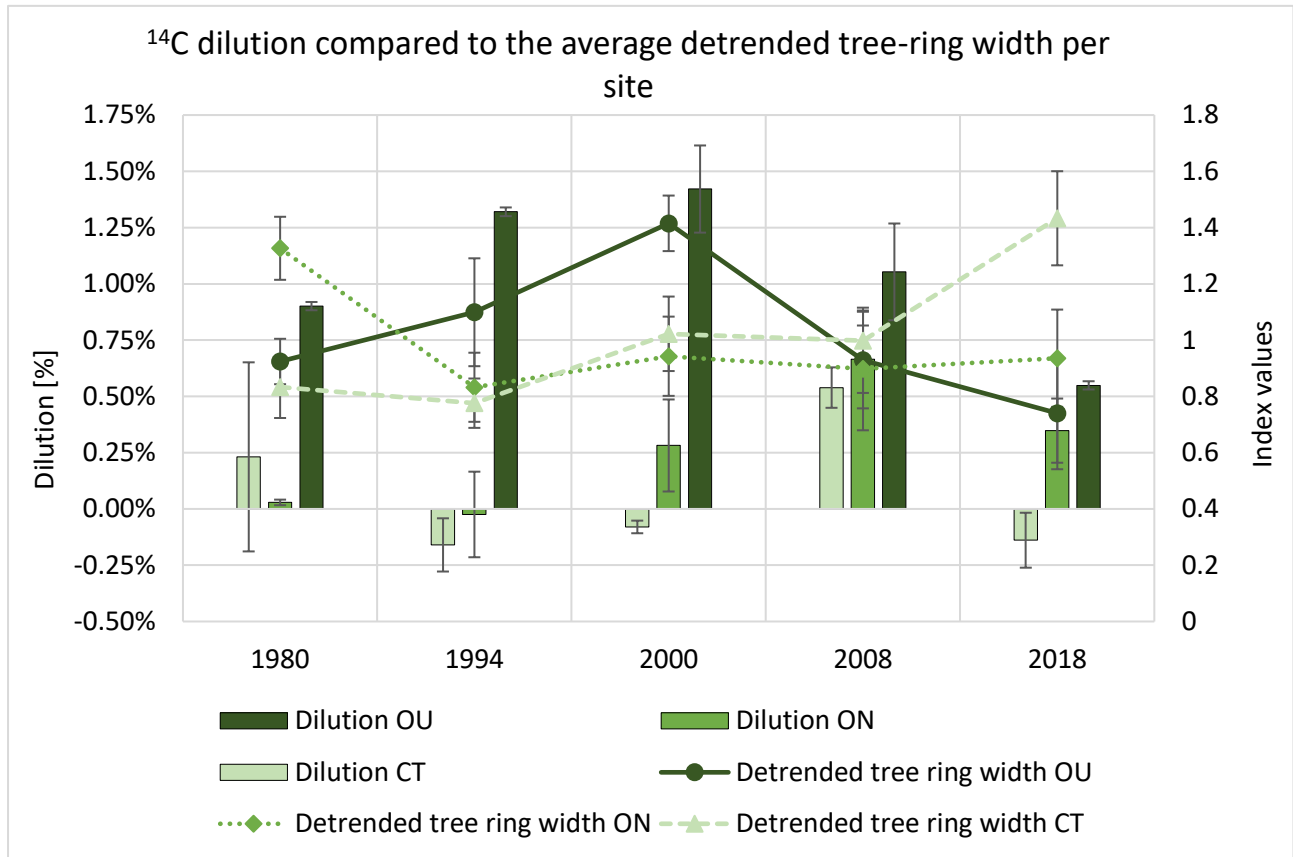


Figure 25: Comparison between the radiocarbon dilution per site ($\pm SE$) with the tree-ring growth of the equivalent year ($\pm SE$).

The comparison between the dilution of ^{14}C and the detrended tree-ring width for each site is presented in Figure 25. Given that the ^{14}C analysis are conducted only over precise years, in Figure 25 it is represented only the detrended average tree-ring width of the site corresponding to the measured ^{14}C year. Therefore, unlike Figure 23 and Figure 24, 5-year average clusters are not necessary. The two variables (detrended tree-rings width and ^{14}C dilution) were checked with the Pearson correlation coefficient. Site ON and site CT reports a slightly negative r value, meaning that the correlation is weak. In contrast, site OU registered a very high correlation value is also statistically significant ($P < 0.05$). Thus, in site OU the strong correlation between the ^{14}C dilution and the detrended tree-ring width indicates that high dilution rates are reflected in high growth rates and vice versa.

4 Discussion

4.1 Nitrogen isotope analysis ($\delta^{15}\text{N}$)

The implementation of nitrogen isotope analysis in studies about local pollution history is possible, and it has been documented by the various examples. However, particular caution is required due to the intrinsic complication of the internal interaction between nitrogen and plant, as well as the multitude of external variables that can influence the results. The $\delta^{15}\text{N}$ results of the current investigation are fairly similar to what was found by Saurer et al. (2004) and Guerrieri et al. (2009), two studies carried out in settings similar to this research. For example, both were performed near a motorway in Switzerland, and analysed the presence of N within the tree rings of Norway spruce trees. In the case of the current investigation, however, the $\delta^{15}\text{N}$ data fail to depict a clear temporal trend that can be related with the polluting events which took place in the area of Klosters in the last 50 years. As it is visible in Table 3 (and Figure 12d), site ON has only slightly higher $\delta^{15}\text{N}$ value than the control site, whereas site OU is the one reporting the highest values. It appears that the construction works for the bypass road, as well as its opening did not leave a clearly detectable sign in the data. This result is comparable to the finding of Leonelli et al. (2012), who also did not report a clear response of $\delta^{15}\text{N}$ in tree rings (of European larch – *Larix decidua* Mill.) for the variation of traffic volumes along the Mont Blanc motorway in Italy.

The natural average $\delta^{15}\text{N}$ value for a temperate forest is usually slightly in the negative range, between -2‰ and -5‰ (Amman et al., 1999). According to Table 3 the closest value to the “natural one”, is -1.55‰ found in the period 1976-1980 for site CT. This site was chosen as control, since it is distant enough to avoid being under the influence of atmospheric pollution from both the bypass and the old road. Already at the distance of 1 km the effects of a motorway over the concentration of nitrogen are negligible (Saurer et al., 2004). Therefore, the nitrogen isotope ratio found in the tree rings of site CT should also be somewhat close to the local value of the soil (Gebauer et al., 1994). Considering that the values reported for site OU and ON differs from the ones of the control site and are relatively far from the natural value for temperate forests, we can assume that in the two sites during the last 50 years there has been an ongoing perturbation of N, possibly from one, or multiple anthropogenic sources.

4.1.1 Nitrogen uptake and $\delta^{15}\text{N}$ signal in tree rings

Using N for studies reconstructing the atmospheric pollution history presents some issues. Firstly, when dealing with different polluting sources, it has to be taken into account that they most likely have differing nitrogen isotopic ratios (Heaton, 1990). For this reason, disturbances in the $\delta^{15}\text{N}$ signal might be recorded as either a decrease or increase of the ^{15}N isotope, because they represent the resulting signature from the sum of different signatures values of the various sources (Guerrieri et al., 2009; Savard, 2010). The difficulties in the interpretation of the $\delta^{15}\text{N}$ signal are also related to the fact that the absorption of N is dual, meaning that it can happen through different processes, i.e, the leaves and the root system (Vallano and Sparks, 2007).

Table 3: average $\delta^{15}\text{N}$ [‰] values recorder per site

Period	Average $\delta^{15}\text{N}$ [‰]		
	Site OU	Site ON	Site CT
2016-2020	4.98	-0.63	-0.46
2006-2010	2.15	2.24	1.55
1996-2000	2.58	-0.49	-0.64
1991-1995	4.95	2.69	-0.55
1976-1980	0.19	2.22	-1.51

4. Discussion

The $\delta^{15}\text{N}$ value found in tree rings is also related to the nitrogen cycle in the soil, therefore, changes in the cycle can have consequences over the isotopic ratio (Bukata and Kyser, 2007). Such disturbances are often induced by the local climatic conditions (Savard et al., 2009), which can manifest themselves as variations in the soil pH, increment in temperature of the soil, changes in the soil microbe communities or modification of the regional hydrology (Bukata and Kyser, 2007). In the soil, the main source of N for the plants is represented mostly by either nitrate (NO_3^-) or ammonium (NH_4^+) and in smaller part by organic nitrogen (Vallano and Sparks, 2007). The transformation process of organic N into an inorganic form (NO_3^- , NH_4^+ or NO_2) is known as mineralisation. During this process, fractionation takes place within the soil (Guerrieri et al., 2009). However, it has been reported to not have a major influence over the $\delta^{15}\text{N}$ value of nitrogen taken up through the roots (Evans, 2007; Savard, 2010). What could instead have an influence over the $\delta^{15}\text{N}$ value assimilated by the root is any process that can potentially modify the ratio between NO_3^- and NH_4^+ (Savard, 2010). In fact, NO_3^- typically has a more depleted nitrogen isotopic ratio than NH_4^+ . NO_3^- is produced by the nitrification process, namely, a microbe mediated transformation of ammonium into nitrate. This compound (NO_3^-) presents higher mobility in water than ammonium, nonetheless NH_4^+ is preferably assimilated by the trees (Savard et al., 2009). This means that there is a discrimination process during the nitrogen uptake from the roots in favour of NH_4^+ , possibly because, in the tree, NO_3^- before being synthesised into amino acids still requires to be reduced (Cole, 1981). High rates of N deposition have been reported to increase the net nitrification process, increasing thus the concentration of NO_3^- into the soil (Savard, 2009). Moreover, Norway spruce is a species whose roots are often converted to mycorrhizas. The fungi are known to be able to influence the nutrition of the tree and its reaction to environmental disturbances (Taylor et al., 2000). This symbiotic relationship has been reported to lead to lower $\delta^{15}\text{N}$ values in the plants, due to elevated rates of isotopic fractionation happening within the fungi (Marshall et al., 2007). This phenomenon seems to be more prominent under N-limited conditions, since the tree has to rely more heavily on the nutrients provided by the mycorrhizae (Marshall et al., 2007; Vallano and Sparks, 2007).

The second way in which plants assimilate N is through foliar uptake. Thanks to the implementation of models, it has been demonstrated that this pathway is responsible for the uptake of 3-16% of reactive nitrogen (i.e., the combination of oxidized, reduced, and organically bound nitrogen) used by the tree for the growth of new tissues (Vallano and Sparks, 2007). The foliar assimilation happens mainly through stomatal diffusion. This process is dependent on two main factors: firstly, the physical and chemical characteristics of the pollutant. Secondly the plant species and its physiological properties, such as its stomatal conductance and rate of N metabolism (Vallano and Sparks, 2007).

The $\delta^{15}\text{N}$ value in the tree rings is therefore a resulting combination of the N taken up by both leaves, from the atmosphere, and roots, from the soil. For this reason, it is important to be able to differentiate between the sources of nitrogen (Vallano and Sparks, 2007), and possibly isolate atmospheric signal. This step has often proven difficult to be put into practice in field studies, especially due to discrimination during uptake and assimilation of N, as well as the aforementioned mycorrhizal interaction (Vallano and Sparks, 2007). Nonetheless, although not perfectly, with the help of mixing models, it is possible to extrapolate general deductions regarding the uptake from the leaves (Marshall et al., 2007). As it is shown in Figure 15, in the current investigation we managed to isolate and reconstruct the $\delta^{15}\text{N}\text{-NO}_x$ signal with a two-component mixing model in order to highlight the role of atmospheric pollution.

4.1.2 Reconstructed $\delta^{15}\text{N}\text{-NO}_x$ signal

The interpretation of $\delta^{15}\text{N}\text{-NO}_x$ signal is not straightforward, since its value has been proven to also be highly different depending on the emitting source (Heaton, 1990; Walters et al., 2015). For

4. Discussion

example, Heaton (1990) confirmed that the $\delta^{15}\text{N}$ value emitted by a combustion engine can vary from -2‰ to -13‰. The emission difference is tied to the type of engine, the speed at which it is rolling and its load. The result showed that higher loads are reflected in a higher nitrogen isotope ratio, for both gasoline and diesel engines (Heaton, 1990). A more recent study by Walters et al. (2015) suggested that there is an even bigger excursion range of $\delta^{15}\text{N}$ values for vehicle exhausts, from -23.3 to 15.9‰ for diesel-fuelled vehicles and from -15 to 10.5‰ for gasoline-powered ones. A relationship was found between the concentration of NO_x and the $\delta^{15}\text{N}\text{-NO}_x$ value, namely, a higher concentration is reflected by a lower isotopic ratio (Walters et al., 2015). Most of the emissions (around 70%) are expelled in the first 200 s of engines' operation, since the catalyst is still cold (Walters et al., 2015), whereas, once the catalyst is warm, the emission of NO_x tends to enrich in ^{15}N .

An important role in the regulation of the emissions of nitrogen is also played by catalysts, since after their introduction, the emissions from vehicles' engines have been largely reduced, especially in terms of NO_x . Fundamental in this abatement, is the role played by selective catalytic reduction (SCR) – which falls into the category of post-combustion control (Cheng and Bi, 2014). SCR catalysts were first introduced in the early 2000s with the Euro IV standards (Johnson, 2015), and are now one of the most efficient post-combustion technologies for the control of NO_x emissions (Liu et al., 2016).

4.1.3 Alternative sources affecting the $\delta^{15}\text{N}$ value of tree rings

Other perturbances affecting the $\delta^{15}\text{N}$ value are related to the deposition of domestic animals (Battipaglia et al., 2010). The general average $\delta^{15}\text{N}$ value for raw manure from various livestock is 7.2‰ – while for cattle only it is slightly higher, 8.4‰ – (Bateman and Kelly, 2007; Choi et al., 2017; Lim et al., 2010). However, once the manure is deposited on a surface, the phenomenon of NH_3 volatilisation takes place, stripping away the lighter ^{14}N isotopes and creating thus an enrichment of ^{15}N in the remaining N, up to 14‰ (Choi et al., 2017). Another issue is posed by the use of fertilisers, either in the form of composted manure or of synthetic nature, given that they both contain nitrogen. The $\delta^{15}\text{N}$ value of composted manure is usually more enriched in ^{15}N than raw manure, displaying a mean value of 16.3‰, but ranging between +4.9 and 20.9‰ (Choi et al., 2017), whereas the typical signature of N from synthetic fertilisers ranges from -3 to +3‰ in 90% of the cases (Choi et al., 2017). The use of fertilisers might not represent an issue for site OU and ON, due to the fact that they are mostly comprised of forested areas – even though accidental contamination due to spillage could still happen (especially for site OU, given its closer proximity to the road). Furthermore, random deposition from wild animals cannot be excluded. In contrast, for site CT, fertilisers and manure might represent an issue, since there the trees are more spaced between each other, and the area might be used as a pasture for cattle.

4.1.4 Nitrogen concentration in tree rings

Similar to the results of $\delta^{15}\text{N}$ and $\delta^{15}\text{N}\text{-NO}_x$, the concentration of nitrogen in the tree rings (Figure 13) does not provide specific evidence for the main events that took place in Klosters. There could be multiple reasons to explain this behaviour. As a matter of fact, whenever employing methods involving important nutrients for the plant physiology, such as nitrogen, there is an important level of uncertainty that has to not be neglected. Due to its metabolic utility for the tree, the plant can manage N according to its physiological necessity (Saurer et al., 2004), with the aim of increasing the N use efficiency (Meerts, 2002). This phenomenon, which is known as lateral/radial transport (or translocation), constitutes an issue for the application of dendrochemical analyses on tree rings. (Saurer et al., 2004; Tomlison et al., 2014). Lateral translocation generally takes place during the cellular transformation procedure of sapwood into heartwood. When the cells die, the tree usually recovers nitrogen from them and moves it to the living and younger parts of the tree, namely, the sapwood and developing leaves (Saurer et al., 2004; Tomlison et al., 2014). The presence of such a

phenomenon can potentially invalidate the use of tree-ring N-concentration as a reliable tool to track the nitrogen deposition rates. One of the main reasons is that due to this process, nitrogen from past polluting events might be displaced to younger sections of the tree (Battipaglia et al., 2010). Consequently, annual resolution is precluded a priori, however the $\delta^{15}\text{N}$ signal can potentially be affected only minorly, if during the process of nitrogen-recovery fractionation is not prominent. Thus N-concentration can still retain a certain degree of utility (Saurer et al., 2004; Savard, 2010).

4.1.5 Limitations of nitrogen isotope analysis in this investigation

The study carried out by Saurer et al. (2004), was able to benefit from the data about the nitrogen condition in the soil collected by Amman et al. (1999), since the two research were conducted in the same location. For the present project, no assessment of the soil N was made, which could have helped to discriminate between the various sources of N. Furthermore, a total of 3 trees were analysed per each site, which is a relatively low number; therefore, in a successive study, using a higher number of samples could be helpful to give more robust results which are less influenced by outliers. Moreover, the distance of the trees from the road is dependent on the site and on the individual, and thus it is uneven between the samples. This changes the level of exposition to the pollution, since individuals closer to the road interact with the higher quantity of pollutants. The quantity of pollutants to which a tree is exposed, is also influenced by the wind speed and direction (Guerrieri et al., 2009), thus having a deeper insight into this aspect could be highly beneficial for the interpretation for the results.

4.2 Radiocarbon analysis (^{14}C)

As shown in Figure 16 and 17, the radiocarbon results do not match the expectations, and partially fail to show the polluting effect of road traffic in terms of fossil carbon emissions. Most surprising is the low signal response in site ON, which should be particularly exposed to such pollution. A somewhat similar result was obtained by Sensula et al. (2018). In their case, Scots pine (another coniferous species) was sampled in proximity of heavy industrial factories, and radiocarbon analysis over tree rings were carried out. Analogously, in some of the sites which the authors hypothesised to be particularly affected by an important local Suess effect, no clues regarding pollution were found by the radiocarbon analysis. The absence of dilution in the ^{14}C isotope was mainly attributed to physiological factors of the trees, i.e., how carbon is stored as well as external factors – such as nuclear power plants (Sensula et al., 2018).

Among the sampled sites, the ratio $^{14}\text{C}/^{12}\text{C}$ is always the lowest in site OU. However, Figure 16 highlights a clear decrease in ^{14}C dilution, starting in year 2000. On the one hand, this behaviour could be suggesting that the opening of the bypass road in late 2005, by diverting the majority of the traffic, affected the local concentration of radiocarbon. As a matter of fact, the environmental impact assessment report states that in 1987 approximately two thirds of the carbon emission in Klosters were produced by road traffic, while the remaining one third was attributed to other sources of fossil fuel combustion, such as heating implants (Tiefbauamt des Kantons Graubünden, 1991). In 2005, once the bypass road would have opened, the prediction in the environmental impact assessment report states that the carbon emission percentages in the village would have shifted from 66.6% to 8.5% for road traffic and from 33.3% to 91.5% for combustion and heating implants (Tiefbauamt des Kantons Graubünden, 1991). On the other hand, another possible explanation for the decreased dilution could be found by glancing at the location of the sites (Figure 8). Given that site OU is much closer to the village and its buildings than site ON, the local trees could be primarily affected by the pollution produced by “*Feuerungen*”, i.e., the burning of fuels for industrial production and heating

4. Discussion

of building (FOEN, 2021). Moreover, the role of “*Feuerungen*” is possibly enhanced by the geographical location of Klosters. The village lays de facto in a mountainous region at 1200m a.s.l. with an average annual temperature of 2.2 °C, and therefore the higher number of heating degrees induces larger quantities of CO₂ emitted per capita in comparison to cities in warmer conditions (Bergeron and Strachan, 2011). Thus, the drop in the dilution signal could be also partially reconducted to a technological improvement of the combustion plants fuelled by either oil or gas. This improvement took place (in Switzerland) at a national level during the 90’s and helped greatly in the mitigation of atmospheric pollution (FOEN, 2021). The key elements of the emission’s curbing can be identified in better combusting techniques, higher fuel quality and periodical controls once the new air quality law (Luftreinhalte-Verordnung) was introduced in 1986 (FOEN, 2021).

4.2.1 Trees’ uptake of carbon and ¹⁴C signal

Green plants are able to fix carbon dioxide (CO₂) from the atmosphere by bounding it with water (H₂O) into glucose (C₆H₁₂O₆). This process, known as photosynthesis, requires the energetic input of light to produce chemical energy. The photosynthetic reaction takes place into the chloroplast of the chlorophyll – the green parts of the plant (Agrios, 2005). Trees play an important role in this section of the carbon cycle, i.e., the atmospheric carbon fixation and storing through photosynthesis. For this reason, forests are considered as major carbon sinks (Saurer et al., 2003). The carbon present in the atmosphere can be found in the stable forms of ¹²C and ¹³C or in the radioactive form of ¹⁴C. During the photosynthesis, plants take up one of the three isotopic forms of carbon, fix it into glucose and use it to sustain their metabolic functions. Therefore, part of this carbon consists of ¹⁴C, and it reflects the fractions of carbon isotopes in the atmosphere (Suess, 1980). Unlike the quantity of ¹³C, whose assimilation depends on the in-situ conditions during the tree growth, the quantity of radiocarbon uptake is for the most part independent by the geographic location (Suess, 1980). A decrease of the ¹⁴C/¹²C ratio in the atmosphere, which is not attributable to the natural decay of the radioactive isotope ¹⁴C, is known as Suess effect. This effect can have global, regional, or local character (Levin et al., 2008), and can be induced by the burning of fossil fuels.

4.2.2 Radiocarbon concentration in tree rings

Tree rings are generally believed to be an optimal passive record of ¹⁴C, since the cellulose of the plant is usually a direct sample of the atmospheric carbon concentration (Kromer, 2009). For this reason, the ¹⁴C curves for the radiocarbon dating method are calibrated on the value retrieved by tree rings (Kromer, 2009). Nonetheless, although not as prominent as with nitrogen, even for ¹⁴C there are both internal and external factors that influence the concentration of radiocarbon present within the tree rings. One of the most important internal factors related to such variabilities is represented by nonstructural carbon – NSC (McDonald et al., 2019). NSC is carbon that has been recently photosynthesised but was nonetheless not integrated into structural tissue – as instead it is the case for the majority of the photosynthesised C – but it is stored to be used in other circumstances, such as stressful events (McDonald et al., 2019; Sensula et al., 2018). As a matter of fact, when the tree is under stress it tends to reallocate carbon as a response, and if this reallocation is not sufficient to overcome the stress-related disruption, the plant might die (Cherubini et al., 2021). It has been demonstrated that trees having a higher amount of NSC stored and ready to be used, are most likely to survive the impact of important disturbances. In some cases, carbon older than 10 years was reallocated in order to cope with extremely stressful events (McDonald et al., 2019). Droughts represent one of these major, and always more frequent, stress factors for forests worldwide. Prolonged periods of dryness can disrupt the hydraulics of the tree, the quantity of nutrients taken up and the assimilation of carbon (Joseph et al., 2021). Extended droughts can lead the tree to repeatedly

recur to the use of stored C so as to sustain vital processes such as respiration (Gessler and Treydte, 2016). Thus, when a summer is particularly hot and dry, the isotopic signatures of carbon found in tree rings might not reflect the atmospheric composition (Gessler and Treydte, 2016).

4.2.3 External variables radiocarbon concentration

Among the external variables that can affect the atmospheric radiocarbon value, except for local and regional Suess effects, the most important one is the interaction between the sun and the Earth's geomagnetic field, which determines the rate of ^{14}C production (McDonald et al., 2019). The solar winds do determine the subannual ^{14}C variation amplitude, which was found to be particularly high (up to 5-6 ‰) at the Jungfrauoch measuring station, in Switzerland (Levin and Kromer, 2004). These fluctuations however take place at a global or regional scale, whereas the focus of the current investigation regards the local scale. What could instead influence differently the sampled sites in Klosters, is the effect caused by the presence of biogenic CO_2 in the soil (Sensula et al., 2018). As a matter of fact, biogenic CO_2 can lead to increases in the concentration of ^{14}C in tree rings (Piotrowska et al., 2019), thus masking the local Suess effect. It refers to the decomposition of older plant material that was incorporated into the organic matter of the soil, which might conceal the atmospheric ^{14}C value, given that this material contains higher ^{14}C concentrations – since this is age dependent (Piotrowska et al., 2019). This effect could apply for the higher values found for site ON, and the seemingly absence of a strong Suess effects – especially in 1980, since in this year the site shows a concentration higher than site CT; although not higher than the Jungfrauoch data. Nevertheless, this is just a speculation. Other factors that influence the radiocarbon value are for example nuclear power plants, which do exert an enriching effect over the local concentration of ^{14}C (Sensula et al., 2018). However their effect is spatially limited up to 2.5 km of radius (Monlnar et al., 2007), therefore, for this investigation their influence is absent.

4.2.4 Limitations of radiocarbon analysis in this investigation

The obtained results are difficult to compare. The dilution graph shows that the ratio $^{14}\text{C}/^{12}\text{C}$ starting from 2008 is decreasing for both sites, OU and ON. While simultaneously it appears that in the same period the CO_2 fossil fuel component emitted is strongly increasing. Nevertheless, the dilution effect is arguably more trustworthy, because it is based only on measured data obtained by Levin and Kromer (2004), from the Jungfrauoch station. In contrast, the estimation of fossil fuel component of CO_2 requires an additional input data – i.e., the atmospheric concentration of CO_2 , for which the concentration of Mauna Loa, from Keeling et al. (2001) was chosen, and it relies on various calculations and simplifications. As a matter of fact, for the calculation of the CO_2 fossil fuel component of the current investigation, the influence on $\Delta^{14}\text{C}$ of the biospheric component was not taken into account. Levin et al. (2008) suggest that if the magnitude of the local biospheric component is important, it should not be disregarded. However, given its unknown magnitude for the study area of Klosters, this component was neglected. Furthermore, similar to nitrogen, the unequal distance between the road and the trees that were sampled plays an important role in the intensity of the recorded ^{14}C signal, due to the very high sensitivity levels of the radiocarbon analysis (Battipaglia et al., 2010).

4.3 LA-ICP-MS analysis

The low signals detected for Cd are surprising since in Switzerland it is considered as a priority heavy metal, and according to Table 4 it is present in the traffic emissions with a signal twice as high as the one of Hg. In general, on a national level the emissions of Pb, Hg and Cd drastically decreased since

4. Discussion

1980 (Bass et al., 2021). The emissions of Pb reduced by as much as 98.8% until 2019, Cd by 87.2% and Hg by 91.1% for the same period (Bass et al., 2021). For Hg and Cd, the main improvements in emissions curbing are tied to the implementation of more severe regulations and limits imposed to the waste incinerations plants (Bass et al., 2021). In contrast, the important decrease showed by Pb is mainly attributable to the countrywide ban on leaded gasoline in the year 2000 (Bass et al., 2021). Table 4 represents the evolution of the emissions of priority heavy metals in Switzerland and their relevance in the transportation sector. The evolution of Hg is relatively stable throughout time, thus its signal found in tree rings is not particularly surprising. In contrast, the results for Cd are unexpected, since most of the time, the signals found in tree rings in Klosters were not higher than its LOD. Pb shows the biggest differences in terms of index values between the two sites. In site OU it appears that Pb is following the Swiss trend, with a steep decrease since the 1980, whereas in site ON, no such trend is present, but there are rather higher oscillations trough time (Figure 18a). Such comparisons cannot be made for Cr and the other non-priority heavy metals, since they are not measured on a national level and are therefore missing from the Swiss inventory (Bass et al., 2021).

Table 4: Emissions of the transportation sector in Switzerland in tonnes (data from Bass et al., 2021).

Element	1990	2005	2010	2019
Pb	230	4.3	3.7	2.8
Cd	0.070	0.077	0.083	0.093
Hg	0.034	0.037	0.037	0.035

4.3.1 Heavy metal signal in tree rings

The signals of heavy metals found in tree rings is dependent on several factors, such as: (i) the quantity of anthropogenic emissions, (ii) the metabolism of the tree, (iii) the mobility of metals in the soil due to the pH variations and redox potential and (iv) the uptake mechanism – roots, leaves or bark (Jonsson et al., 1997).

The mobility of the elements in the xylem is related to their solubility in the solution transported by the xylem – i.e., the sap (Cutter and Guyette, 1993). The sap is the liquid flowing in cells of the wood (Taiz and Zeiger, 2002). The rings that usually conduct the sap are the younger ones, usually 10 to 12, and among those, the transport happens through the outer-most ones, since they are the most efficient (Bodo and Arain, 2021). For Norway spruce the exact dimension of the sapwood is not always constant but varies according to the age of the tree, and also whether the tree is dominant – which translates to bigger sapwood – or suppressed – which equals to smaller sapwood – (Sellin, 1996). Longuetaud et al. (2006) reported a range of 2.4 to 7.1 cm for the sapwood width of Norway spruce. The number of tree rings that compose the sapwood are higher at the bottom of the trees and lower at the top (Longuetaud et al., 2006). Therefore, the height at which a tree is sampled defines the sapwood width, which presents a higher concentration of heavy metals in comparison to the heartwood. As a matter of fact, the sapwood transport allows for the translocation of trace metals from ring to ring influencing the detected signal, especially where most of the sap transits (Prohaska et al., 1998). There are multiple ways in which this kind of transport can influence the final elemental concentration in the tree rings, including: i) the amount of time for which the ring is an active part of the sap transport, ii) the concentration of the element in the sap passing through the ring, iii) the ability of the xylem matrix of a tree ring to bind cations (Hagenmeyer and Hübner, 1999), iv) the heartwood-sapwood equilibrium and v) the pH of the sap (Prohaska et al., 1998). The effect of the sap transport is identifiable in an accumulation of the trace elements in the outer most rings of the sapwood, as well as an increased concentration in the cell walls of the vessels transporting the sap (Locosselli et al., 2018).

4. Discussion

Prohaska et al. (1998) highlighted the role of compression wood for the concentration of heavy metals. This kind of wood is much likely to attract and to bind ions in comparison to its opposite wood; thus, higher trace metals concentrations, up to a factor of 4-6, are to be found if compression wood is present (Prohaska et al., 1998). The selected trees for this study were seemingly unaffected by compression wood, however no further analyses, other than in-situ observations, were performed to exclude this option. The elemental concentration of heavy metals in tree rings could also be related to the effects of injuries or infections, since these can change the properties of the wood and lead to substantial increases of element concentrations in tree rings (Danek et al., 2015). Higher concentration of pollutants near the outer most rings (visible in Figure 19) could also be the result of airborne uptake from the bark (Garbe Schönberg et al., 1997). Most trees tend to show a decrease in the quantity of elements present in recent tree rings as the plant ages, mostly due to the lower binding ability of its woody tissues (Prohaska et al., 1998). For Ca and Mn (Figure 22) this tendency is clearly observable, it is not the case for Hg and Pb (Figure 20).

In some cases, despite the soil having a notably high concentration of heavy metals, if the tree is growing at particularly fast rates, the signal of the element might not be detected (Prohaska et al., 1998). Alternatively, due to the extreme level of pollution, causing severe stress, the plant might behave abnormally (Garbe Schönberg et al., 1997). Individual trees can display different behaviours, and their uptake of trace elements is not always consistent. As a matter of fact, when in presence of heavily polluted soils, they can move the location of their roots to less polluted spots, such as deeper horizons, where the concentration of chemical compounds is different (Garbe Schönberg et al., 1997). The horizon depth that the roots reach to absorb the nutrients is also dependent on the water regime (Mihailjevic et al., 2011). In case of dry period the uptake of heavy metals happens more deeply in the soil, whereas when enough water is available, the trace metals are absorbed mostly from the upper layers (Mihailjevic et al., 2011).

4.3.2 Pb

The ban on leaded gasoline introduced in 2000 seems to not have affected the signal of Pb in site ON (Figure 20a). Pb is usually considered as an element having low mobility between tree rings. The reason is tied to its low solubility in the sap that hinders its translocation between the ring's boundaries (Cutter and Guyette, 1993). The establishment of the uptake mechanism for Pb, either root, leaves or bark is not possible to verify with precision and for this reason, a consensus has still not been reached, leading to diverging answers. For example, Bindler et al. (2004), favoured the theory of the bark uptake mechanism being the most prominent; Novak et al. (2010) and Kim et al. (2020) suggested that the preferred way is through foliar uptake, whereas various studies focused on the absorption of lead from the soil, such as Hagemeyer and Hübner (1999). The latter authors conducted a controlled experiment regarding the growth of Norway spruce in Pb contaminated soil and they noticed that the highest signal of the element in the tree rings do not always reflect the year in which its signal was at highest levels in the soil. Previous studies on the concentration of Pb in tree rings (Hagemeyer and Weinland, 1996; Prohaska et al., 1998) found a radial distribution pattern, where the rings closest to the pith recorded the highest values, whereas the youngest rings recorded the lowest values. Prohaska et al. (1998) concluded however that, despite the radial distribution pattern, the concentration of lead in the rings did not reflect the applied change of Pb in the soil. Furthermore, according to studies over lead isotopes, the uptake via roots might not be the preferred absorption way for this trace metal (Mihailjevic et al., 2011). Stille et al. (2012) suggest that the uptake of Pb and its presence is the result of all the three mechanisms. As a matter of fact, there is a relationship regarding the soil pH and the concentration of Pb in tree rings (Bukata and Kyser, 2008). Lower pH values in the soil correspond to higher quantities of Pb in tree rings (Stille et al., 2012). This condition is mainly due to the fact

that in such soils more Pb is mobilized and available for the plant to be absorbed (Stille et al., 2012). Thus, for the monitoring of historical Pb fluctuations in the atmosphere, it is important that the chosen soil has an elevated pH, especially when using Norway spruce (Stille et al., 2012).

4.3.3 Hg

Mercury is emitted by both anthropogenic and natural sources. In case of natural sources, it is either released by volcanoes eruption or through re-emission from the burning of biomass that was previously contaminated by Hg and acting as a storage unit (Cooke et al., 2020). In case of the anthropogenic sources, the main emissions are derived from the burning of fossil fuels. Among several other natural archives, such as ice, firn, peat, as well as lake and marine sediments, tree rings are a sink for mercury (Cooke et al., 2020). Conifers in particular represent good interceptors of Hg, due to their all-year-round presence of needles, in comparison to deciduous species (Arnold et al., 2018). Unlike Pb, where the uptake mechanism still represents an ongoing debate, for Hg it has been recently proven that foliar uptake and subsequent phloem transportation to the ring is the predominant way of absorption (Arnold et al., 2018; Pekham et al., 2019). Furthermore, concentration of Hg in foliage, bark and tree rings are seemingly not influenced by its quantities in the soil, thus the measurements recorded in the tree represent potential proxies for the monitoring of the atmospheric concentration of Hg (Arnold et al., 2018). The main concerns and debates are tied to the radial translocation. According to Peckham et al. (2019), it appears to not represent an issue for Hg, at least in their experiment, since no signs of the phenomenon were found. In contrast, Arnold et al. (2018) and Wang et al. (2021) call for caution when studying long term trends of mercury concentration in tree rings, due to the presence of radial translocation, which was assessed in their investigations. This finding would invalidate the annual resolution of Hg chronologies.

Unlike the study conducted by Perone et al. (2018), in the current investigation (Figure 20b) we did not find a decrease of the signal of Hg, but rather a slight increase over time. The discrepancy in Hg records found in tree rings, with the development of the local traffic situation in Klosters could be reconducted to biological and physiological processes of the plants, such as asymmetrical growth, stomata conductance, tree age and canopy dynamics (Wang et al., 2021). Thus, due to the latter reasons, the concentration of Hg seems to be particularly specific to the individual tree, showing a high degree of variation within the same site (Wang et al., 2021).

4.3.4 Cr

Cr is considered to be an element with moderate levels of mobility within tree rings, thus showing higher solubility in the sap than Pb (Prohaska et al., 1998). Therefore, the effect of the sapwood transport, displaying an enrichment of the element in, at least, the outermost ring, should be visible in Figure 21. In contrast, the raw signal of Cr is similar to the findings of Prohaska et al. (1998), for both sites. OU and ON. The signals remain at stable levels throughout all the investigated timespan and do not show any particular fluctuations for neither site.

4.3.5 Ca and Mn

Ca and Mn, in addition to being part of the exhausts of fossil fuel combustion, they are also plants' nutrients. Within the wood structure, they tend to show a moderate radial mobility between tree rings (Tendel and Wolf, 1988). Their measured signals in this investigation (Figure 22) are similar to what was also observed by previous studies on tree rings (Prohaska et al., 1998; Rodriguez et al., 2015), showing a decreasing radial trend with highest values near the pith and the lowest in proximity of the bark. The presence of Al in the soil has been reported to favour the immobilisation of both Ca and

Mn, reducing thus their uptake and consequently their presence within tree rings (Hoffmann et al., 1994). The content of these two nutrients has been found to be also moderately dependent on the pH values of the soil (Augustin et al. 2005; Prohaska et al., 1998).

4.3.6 Limitations of LA-ICP-MS analysis in this investigation

The choice of using unprocessed cores, although it minimises the risk of contamination from external sources, presents two new challenges for the LA-ICP-MS analysis. Firstly, the fact that the surface of a sample extracted with an increment borer is rugged and presents a cylindrical shape, can be an issue. The reason is that relatively large wood particles can always detach from the surface of the core, and especially if it is unprocessed, which translates into a loss of material, which in the analysis yields to unreliable results (Danek et al., 2015; Monticelli et al., 2009). Secondly, due to the roughness of the surface of the core, the laser might penetrate at differing depths, leading to uneven quantities of material analysed and consequently to misleading results (Danek et al., 2015).

Considering the various factor that influences the uptake and the storage of heavy metals within trees, increasing the number of sampled individuals per site, possibly more than 10, so as to obtain more measures per year leads to have results that are less dependent on extremes values (Wang et al., 2021). Moreover, in successive studies it is recommended to carefully study the location of the sampled trees. Both in terms of physical position respect to the polluting source, as well as in terms of soil condition (including presence of above- or underground streams and possibly land use changes), since even small-scale changes can lead to highly different results, as it is the case for Tree 3.2 in site OU.

4.4 Tree-ring width analysis

4.4.1 Detrended tree-ring width compared with nitrogen isotope analysis results

The addition of nitrogen to an environment can exert a fertiliser effect, since this nutrient is very often limiting the biomass production (Evans, 2001; Vallano and Sparks, 2007). In previous studies (Schleppi et al., 1999; Hart and Classen, 2003; Guerrieri et al., 2009) a relationship was found between the tree rings having a higher $\delta^{15}\text{N}$ value and a fertilisation effect. In this research however, none of the comparison between the $\delta^{15}\text{N}$ value of nitrogen of the 5-years clusters and the average detrended tree-ring width for the equivalent period showed a statistically significant correlation. Likewise, higher concentrations of nitrogen were not correlated significantly with higher growth rates. Only site OU reported an elevated correlation value between the detrended tree-ring growth and the $\delta^{15}\text{N}$ - NO_x value, showing although a non-significant statistical correlation ($P > 0.05$). These results are not unprecedented in N deposition studies using Norway spruce. For example, Guerrieri et al. (2009), for their sampled site near a Swiss freeway, did not report a fertilisation effect in relation to the $\delta^{15}\text{N}$ value, or to the N-concentration. The absence of fertilisation effect was also found by Saurer et al. (2004); however, the presence of the effect was not ruled out. As a matter of fact, it is possible that the fertilisation effect is masked behind the mutual existence of positive and negative effects for the tree-ring growth, which, once added together result in a neutralisation of the fertilisation effect (Saurer et al., 2004). Guerrieri et al. (2009) stated that over short terms N-fertilisation affects positively the plant, however if the accumulation of inorganic nitrogen persists over longer periods of time, it can disrupt the biogeochemical cycles of forest ecosystems. Furthermore, these experiments are conducted in proximity of a trafficked road which emits a conspicuous amount of environmentally toxic pollutants, among which, also Ozone (O_3) is present. O_3 is produced in the troposphere due to the reaction of NO_x emissions from traffic exhaust with

4. Discussion

volatile organic compounds, under the irradiance of the sun (Zhang et al., 2019). Ozone is currently considered to be one of the most harmful pollutants for the environment (De Temmerman et al., 2002; Vacek et al., 2015). Long term exposure to O₃ can severely hinder the trees' production of biomass and therefore limit the radial stem growth (De Temmerman et al., 2002; Matyssek and Sandermann, 2003). This chemical compound induces the closure of the stomata, and consequently, the trees' photosynthesis is reduced (Cherubini et al., 2021). An additional explanation to the seemingly absent N-fertilisation could be reconducted to the fact that this specific forested ecosystem might be particularly resistant to the effect of pollution, and thus the variations in $\delta^{15}\text{N}$ or N-concentration do not noticeably affect the trees (Saurer et al., 2004).

4.4.2 Detrended tree-ring width compared with radiocarbon analysis results

In contrast to the comparisons with nitrogen, there is a statistically significant result obtained with the Pearson correlation coefficient between the detrended tree-ring width of site OU and its local Suess effect (r value = 0.91, $P < 0.05$). This correlation indicates that when the dilution of ¹⁴C is higher, possibly due to the emission of radioactively dead carbon from the burning of fossil fuels, the trees of site OU tend to produce radially larger tree rings. In general, the topic of CO₂-related fertilisation in unlimited N environments presents conflicting results (Klein et al., 2016). At the global level, up to 20% of the forested ecosystems are expected to experience forms of CO₂-fertilisation effects on the growth rate of tree rings, due to the increased greenhouse gases emissions and consequently higher atmospheric concentration of carbon dioxide (Martinelli, 2004; Huang et al., 2007; Gedalof and Berg, 2010). CO₂ can stimulate the plant growth mainly in two ways: firstly, by increasing the carbon dioxide reaction rate with the rubisco enzyme during photosynthesis (due to its higher atmospheric concentration, and consequent larger pressure) while simultaneously inhibiting photorespiration. Secondly, by fostering reduced stomatal conductance that could increase water use efficiency, and therefore increase the plant resistance to droughts (Gedalof and Berg, 2010).

On the one hand, Telewsky et al. (1999) conducted a controlled experiment on loblolly pine (*Pinus taeda* L.), where they supplied the trees with the necessary nutrients, in an environment with a CO₂-enriched atmosphere. The results showed that when there is no nitrogen limitation, the enrichment of CO₂ was reflected in an increased radial growth (Telewsky et al., 1999). Similar findings, with positive association between CO₂ concentration and higher tree-ring growth were also drawn by Huang et al. (2007). Kienast and Luxmoore (1988), investigated conifer trees growing into different natural environments and conditions, and concluded that CO₂-fertilisation was found on a relatively small portion of the trees sampled. Thus, they concluded that for this phenomenon to happen specific environmental conditions have to be met, especially favourable climatic condition, including moderate temperature and/or low water stress (Kienast and Luxmoore, 1988). On the other hand, the growth of tree rings is dependent on several factors (Schweingrüber, 1996), and the CO₂-fertilisation effect could be attributable to spurious correlations driven by the choice of the samples and population dynamics (Brienen et al., 2012). As a matter of fact, studies on Norway spruce (Hättenschwiler et al., 1996; Klein et al., 2016), as well as several Mediterranean species (Tognetti et al., 2000) did not find evidence of CO₂-fertilisation. Tognetti et al. (2000) documented that despite the presence of a natural CO₂ spring enriching the local atmosphere, the nearby plants did not show an increased production of biomass. Hättenschwiler et al. (1996) conducted instead, a controlled experiment over Norway spruce trees by supplying the plants with nutrients and increased amount of CO₂, however, no increased radial growth was found. Likewise, Klein et al. (2016) concluded that higher atmospheric CO₂ concentrations do not lead to a fertilisation effect for tall Norway spruce trees, even when larger quantities of N are available. The CO₂ effect due to higher concentrations has only subtle effects on the growth of Norway spruce trees (Klein et al., 2016). Moreover, photosynthetic activities of trees, C storage, respiration and their radial growth are seemingly regulated by other limiting soil nutrients

4. Discussion

than nitrogen (Klein et al., 2016), such as phosphorus, potassium, or manganese (Hättenschwiler et al., 1996). The exact circumstances in which CO₂-fertilisation verifies are not yet completely clear, however, relatively warm climatic conditions with moderate water stress levels and large N availability appear to be prerequisites (Huang et al., 2007).

4.4.3 Limitations of nitrogen isotope and radiocarbon analyses in this investigation

The comparison of the tree-ring width with the nitrogen isotope analysis and the radiocarbon analysis, in order to find temporal trends was mainly hindered by the limited number of measurements performed and samples available. As a matter of fact, the relatively high correlations found with the Pearson test, were often not significant, possibly due to the low number of points, in both the number of sampled trees used (3 per site), as well as the measurements performed on each tree core (5). Additionally, the chosen years for the analyses were not over regular temporal intervals, thus, the pattern might result weighted towards the periods with higher concentration of measurements. Lastly, the N analysis were performed using 5-years clusters instead of single year. Although, this procedure might help mitigating the effect of radial translocation, in also preclude the analysis of exact years, which can be important when investigating events taking place in a specific year.

5 Conclusion

The construction of the bypass road of Klosters has certainly improved the livelihood of the village, restoring its image of a clean, quiet, and picturesque mountain resort. Traffic congestion is no longer a daily hassle for the local population, but rather a distant memory. However, assessing the magnitude of the presumed beneficial effects on the local air quality brought by the opening of the new A28 road is not as trivial as noticing the absence of traffic. In this investigation, the characteristic of trees as environmental archives was taken into account by testing the efficacy of a combination of three different dendrochemical approaches, usually employed individually, and aimed at detecting temporal patterns of pollutants within tree rings.

In order to reconstruct the history of the local pollution for the last 50 years, from 1970 to 2020, Norway spruce trees were sampled at three locations. The first site is located along the old road, close to the village, the second site lays along the old and the new bypass road, and the last one, serving as control site, was selected as far away as possible from both roads and other major polluting sources. Given the profound changes in traffic flow dynamics that took place since the opening of the bypass road, the site near both the old road and the new A28 was expected to record a much higher quantity of pollutants than the site in the village.

The signal of various elements within the tree rings of the extracted cores of Norway spruce trees from each site was examined. Nitrogen analysis was performed to determine the N isotope ratio, and the N-concentration. The results did not yield unequivocal evidence for a clear pattern ascribable to the local historic pollution. The LA-ICP-MS analysis, applied to monitor the presence of heavy metals showed feeble differences among the investigated sites that could be due to changes in traffic flows. Moreover, the majority of the trace metals displays vastly different behaviours, indicating the lack of a general pattern in the data. On the other hand, radiocarbon analysis demonstrated that air quality in the village is not mainly influenced by road traffic, but by other factors, such as fossil fuels burned for heating. Thus, events related to the bypass road do not appear to be clearly visible in the measured data.

All the methods applied in this investigation over tree rings are subject to a multitude of internal physiological factors, as well as external influences that could swing the results to different outcomes. Therefore, it is hard to draw conclusions on which method is the most suitable for the investigation of local pollution histories. The previous studies conducted using similar approaches were located in areas subject to higher emissions of atmospheric pollutants. Thus, the relatively low traffic rates registered in Klosters (less than 10'000 daily vehicles) might not be sufficient to unequivocally affect the local vegetation with clear-cut evidence. The outcome of this survey suggests that although tree rings are able to record environmental pollution data, if the target source is not the most prominent, then it is particularly difficult to isolate its signal and separate it from the noise produced by the other surrounding sources.

For future pollution monitoring studies using tree rings, it is advised to improve the experimental settings. Due to the complicated, intertwined interactions between soil and trees, studying the soil conditions beforehand is firmly recommended. The pH value in particular can provide useful information, since it affects the roots' uptake of several elements. Increasing the number of sampled individuals can increase the sturdiness of the results and mitigate the level of uncertainty, while a higher number of measurement per samples allows the application of more thorough statistical calculations. Lastly, considering the sensitivity of the analytical methods employed, either precise measurements of distances between the pollution sources and the sampled trees should be recorded, or only trees at a similar distance, independently of the site, should be sampled.

References

- Abrams, M. D. (2011). Adaptations of forest ecosystems to air pollution and climate change. *Tree Physiology*, 31(3) 258-261.
- Achim, A., Gardiner, B., Leban, J. M., & Daquitaine, R. (2006). Predicting the branching properties of Sitka spruce grown in Great Britain. *New Zealand Journal of Forestry Science*, 36(2/3), 246-264.
- Agarwal, A. K., Gupta, T., & Kothari, A. (2011). Particulate emissions from biodiesel vs diesel fuelled compression ignition engine. *Renewable and Sustainable Energy Reviews*, 15(6), 3278-3300.
- Agrios, G. N. (2005). Effects of pathogens on plant physiological functions. *Plant Pathology*, 54, 1157-1167.
- Al-Thani, H., Koç, M., & Isaifan, R. J. (2018). A review on the direct effect of particulate atmospheric pollution on materials and its mitigation for sustainable cities and societies. *Environmental Science and Pollution Research*, 25(28), 27839-27857.
- Arnold, J., Gustin, M. S., & Weisberg, P. J. (2018). Evidence for nonstomatal uptake of Hg by aspen and translocation of Hg from foliage to tree rings in Austrian pine. *Environmental Science & Technology*, 52(3), 1174-1182.
- Augustin, S., Stephanowitz, H., Wolff, B., Schröder, J., & Hoffmann, E. (2005). Manganese in tree rings of Norway spruce as an indicator for soil chemical changes in the past. *European Journal of Forest Research*, 124(4), 313-318.
- BAK Economics AG. (2018). Die Bündner Tourismuswirtschaft im internationalen Vergleich. Retrieved from https://www.gr.ch/DE/institutionen/verwaltung/dvs/awt/Dokumente/Tourismus_Benchmarking_-_Die_Buendner_Tourismuswirtschaft_im_internationalen_Vergleich_Juni_2018.pdf
- Bardule, A., Bertins, M., Busa, L., Lazdina, D., Viksna, A., Tvrdonova, M., Kanicky, V., & Vaculovic, T. (2020). Variation of major elements and heavy metals occurrence in hybrid aspen (*Populus tremuloides* Michx. × *P. tremula* L.) tree rings in marginal land. *iForest-Biogeosciences and Forestry*, 13(1), 24-32.
- Bass, A. A., Kegel, R., Leuenberger, D., Müller, B. & Schenker, S. (2021). Switzerland's Informative Inventory Report 2021. Submission of March 2021 to the United Nations ECE Secretariat. Berne, Federal Office for the Environment, 380 pp.
- Bateman, A. S., & Kelly, S. D. (2007). Fertilizer nitrogen isotope signatures. *Isotopes in Environmental and Health Studies*, 43(3), 237-247.
- Battipaglia, G., Campelo, F., Vieira, J., Grabner, M., De Micco, V., Nabais, C., Cherubini, P., Carrer, C., Bräuning, A., Cufar, K., Di Filippo, A., Garcia-Gonzalez, I., Koprowski, M., Klisz, M., Kirdeyanov, A. V., Zafirov, N. & De Luis, M. (2016). Structure and function of intra-annual density fluctuations: mind the gaps. *Frontiers in Plant Science*, 7, 595.
- Battipaglia, G., Marzaioli, F., Lubritto, C., Altieri, S., Strumia, S., Cherubini, P., & Cotrufo, M. F. (2010). Traffic pollution affects tree-ring width and isotopic composition of *Pinus pinea*. *Science of the total Environment*, 408(3), 586-593.
- Beramendi-Orosco, L. E., Rodriguez-Estrada, M. L., Morton-Bermea, O., Romero, F. M., Gonzalez-Hernandez, G., & Hernandez-Alvarez, E. (2013). Correlations between metals in tree-rings of *Prosopis juliflora* as indicators of sources of heavy metal contamination. *Applied geochemistry*, 39, 78-84.

References

- Bernhardt-Römermann, M., Kirchner, M., Kudernatsch, T., Jakobi, G., & Fischer, A. (2006). Changed vegetation composition in coniferous forests near to motorways in Southern Germany: the effects of traffic-born pollution. *Environmental Pollution*, 143(3), 572-581.
- Bernhardt-Römermann, M., Kudernatsch, T., Pfadenhauer, J., Kirchner, M., Jakobi, G., & Fischer, A. (2007). Long-term effects of nitrogen deposition on vegetation in a deciduous forest near Munich, Germany. *Applied Vegetation Science*, 10(3), 399-406.
- Bignal, K. L., Ashmore, M. R., Headley, A. D., Stewart, K., & Weigert, K. (2007). Ecological impacts of air pollution from road transport on local vegetation. *Applied Geochemistry*, 22(6), 1265-1271.
- Binda, G., Di Iorio, A., & Monticelli, D. (2021). The what, how, why, and when of dendrochemistry:(paleo) environmental information from the chemical analysis of tree rings. *Science of The Total Environment*, 758, 143672.
- Bindler, R., Renberg, I., Klaminder, J., & Emteryd, O. (2004). Tree rings as Pb pollution archives? A comparison of 206Pb/207Pb isotope ratios in pine and other environmental media. *Science of the Total Environment*, 319(1-3), 173-183.
- Bobbink, R., Hicks, K., Galloway, J., Spranger, T., Alkemade, R., Ashmore, M., Bustamante, M., Cinderby, S., Davidson, E., Dentener, F., Emmet, B., Erisman, J.W., Fenn, M., Gilliam, F., Nordin, A., Pardo, L., & De Vries, W. (2010). Global assessment of nitrogen deposition effects on terrestrial plant diversity: a synthesis. *Ecological applications*, 20(1), 30-59.
- Bodo, A. V., & Arain, M. A. (2021). Radial variations in xylem sap flux in a temperate red pine plantation forest. *Ecological Processes*, 10(1), 1-9.
- Brandão, G. P., de Campos, R. C., & Luna, A. S. (2005). Determination of mercury in gasoline by cold vapor atomic absorption spectrometry with direct reduction in microemulsion media. *Spectrochimica Acta Part B: Atomic Spectroscopy*, 60(5), 625-631.
- Brienen, R. J., Gloor, E., & Zuidema, P. A. (2012). Detecting evidence for CO₂ fertilization from tree ring studies: The potential role of sampling biases. *Global Biogeochemical Cycles*, 26(1), GB1025.
- Bukata, A. R., & Kyser, T. K. (2007). Carbon and nitrogen isotope variations in tree-rings as records of perturbations in regional carbon and nitrogen cycles. *Environmental Science & Technology*, 41(4), 1331-1338.
- Bukata, A. R., & Kyser, T. K. (2008). Tree-ring elemental concentrations in oak do not necessarily passively record changes in bioavailability. *Science of the total environment*, 390(1), 275-286.
- Bunn, A. G. (2008). A dendrochronology program library in R (dplR). *Dendrochronologia*, 26(2), 115-124.
- Bunn, A., Korpela, M., Biondi, F., Campelo, F., Mérian, P., Qeadan, F. & Zang, C. (2021). dplR: Dendrochronology Program Library in R. R package version 1.7.2. <https://github.com/AndyBunn/dplR>
- Capano, M., Marzaioli, F., Sirignano, C., Altieri, S., Lubritto, C., D'onofrio, A., & Terrasi, F. (2010). 14C AMS measurements in tree rings to estimate local fossil CO₂ in Bosco Fontana forest (Mantova, Italy). *Nuclear Instruments and Methods in Physics Research Section B: Beam Interactions with Materials and Atoms*, 268(7-8), 1113-1116.
- Cheng, X., & Bi, X. T. (2014). A review of recent advances in selective catalytic NO_x reduction reactor technologies. *Particuology*, 16, 1-18.
- Cheung, K. L., Ntziachristos, L., Tzamkiozis, T., Schauer, J. J., Samaras, Z., Moore, K. F., & Sioutas, C. (2010). Emissions of particulate trace elements, metals and organic species from gasoline, diesel, and biodiesel passenger vehicles and their relation to oxidative potential. *Aerosol Science and Technology*, 44(7), 500-513.

References

- Choi, W. J., Kwak, J. H., Lim, S. S., Park, H. J., Chang, S. X., Lee, S. M., Arshad, M. A., Yun, S. I., & Kim, H. Y. (2017). Synthetic fertilizer and livestock manure differently affect $\delta^{15}\text{N}$ in the agricultural landscape: a review. *Agriculture, Ecosystems & Environment*, 237, 1-15.
- Clark, C. M., & Tilman, D. (2008). Loss of plant species after chronic low-level nitrogen deposition to prairie grasslands. *Nature*, 451(7179), 712-715.
- Clarke, L. J., Robinson, S. A., Hua, Q., Ayre, D. J., & Fink, D. (2012). Radiocarbon bomb spike reveals biological effects of Antarctic climate change. *Global Change Biology*, 18(1), 301-310.
- Cole, D. W. (1981). Nitrogen uptake and translocation by forest ecosystems. *Ecological Bulletins*, 219-232.
- Cooke, C. A., Martínez-Cortizas, A., Bindler, R., & Gustin, M. S. (2020). Environmental archives of atmospheric Hg deposition—A review. *Science of the Total Environment*, 709, 134800.
- Coufalík, P., Matoušek, T., Krůmal, K., Vojtišek-Lom, M., Beránek, V., & Mikuška, P. (2019). Content of metals in emissions from gasoline, diesel, and alternative mixed biofuels. *Environmental Science and Pollution Research*, 26(28), 29012-29019.
- Cutter, B. E., & Guyette, R. P. (1993). *Anatomical, chemical, and ecological factors affecting tree species choice in dendrochemistry studies* (Vol. 22, No. 3, pp. 611-619). American Society of Agronomy, Crop Science Society of America, and Soil Science Society of America.
- Danek, M., Bell, T., & Laroque, C. P. (2015). Some considerations in the reconstruction of lead levels using laser ablation: Lessons from the design stage of an urban dendrochemistry study, St. John's, Canada. *Geochronometria*, 42(1), 217-231.
- Davos-Klosters. (n.d.). *Holiday classic for connoisseurs*, Retrieved 28.12. 2020, from <https://www.davos.ch/en/information/portrait-image/klosters>
- de Castro, M. L., & Ayuso, L. E. (2000). Soxhlet extraction. *Environmental Applications*, 2000, 2701-2705.
- De Temmerman, L., Vandermeiren, K., D'Haese, D., Bortier, K., Asard, H., & Ceulemans, R. (2002). Ozone effects on trees, where uptake and detoxification meet. *Dendrobiology*, 47, 9-19.
- Di, Q., Wang, Y., Zanobetti, A., Wang, Y., Koutrakis, P., Choirat, C., Dominici, F. & Schwartz, J. D. (2017). Air pollution and mortality in the Medicare population. *New England Journal of Medicine*, 376(26), 2513-2522.
- Djuricin, S., Xu, X., & Pataki, D. E. (2012). The radiocarbon composition of tree rings as a tracer of local fossil fuel emissions in the Los Angeles basin: 1980–2008. *Journal of Geophysical Research: Atmospheres*, 117, D12302.
- Douglass, A. E. (1941). Crossdating in dendrochronology. *Journal of Forestry*, 39(10), 825-831.
- Dünser, Y. (n.d.). *20 Jahre Vereinalinie – eine Erfolgsgeschichte: Seit 1999 wintersicher vom Prättigau ins Engadin*. Retrieved 29.12.2020, from https://www.rhb.ch/fileadmin/user_upload/redaktion/Ueber_die_RhB/Medien/Dokumente/Medienmitteilungen/Medienmitteilungen_2019/20191028_20_Jahre_Vereina_Geschichte_und_Entwicklung.pdf
- Engler, S. (2005). *Umfahrung Klosters eröffnet* (Report No. 67). Retrieved from http://tools.tiefbauamt.gr.ch/pdf/tba-info-67_eroeffnung_klosters.pdf

References

- Esper, J., Niederer, R., Bebi, P., & Frank, D. (2008). Climate signal age effects—evidence from young and old trees in the Swiss Engadin. *Forest Ecology and Management*, 255(11), 3783-3789.
- Evans, R. D. (2001). Physiological mechanisms influencing plant nitrogen isotope composition. *Trends in Plant Science*, 6(3), 121-126.
- Evans, R. D. (2007). Soil nitrogen isotope composition. *Stable Isotopes in Ecology and Environmental Science*, 2, 83-98
- Federal Roads Office – FEDRO . (2020). Klosters, Mezzaselva: counting station. [Dataset]. Available upon request at the FEDRO.
- Federal Statistical Office. (n.d.) *Road vehicles - Stock, level of motorisation*. Retrieved 10.02.2021, from <https://www.bfs.admin.ch/bfs/en/home/statistics/mobility-transport/transport-infrastructure-vehicles/vehicles/road-vehicles-stock-level-motorisation.html>
- Ferretti, M., Innes, J. L., Jalkanen, R., Saurer, M., Schäffer, J., Spiecker, H., & von Wilpert, K. (2002). Air pollution and environmental chemistry—what role for tree-ring studies?. *Dendrochronologia*, 20(1-2), 159-174.
- FOEN - Federal Office for the Environment (2021). *Feuerungen und Heizungen als Luftschadstoffquellen*. Retrieved 28.07.2021, from <https://www.bafu.admin.ch/bafu/de/home/themen/luft/fachinformationen/luftschadstoffquellen/feuerungen-und-heizungen-als-luftschadstoffquellen.html>
- Garbe-Schönberg, C. D., Reimann, C., & Pavlov, V. A. (1997). Laser ablation ICP-MS analyses of tree-ring profiles in pine and birch from N Norway and NW Russia—a reliable record of the pollution history of the area?. *Environmental Geology*, 32(1), 9-16.
- García, M., Aguirre, M. Á., & Canals, A. (2017). Determination of As, Se, and Hg in fuel samples by in-chamber chemical vapor generation ICP OES using a Flow Blurring® multinebulizer. *Analytical and Bioanalytical Chemistry*, 409(23), 5481-5490.
- Gebauer, G., Giesemann, A., Schulze, E. D., & Jäger, H. J. (1994). Isotope ratios and concentrations of sulfur and nitrogen in needles and soils of *Picea abies* stands as influenced by atmospheric deposition of sulfur and nitrogen compounds. *Plant and Soil*, 164(2), 267-281.
- Gedalof, Z. E., & Berg, A. A. (2010). Tree ring evidence for limited direct CO₂ fertilization of forests over the 20th century. *Global Biogeochemical Cycles*, 24(3), GB3027.
- Gemeinde Klosters. (n.d. a). *Zahlen - Daten – Fakten*. Retrieved 28.12.2020, from <http://www.klosters-serneus.ch/de/portrait/gemeindeinzahlen/>
- Gemeinde Klosters. (n.d. b). *Verkehrsmittel*. Retrieved 28.12.2020, from <http://www.klosters-serneus.ch/de/portrait/verkehrsmittel/>
- Gessler, A., & Treydte, K. (2016). The fate and age of carbon—insights into the storage and remobilization dynamics in trees. *New Phytologist*, 209(4), 1338-1340.
- Gómez-Moreno, F. J., Artíñano, B., Ramiro, E. D., Barreiro, M., Núñez, L., Coz, E., Dimitroulopoulou, C., Vardoulakis, S., Yagüe, C., Maqueda, G., Sastre, M., Roman-Cascon, C., Santamaria, J.M. & Borge, R. (2019). Urban vegetation and particle air pollution: Experimental campaigns in a traffic hotspot. *Environmental Pollution*, 247, 195-205.
- Grantz, D. A., Garner, J. H. B., & Johnson, D. W. (2003). Ecological effects of particulate matter. *Environment International*, 29(2-3), 213-239.
- Guerrieri, M. R., Siegwolf, R. T. W., Saurer, M., Jäggi, M., Cherubini, P., Ripullone, F., & Borghetti, M. (2009). Impact of different nitrogen emission sources on tree physiology as assessed by a triple stable isotope approach. *Atmospheric Environment*, 43(2), 410-418.

References

- Günther, D., & Hattendorf, B. (2005). Solid sample analysis using laser ablation inductively coupled plasma mass spectrometry. *TrAC Trends in Analytical Chemistry*, 24(3), 255-265.
- Gupta, J. (2010). A history of international climate change policy. *Wiley Interdisciplinary Reviews: Climate Change*, 1(5), 636-653.
- Hagemeyer, J., & Hübner, C. (1999). Radial Distributions of Ph in Stems of 6-Year-Old Spruce Trees (*Picea Abies* (L.) Karst.) Grown for 2 Years in Ph-Contaminated Soil. *Water, Air, and Soil Pollution*, 111(1), 215-224.
- Hagemeyer, J., & Weinand, T. (1996). Radial distributions of Pb in stems of young Norway spruce trees grown in Pb-contaminated soil. *Tree Physiology*, 16(6), 591-594.
- Hagemeyer, J., Schäfer, H., & Breckle, S. W. (1994). Seasonal variations of nickel concentrations in annual xylem rings of Beech trees (*Fagus sylvatica* L.). *Science of the Total Environment*, 145(1-2), 111-118.
- Hart, S. C., & Classen, A. T. (2003). Potential for assessing long-term dynamics in soil nitrogen availability from variations in δ ¹⁵N of tree rings. *Isotopes in Environmental and Health Studies*, 39(1), 15-28.
- Hättenschwiler, S., Schweingruber, F. H., & Körner, C. H. (1996). Tree ring responses to elevated CO₂ and increased N deposition in *Picea abies*. *Plant, Cell & Environment*, 19(12), 1369-1378.
- Heaton, T. H. E. (1990). ¹⁵N/¹⁴N ratios of NO_x from vehicle engines and coal-fired power stations. *Tellus B*, 42(3), 304-307.
- Henriques, S. T., & Borowiecki, K. J. (2017). The drivers of long-run CO₂ emissions in Europe, North America and Japan since 1800. *Energy Policy*, 101, 537-549.
- Hoffmann, E., Lüdke, C., Scholze, H., & Stephanowitz, H. (1994). Analytical investigations of tree rings by laser ablation ICP-MS. *Fresenius' Journal of Analytical Chemistry*, 350(4), 253-259.
- Hua, Q., Barbetti, M., & Rakowski, A. (2013). Atmospheric Radiocarbon for the Period 1950–2010. *Radiocarbon*, 55(4), 2059-2072.
- Huang, J. G., Bergeron, Y., Denneler, B., Berninger, F., & Tardif, J. (2007). Response of forest trees to increased atmospheric CO₂. *Critical Reviews in Plant Sciences*, 26(5-6), 265-283.
- Huber, M., Welker, A., & Helmreich, B. (2016). Critical review of heavy metal pollution of traffic area runoff: Occurrence, influencing factors, and partitioning. *Science of the Total Environment*, 541, 895-919.
- Ibalid-Mulli, A., Wichmann, H. E., Kreyling, W., & Peters, A. (2002). Epidemiological evidence on health effects of ultrafine particles. *Journal of Aerosol Medicine*, 15(2), 189-201.
- Johnson, T. V. (2015). Review of vehicular emissions trends. *SAE International Journal of Engines*, 8(3), 1152-1167.
- Keeling, C. D., Piper, S. C., Bacastow, R. B., Wahlen, M., Whorf, T. P., Heimann, M., & Meijer, H. A. (2001). Exchanges of atmospheric CO₂ and ¹³CO₂ with the terrestrial biosphere and oceans from 1978 to 2000. I. Global aspects. SIO Reference Series, No. 01-06. Scripps Institution of Oceanography, San Diego.
- Kienast, F., & Luxmoore, R. J. (1988). Tree-ring analysis and conifer growth responses to increased atmospheric CO₂ levels. *Oecologia*, 76(4), 487-495.
- Kim, J. Y., Park, J., Choi, J., & Kim, J. (2020). Determination of Metal Concentration in Road-Side Trees from an Industrial Area Using Laser Ablation Inductively Coupled Plasma Mass Spectrometry. *Minerals*, 10(2), 175.

References

- Klein, T., Bader, M. K. F., Leuzinger, S., Mildner, M., Schleppei, P., Siegwolf, R. T., & Körner, C. (2016). Growth and carbon relations of mature *Picea abies* trees under 5 years of free-air CO₂ enrichment. *Journal of Ecology*, *104*(6), 1720-1733.
- Klosters Tourismus. (2017). Jahresbericht 2016/2017. Retrieved from https://www.davos.ch/fileadmin/user_upload/dokumente/Service/Medien/DDO/Geschaeftsbericht_Klosters_2016-17_web.pdf
- Klosters Tourismus. (2018). Jahresbericht 2017/2018. Retrieved from https://www.davos.ch/fileadmin/user_upload/dokumente/Service/Medien/DDO/Geschaeftsbericht_Klosters_2017-18_web.pdf
- Koerner, W., Dambrine, E., Dupouey, J. L., & Benoit, M. (1999). $\delta^{15}\text{N}$ of forest soil and understorey vegetation reflect the former agricultural land use. *Oecologia*, *121*(3), 421-425.
- Krzyżanowski, M., Kuna-Dibbert, B., & Schneider, J. (Eds.). (2005). *Health effects of transport-related air pollution*. WHO Regional Office Europe.
- Lee, B. J., Kim, B., & Lee, K. (2014). Air pollution exposure and cardiovascular disease. *Toxicological research*, *30*(2), 71-75.
- Lee, M. A., Davies, L., & Power, S. A. (2012). Effects of roads on adjacent plant community composition and ecosystem function: an example from three calcareous ecosystems. *Environmental Pollution*, *163*, 273-280.
- Leonelli, G., Battipaglia, G., Siegwolf, R. T., Saurer, M., di Cella, U. M., Cherubini, P., & Pelfini, M. (2012). Climatic isotope signals in tree rings masked by air pollution: A case study conducted along the Mont Blanc Tunnel access road (Western Alps, Italy). *Atmospheric Environment*, *61*, 169-179.
- Levin, I., & Kromer, B. (2004). The tropospheric ¹⁴CO₂ level in mid-latitudes of the Northern Hemisphere (1959–2003). *Radiocarbon*, *46*(3), 1261-1272.
- Levin, I., Hammer, S., Kromer, B., & Meinhardt, F. (2008). Radiocarbon observations in atmospheric CO₂: determining fossil fuel CO₂ over Europe using Jungfrauoch observations as background. *Science of the Total Environment*, *391*(2-3), 211-216.
- Lim, S. S., Lee, S. M., Lee, S. H., & Choi, W. J. (2010). Nitrogen isotope compositions of synthetic fertilizer, raw livestock manure slurry, and composted livestock manure. *Korean Journal of Soil Science and Fertilizer*, *43*(4), 453-457.
- Lindsay, R. (2020). Climate Change: Atmospheric Carbon Dioxide. Retrieved 19.04.2021, from <https://www.climate.gov/news-features/understanding-climate/climate-change-atmospheric-carbon-dioxide#:~:text=The%20global%20average%20atmospheric%20carbon,plus%20or%20minus%200.1%20ppm>.
- Liu, C., Shi, J. W., Gao, C., & Niu, C. (2016). Manganese oxide-based catalysts for low-temperature selective catalytic reduction of NO_x with NH₃: A review. *Applied Catalysis A: General*, *522*, 54-69.
- Liu, Z. G., Ottinger, N. A., & Creemeens, C. M. (2015). Vanadium and tungsten release from V-based selective catalytic reduction diesel aftertreatment. *Atmospheric Environment*, *104*, 154-161.
- Locosselli, G. M., Chacón-Madrid, K., Arruda, M. A. Z., de Camargo, E. P., Moreira, T. C. L., de André, C. D. S., Singer, J. M., Saldiva, P. H. N., & Buckeridge, M. S. (2018). Tree rings reveal the reduction of Cd, Cu, Ni and Pb pollution in the central region of São Paulo, Brazil. *Environmental pollution*, *242*, 320-328.
- Longerich, H. P., Jackson, S. E., & Gunther, D. (1997). Laser ablation inductively coupled plasma mass spectrometric transient signal data acquisition and analyte concentration

References

- calculation (vol 11, pg 899, 1996). *Journal of Analytical Atomic Spectrometry*, 12(3), 391-391.
- Longuetaud, F., Mothe, F., Leban, J. M., & Mäkelä, A. (2006). Picea abies sapwood width: variations within and between trees. *Scandinavian Journal of Forest Research*, 21(1), 41-53.
 - Marshall, J. D., Brooks, J. R., & Lajtha, K. (2007). Sources of variation in the stable isotopic composition of plants. *Stable Isotopes in Ecology and Environmental Science*, 2, 22-60.
 - Martinelli, N. (2004). Climate from dendrochronology: latest developments and results. *Global and Planetary Change*, 40(1-2), 129-139.
 - Matyssek, R., & Sandermann, H. (2003). Impact of ozone on trees: an ecophysiological perspective. In *Progress in botany* (pp. 349-404). Springer, Berlin, Heidelberg.
 - Maxwell, R. S., Wixom, J. A., & Hessl, A. E. (2011). A comparison of two techniques for measuring and crossdating tree rings. *Dendrochronologia*, 29(4), 237-243.
 - McDonald, L., Chivall, D., Miles, D., & Ramsey, C. B. (2019). Seasonal variations in the ¹⁴C content of tree rings: Influences on radiocarbon calibration and single-year curve construction. *Radiocarbon*, 61(1), 185-194.
 - Meerts, P. (2002). Mineral nutrient concentrations in sapwood and heartwood: a literature review. *Annals of Forest Science*, 59(7), 713-722.
 - Mihaljevič, M., Ettler, V., Šebek, O., Sracek, O., Kříbek, B., Kyncl, T., Mayer, V. & Veselovský, F. (2011). Lead isotopic and metallic pollution record in tree rings from the Copperbelt mining–smelting area, Zambia. *Water, Air, & Soil Pollution*, 216(1-4), 657-668.
 - Mokgalaka, N. S., & Gardea-Torresdey, J. L. (2006). Laser ablation inductively coupled plasma mass spectrometry: Principles and applications. *Applied Spectroscopy Reviews*, 41(2), 131-150.
 - Molnár, M., Bujtás, T., Futó, I., & Světlík, I. (2007). Monitoring of atmospheric excess ¹⁴C around Paks nuclear power plant, Hungary. *Radiocarbon*, 49(2), 1031-1043.
 - Monticelli, D., Di Iorio, A., Ciceri, E., Castelletti, A., & Dossi, C. (2009). Tree ring microanalysis by LA–ICP–MS for environmental monitoring: validation or refutation? Two case histories. *Microchimica Acta*, 164(1), 139-148.
 - Myung, C. L., & Park, S. (2012). Exhaust nanoparticle emissions from internal combustion engines: A review. *International Journal of Automotive Technology*, 13(1), 9.
 - Němec, M., Wacker, L., Hajdas, I., & Gäggeler, H. (2010). Alternative methods for cellulose preparation for AMS measurement. *Radiocarbon*, 52(3), 1358-1370.
 - Novak, K., De Luis, M., Saz, M. A., Longares, L. A., Serrano-Notivol, R., Raventós, J., Cufar K., Gricar, J., Di Filippo, A., Piovesan, G., Rathgeber, C. B. K., Papadopoulos, A. & Smith, K. T. (2016). Missing rings in Pinus halepensis—the missing link to relate the tree-ring record to extreme climatic events. *Frontiers in Plant Science*, 7, 727.
 - Novak, M., Mikova, J., Krachler, M., Kosler, J., Erbanova, L., Prechova, E., Jackova, I., & Fottova, D. (2010). Radial distribution of lead and lead isotopes in stem wood of Norway spruce: A reliable archive of pollution trends in Central Europe. *Geochimica et Cosmochimica Acta*, 74(15), 4207-4218.
 - Paoletti, E., Schaub, M., Matyssek, R., Wieser, G., Augustaitis, A., Bastrup-Birk, A. M., Bytnerowicz, A., Günthardt-Georg, M.S., Müller-Starck, G. & Serengil, Y. (2010). Advances of air pollution science: from forest decline to multiple-stress effects on forest ecosystem services. *Environmental Pollution*, 158(6), 1986-1989.
 - Peckham, M. A., Gustin, M. S., Weisberg, P. J., & Weiss-Penzias, P. (2019). Results of a controlled field experiment to assess the use of tree tissue concentrations as bioindicators of air Hg. *Biogeochemistry*, 142(2), 265-279.

References

- Piotrowska, N., Tomczyk, J., Pawełczyk, S., & Stanaszek, Ł. M. (2019). Radiocarbon AMS dating of Mesolithic human remains from Poland. *Radiocarbon*, *61*(4), 991-1007.
- Pozebon, D., Scheffler, G. L., Dressler, V. L., & Nunes, M. A. (2014). Review of the applications of laser ablation inductively coupled plasma mass spectrometry (LA-ICP-MS) to the analysis of biological samples. *Journal of Analytical Atomic Spectrometry*, *29*(12), 2204-2228.
- Prohaska, T., Stadlbauer, C., Wimmer, R., Stingeder, G., Latkoczy, C., Hoffmann, E., & Stephanowitz, H. (1998). Investigation of element variability in tree rings of young Norway spruce by laser-ablation-ICPMS. *Science of the Total Environment*, *219*(1), 29-39.
- Przybysz, A., Sæbø, A., Hanslin, H. M., & Gawroński, S. W. (2014). Accumulation of particulate matter and trace elements on vegetation as affected by pollution level, rainfall and the passage of time. *Science of the Total Environment*, *481*, 360-369.
- R Core Team (2020). R: A language and environment for statistical computing. R Foundation for Statistical Computing, Vienna, Austria. URL <https://www.R-project.org/>.
- Rabl, A., & Spadaro, J. V. (2000). Public health impact of air pollution and implications for the energy system. *Annual review of Energy and the Environment*, *25*(1), 601-627.
- Rakowski, A. Z., Nakamura, T., & Pazdur, A. (2008). Variations of anthropogenic CO₂ in urban area deduced by radiocarbon concentration in modern tree rings. *Journal of Environmental Radioactivity*, *99*(10), 1558-1565.
- Rakowski, A. Z., Nakamura, T., Pazdur, A., Charro, E., Villanueva, J. L. G., & Piotrowska, N. (2010). Radiocarbon concentration in modern tree rings from Valladolid, Spain. *Nuclear Instruments and Methods in Physics Research Section B: Beam Interactions with Materials and Atoms*, *268*(7-8), 1110-1112.
- Rauch, S., Hemond, H. F., Barbante, C., Owari, M., Morrison, G. M., Peucker-Ehrenbrink, B., & Wass, U. (2005). Importance of automobile exhaust catalyst emissions for the deposition of platinum, palladium, and rhodium in the northern hemisphere. *Environmental Science & Technology*, *39*(21), 8156-8162.
- Reimer, P. J., Brown, T. A., & Reimer, R. W. (2004). Discussion: reporting and calibration of post-bomb ¹⁴C data. *Radiocarbon*, *46*(3), 1299-1304.
- Rodriguez, D. R. O., de Carvalho, H. W. P., & Tomazello-Filho, M. (2018). Nutrient concentrations of 17-year-old *Pinus taeda* annual tree-rings analyzed by X-ray fluorescence microanalysis. *Dendrochronologia*, *52*, 67-79.
- Rohner, S. (2019). Autoverlad Vereina: Verladene Fahrzeuge 1999 – 2018. Retrieved 29.12.2020, from https://www.rhb.ch/fileadmin/user_upload/redaktion/Ueber_die_RhB/Medien/Dokumente/Medienmitteilungen/Medienmitteilungen_2019/20191028_Autoverlad_1999-2018.pdf
- Rönkkö, T., Pirjola, L., Ntziachristos, L., Heikkilä, J., Karjalainen, P., Hillamo, R., & Keskinen, J. (2014). Vehicle engines produce exhaust nanoparticles even when not fueled. *Environmental science & technology*, *48*(3), 2043-2050.
- Rybski, D., & Neumann, J. (2011). A review on the Pettitt test. In *In extremis* (pp. 202-213). Springer, Berlin, Heidelberg.
- Sala, A., Woodruff, D. R., & Meinzer, F. C. (2012). Carbon dynamics in trees: feast or famine?. *Tree physiology*, *32*(6), 764-775.
- Santos, D. S., Korn, M. G. A., Guida, M. A., Santos, G. L. D., Lemos, V. A., & Teixeira, L. S. (2011). Determination of copper, iron, lead and zinc in gasoline by sequential multi-element flame atomic absorption spectrometry after solid phase extraction. *Journal of the Brazilian Chemical Society*, *22*(3), 552-557.

References

- Sassykova, L. R., Aubakirov, Y. A., Sendilvelan, S., Tashmukhambetova, Z. K., Faizullaeva, M. F., & Bhaskar, K. (2019). The main components of vehicle exhaust gases and their effective catalytic neutralization. *Oriental Journal of Chemistry*, 35(1), 110-127.
- Saurer, M., Cherubini, P., Bonani, G., & Siegwolf, R. (2003). Tracing carbon uptake from a natural CO₂ spring into tree rings: an isotope approach. *Tree Physiology*, 23(14), 997-1004.
- Saurer, M., Cherubini, P., Ammann, M., De Cinti, B., & Siegwolf, R. (2004). First detection of nitrogen from NO_x in tree rings: a ¹⁵N/¹⁴N study near a motorway. *Atmospheric Environment*, 38(18), 2779-2787.
- Savard, M. M., Bégin, C., Smirnoff, A., Marion, J., & Rioux-Paquette, E. (2009). Tree-ring nitrogen isotopes reflect anthropogenic NO_x emissions and climatic effects. *Environmental Science & Technology*, 43(3), 604-609.
- Savard, M. M. (2010). Tree-ring stable isotopes and historical perspectives on pollution—An overview. *Environmental Pollution*, 158(6), 2007-2013.
- Sawidis, T., Breuste, J., Mitrovic, M., Pavlovic, P., & Tsigaridas, K. (2011). Trees as bioindicator of heavy metal pollution in three European cities. *Environmental pollution*, 159(12), 3560-3570.
- Schleppei, P., Bucher-Wallin, L., Siegwolf, R., Saurer, M., Muller, N., & Bucher, J. B. (1999). Simulation of increased nitrogen deposition to a montane forest ecosystem: partitioning of the added ¹⁵N. *Water, Air, and Soil Pollution*, 116(1), 129-134.
- Schweingruber, F. H. (1996). *Tree rings and environment: dendroecology*. Paul Haupt AG Bern.
- Sellin, A. (1996). Sapwood amount in *Picea abies* (L.) Karst. Determined by tree age and radial growth rate. *Holzforschung*, 50(4), 291-296.
- Sensuła, B., Michczyński, A., Piotrowska, N., & Wilczyński, S. (2018). Anthropogenic CO₂ emission records in Scots Pine growing in the most industrialized region of Poland from 1975 to 2014. *Radiocarbon*, 60(4), 1041-1053.
- Sezgin, N., Ozcan, H. K., Demir, G., Nemlioglu, S., & Bayat, C. (2004). Determination of heavy metal concentrations in street dusts in Istanbul E-5 highway. *Environment International*, 29(7), 979-985.
- Slezakova, K., Morais, S., & Carmo Pereir, M. do. (2013). Atmospheric Nanoparticles and Their Impacts on Public Health. In *Current Topics in Public Health*. IntechOpen.
- Sookdeo, A., Kromer, B., Büntgen, U., Friedrich, M., Friedrich, R., Helle, G., Pauli, M., Nievergelt, D., Reinig F., Treydte, K., Synal, H.A. & Wacker, L. (2020). Quality dating: a well-defined protocol implemented at ETH for high-precision ¹⁴C-dates tested on late glacial wood. *Radiocarbon*, 62(4), 891-899.
- Stenström, K., Skog, G., Georgiadou, E., Genberg, J., & Mellström, A. (2011). A guide to radiocarbon units and calculations. Lund University, Nuclear Physics.
- Stewart, G. R., Aidar, M. P., Joly, C. A., & Schmidt, S. (2002). Impact of point source pollution on nitrogen isotope signatures ($\delta^{15}\text{N}$) of vegetation in SE Brazil. *Oecologia*, 131(3), 468-472.
- Stille, P., Schmitt, A. D., Labolle, F., Pierret, M. C., Gangloff, S., Cobert, F., Lucot, E., Guéguen, F., Brioschi, L., Steinmann, M., & Chabaux, F. (2012). The suitability of annual tree growth rings as environmental archives: evidence from Sr, Nd, Pb and Ca isotopes in spruce growth rings from the Strengbach watershed. *Comptes Rendus Geoscience*, 344(5), 297-311.
- swisstopo – Federal office of topography. <https://www.swisstopo.admin.ch/en/home.html>

References

- Taiz, L., & Zeiger, E. (2002). *Plant Physiology*. Sunderland, MA. *Sinauer Associates, Inc., Publishers*, 3, 484.
- Taylor, A. F. S., Martin, F., & Read, D. J. (2000). Fungal diversity in ectomycorrhizal communities of Norway spruce [*Picea abies* (L.) Karst.] and beech (*Fagus sylvatica* L.) along north-south transects in Europe. In *Carbon and nitrogen cycling in European forest ecosystems* (pp. 343-365). Springer, Berlin, Heidelberg.
- Telewski, F. W., Swanson, R. T., Strain, B. R., & Burns, J. M. (1999). Wood properties and ring width responses to long-term atmospheric CO₂ enrichment in field-grown loblolly pine (*Pinus taeda* L.). *Plant, Cell & Environment*, 22(2), 213-219.
- Tendel, J., & Wolf, K. (1988). Distribution of nutrients and trace elements in annual rings of pine trees (*Pinus silvestris*) as an indicator of environmental changes. *Experientia*, 44(11), 975-980.
- Tiefbauamt des Kantons Graubünden (1991). *A 28 a Prättigauerstrasse Umfahrungen Küblis, Saas, Klosters: Abschnitt Büel – Sellfranga*. Holinger AG, Baden.
- Tilako, B. H., Ogbodo, S. O., Okonkwo, I. N., Nubila, I. N., Shuneba, I. L., Ogbonna, E., Odoma, S., Gali, R.M., Basse, E. B.; & Shu, E. N. (2020). Distribution and interactions of priority heavy metals with some antioxidant micronutrients in inhabitants of a lead-zinc mining community of ebonyi state, Nigeria. *Advances in Toxicology and Toxic Effects*, 4(1), 011-017.
- Tiwari, M., Singh, A. K., & Sinha, D. K. (2015). Stable isotopes: Tools for understanding past climatic conditions and their applications in chemostratigraphy. In *Chemostratigraphy* (pp. 65-92). Elsevier.
- Tognetti, R., Cherubini, P., & Innes, J. L. (2000). Comparative stem-growth rates of Mediterranean trees under background and naturally enhanced ambient CO₂ concentrations. *The New Phytologist*, 146(1), 59-74.
- Tomlinson, G., Siegwolf, R. T., Buchmann, N., Schleppi, P., Waldner, P., & Weber, P. (2014). The mobility of nitrogen across tree-rings of Norway spruce (*Picea abies* L.) and the effect of extraction method on tree-ring $\delta^{15}\text{N}$ and $\delta^{13}\text{C}$ values. *Rapid Communications in Mass Spectrometry*, 28(11), 1258-1264.
- Truscott, A. M., Palmer, S. C. F., McGowan, G. M., Cape, J. N., & Smart, S. (2005). Vegetation composition of roadside verges in Scotland: the effects of nitrogen deposition, disturbance and management. *Environmental Pollution*, 136(1), 109-118.
- Turkyilmaz, A., Sevik, H., Isinkaralar, K., & Cetin, M. (2019). Use of tree rings as a bioindicator to observe atmospheric heavy metal deposition. *Environmental Science and Pollution Research*, 26(5), 5122-5130.
- Vacek, S., Hůnová, I., Vacek, Z., Hejčmanová, P., Podrázský, V., Král, J., Putalová, T. & Moser, W. K. (2015). Effects of air pollution and climatic factors on Norway spruce forests in the Orlické hory Mts. (Czech Republic), 1979–2014. *European Journal of Forest Research*, 134(6), 1127-1142.
- Vallano, D. M., & Sparks, J. P. (2007). Foliar ^{15}N values as indicators of foliar uptake of atmospheric nitrogen pollution. In Dawson, T. E., & Siegwolf, T. W. (eds), *Stable isotopes as indicators of ecological change* (pp. 93-109), Elsevier.
- Van der Plicht, J., & Hogg, A. (2006). A note on reporting radiocarbon. *Quaternary Geochronology*, 1(4), 237-240.
- Walters, W. W., Goodwin, S. R., & Michalski, G. (2015). Nitrogen Stable Isotope Composition ($\delta^{15}\text{N}$) of Vehicle-Emitted NO_x. *Environmental Science & Technology*, 49(4), 2278-2285.

References

- Wang, X., Yuan, W., Lin, C. J., Wu, F., & Feng, X. (2021). Stable mercury isotopes stored in Masson Pinus tree rings as atmospheric mercury archives. *Journal of Hazardous Materials*, 415, 125678.
- Watmough, S. A. (1997). An evaluation of the use of dendrochemical analyses in environmental monitoring. *Environmental Reviews*, 5(3-4), 181-201.
- Watmough, S. A. (1999). Monitoring historical changes in soil and atmospheric trace metal levels by dendrochemical analysis. *Environmental pollution*, 106(3), 391-403.
- Weatherbase. (n.d.) *Klosters, Switzerland*. Retrieved 10.05.2021, from <http://www.weatherbase.com/weather/weather-summary.php?s=29760&cityname=Klosters%2C+Grisons%2C+Switzerland&units=&set=metric>
- Zhang, J. J., Wei, Y., & Fang, Z. (2019). Ozone pollution: a major health hazard worldwide. *Frontiers in Immunology*, 10, 2518.
- Zhang, R., Wang, G., Guo, S., Zamora, M. L., Ying, Q., Lin, Y., Wang, W. Hu, M., Wang, Y. & Wang, Y. (2015). Formation of urban fine particulate matter. *Chemical Reviews*, 115(10), 3803-3855.
- Zyskowski, E., Wu, F., & Amarasiriwardena, D. (2021). Investigation of pollution history in XKS mining area in China using dendrochronology and LA-ICP-MS. *Environmental Pollution*, 269, 116107.

Appendix

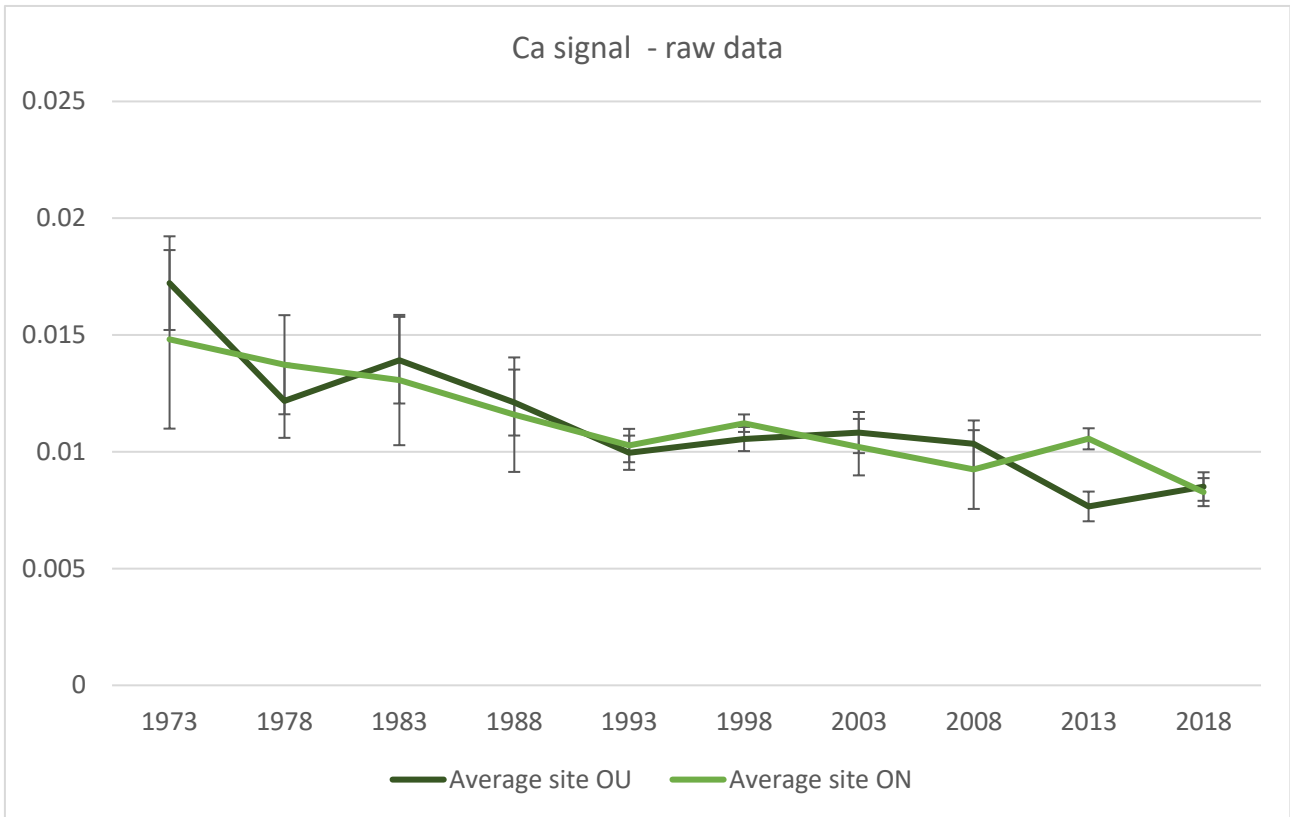


Figure 26: Raw average signal per site for the element Ca (\pm SE).

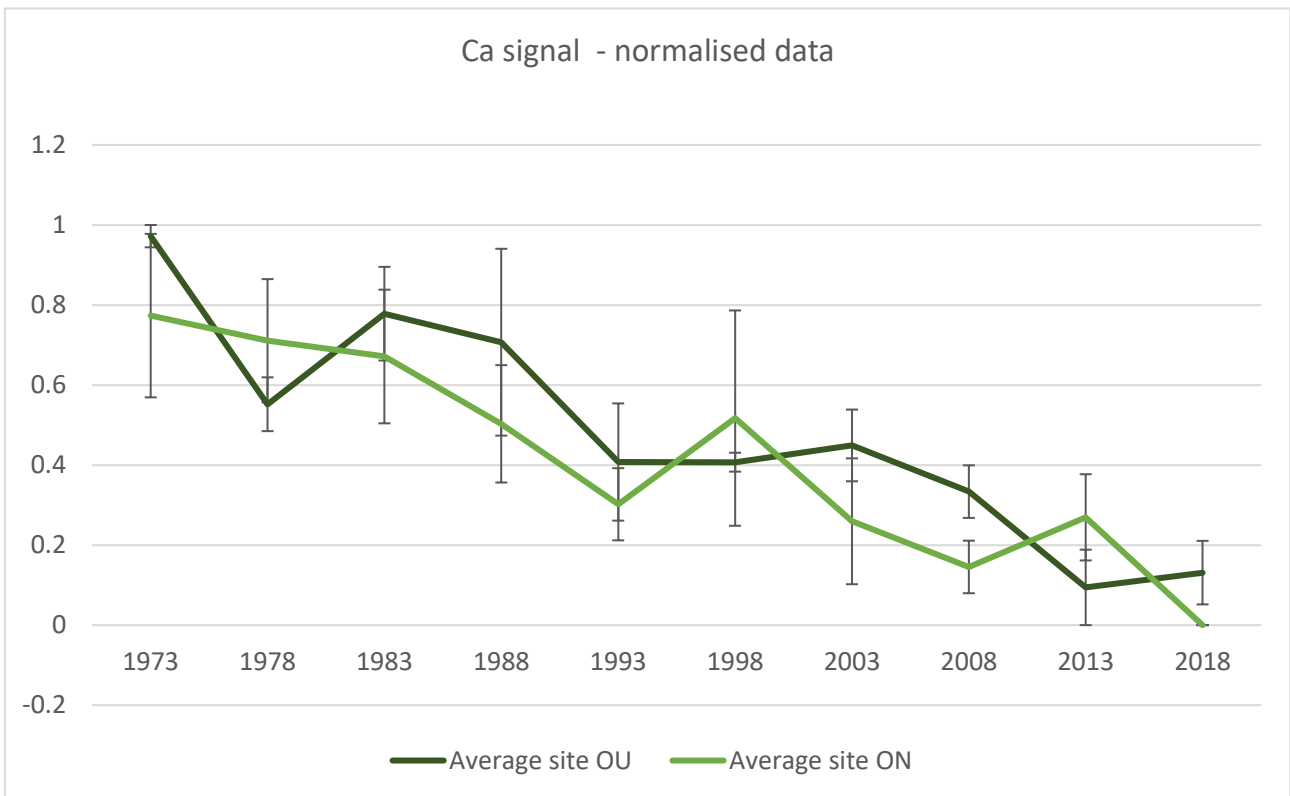


Figure 27: Normalised average signal per site for the element Ca (\pm SE).

Appendix

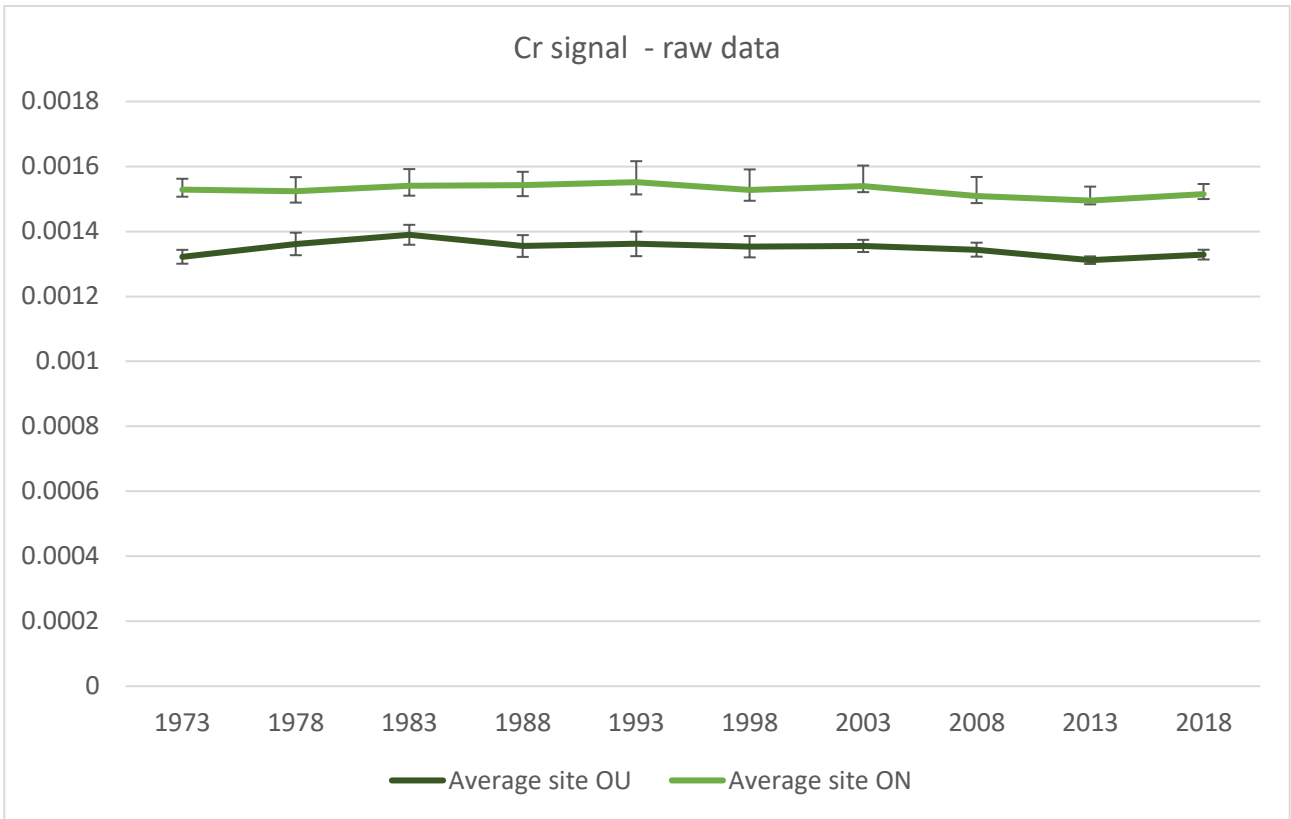


Figure 28: Raw average signal per site for the element Cr ($\pm SE$).

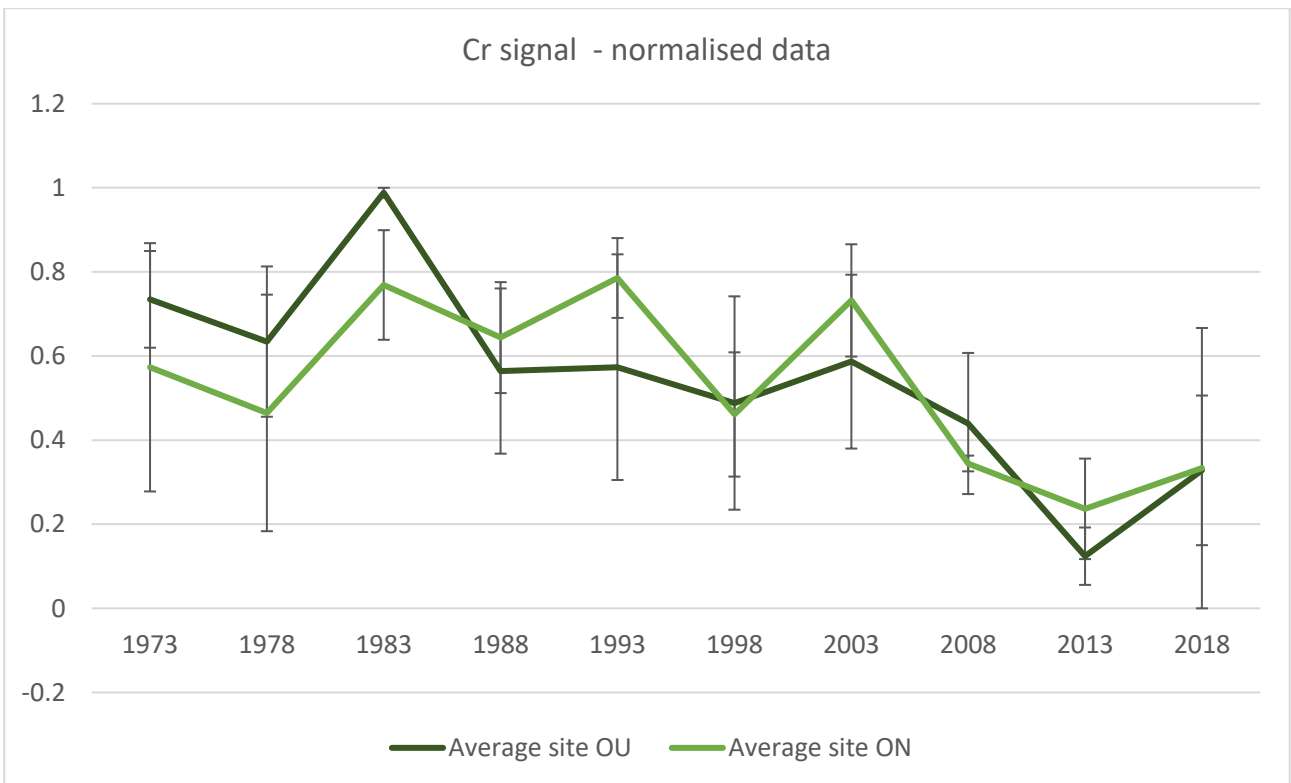


Figure 29: Normalised average signal per site for the element Cr ($\pm SE$).

Appendix

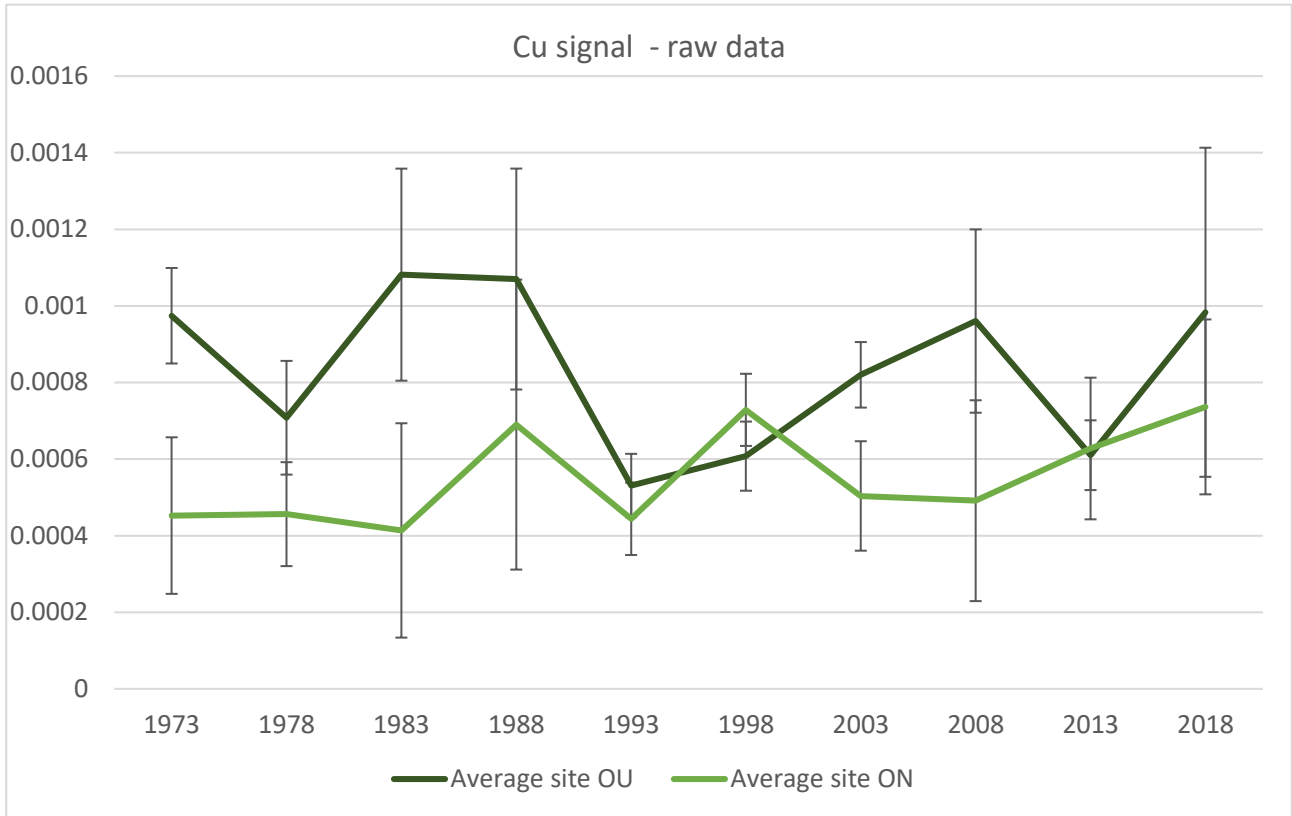


Figure 30: Raw average signal per site for the element Cu (\pm SE).

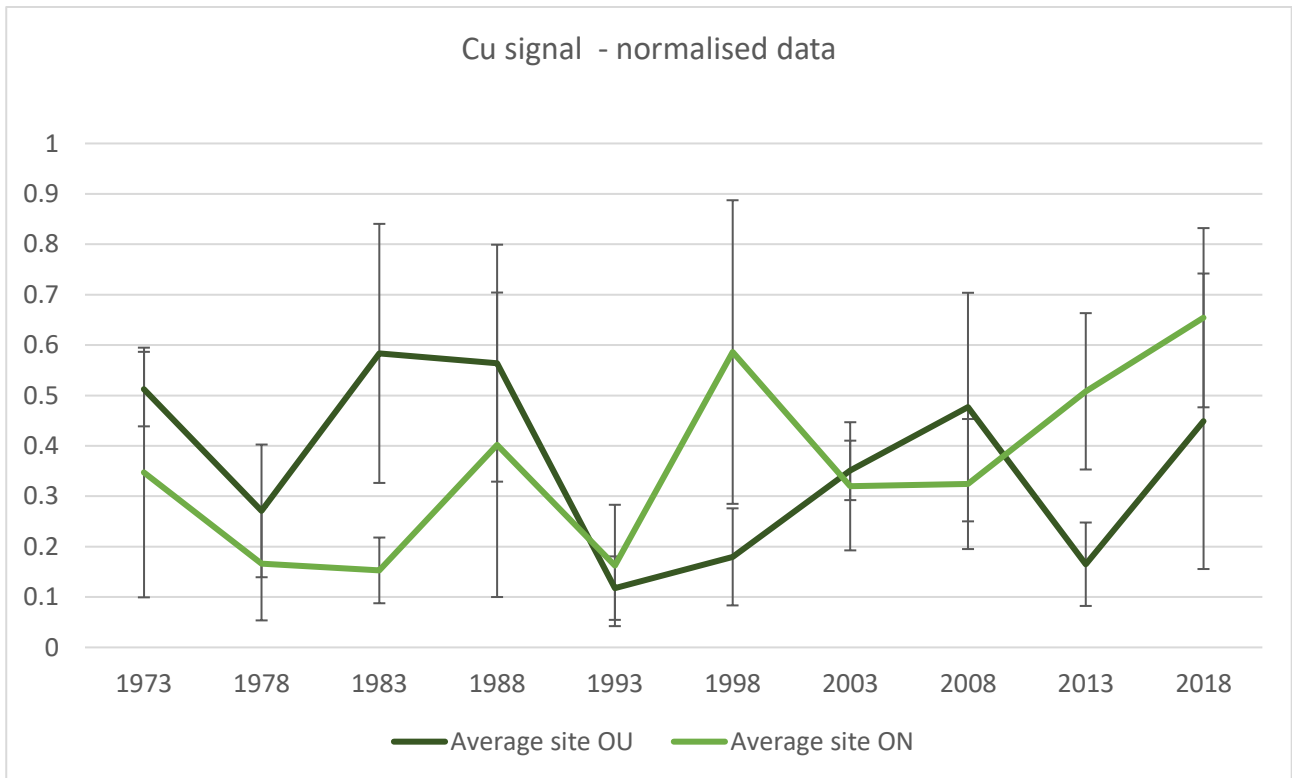


Figure 31: Normalised average signal per site for the element Cu (\pm SE).

Appendix

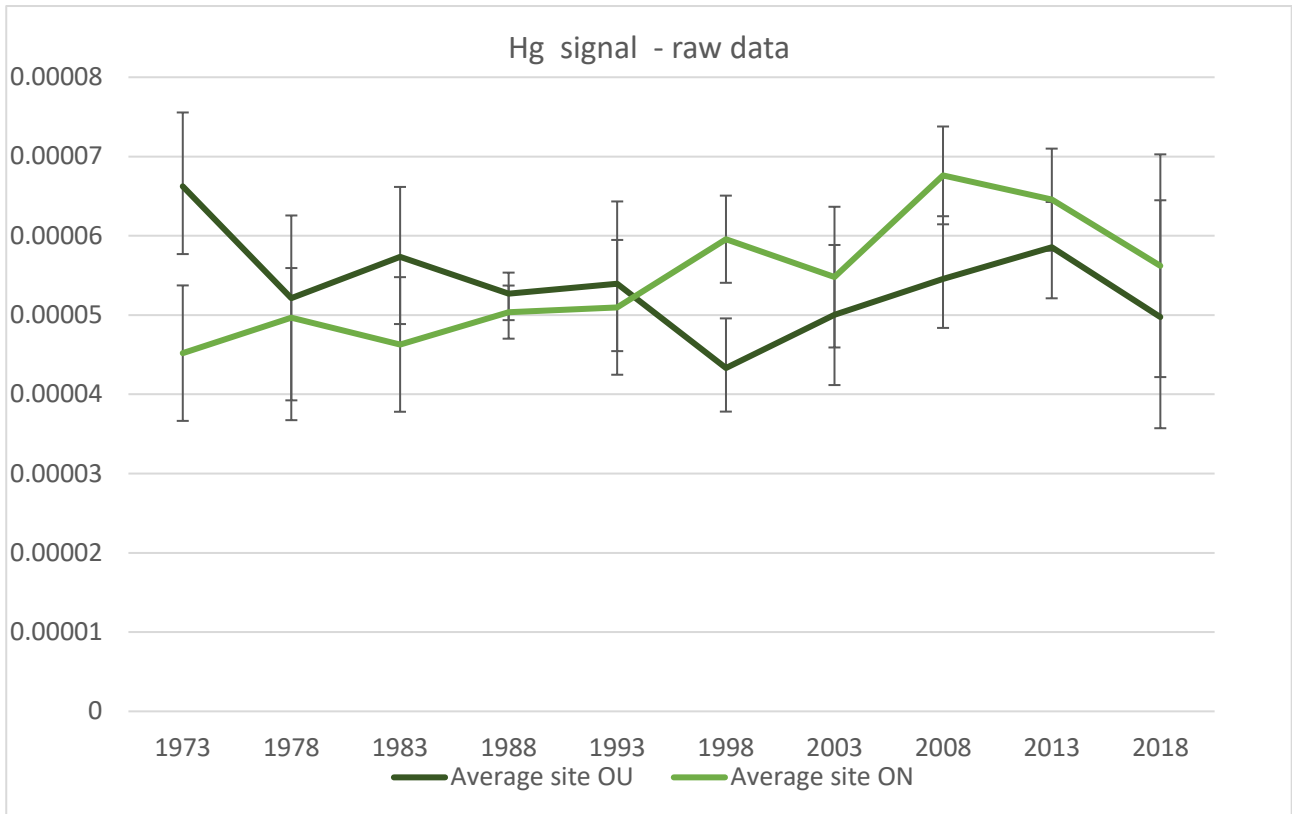


Figure 32: Raw average signal per site for the element Hg ($\pm SE$).

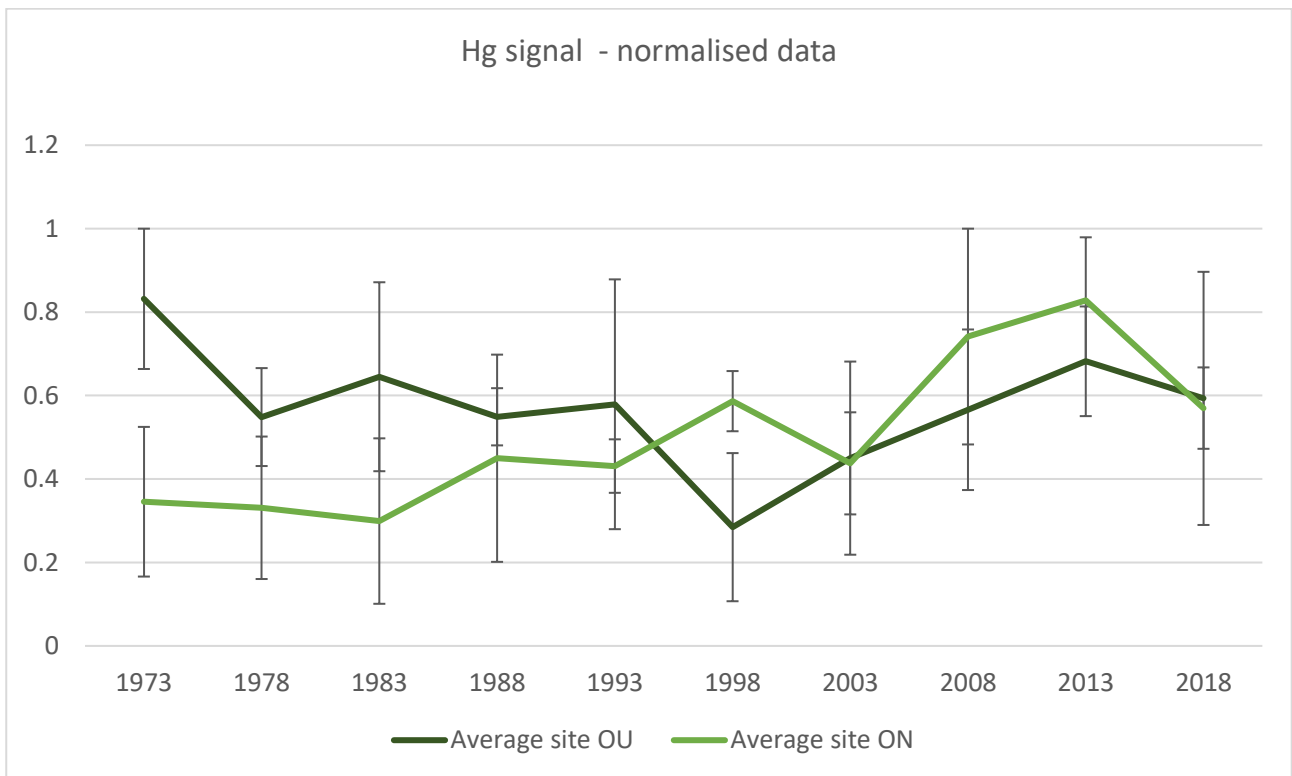


Figure 33: Normalised average signal per site for the element Hg ($\pm SE$).

Appendix

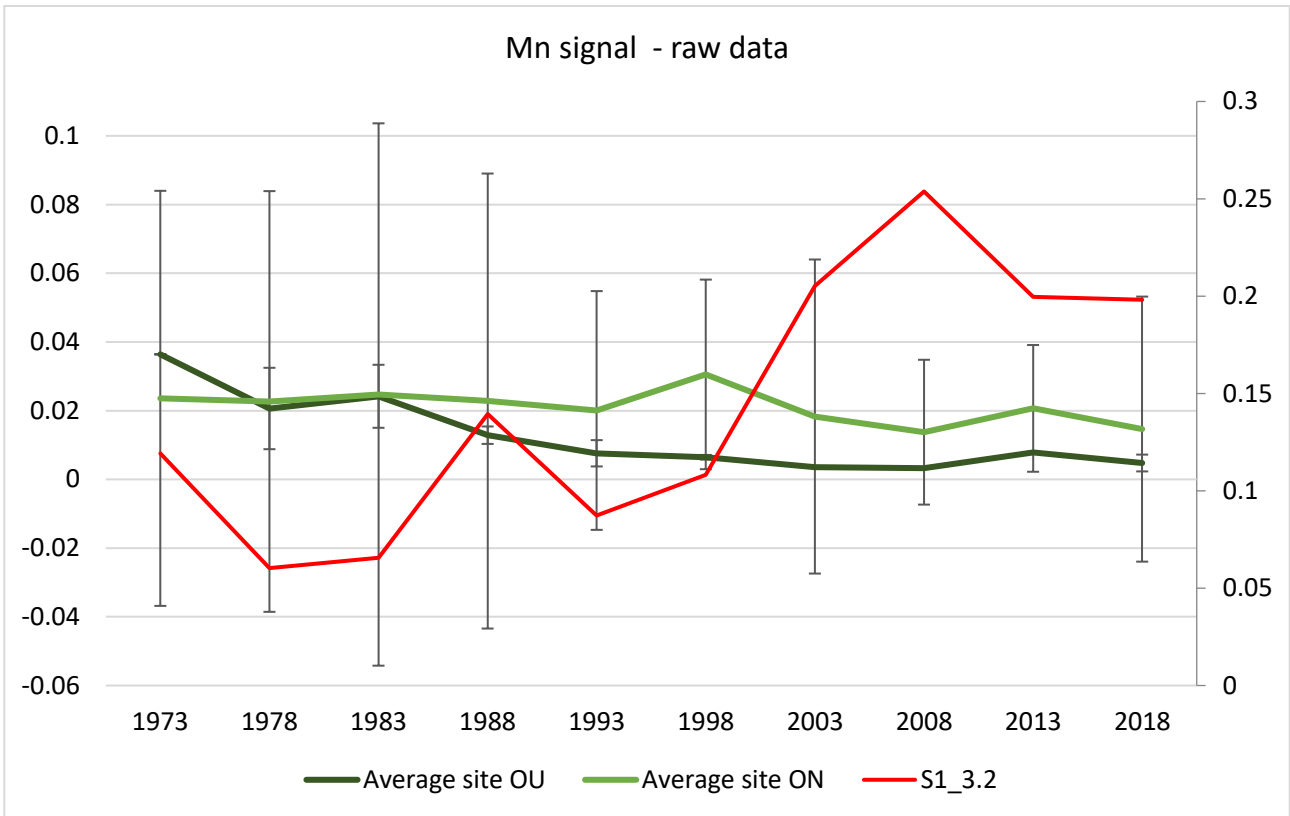


Figure 34: Raw average signal per site for the element Mn (\pm SE), with the concentration of tree 3.2 OU on the secondary y-axis.

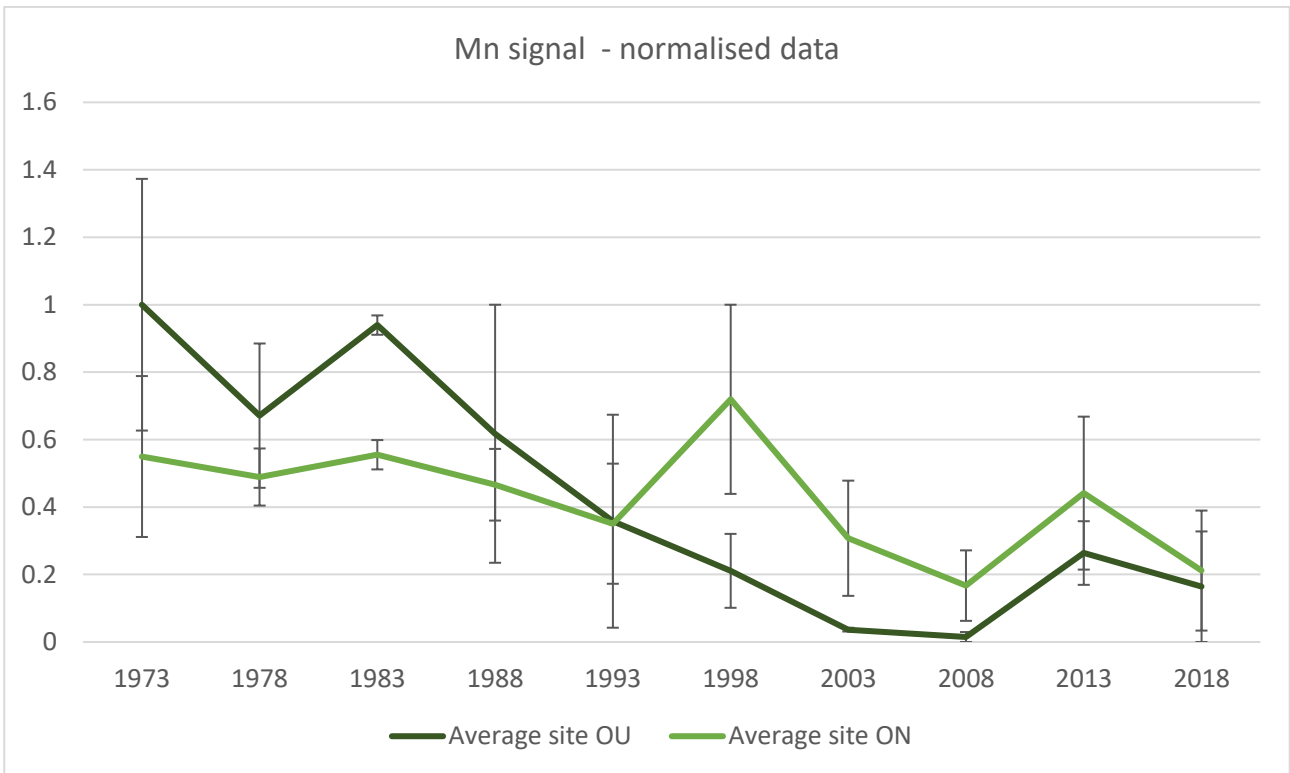


Figure 35: Normalised average signal per site for the element Mn (\pm SE).

Appendix

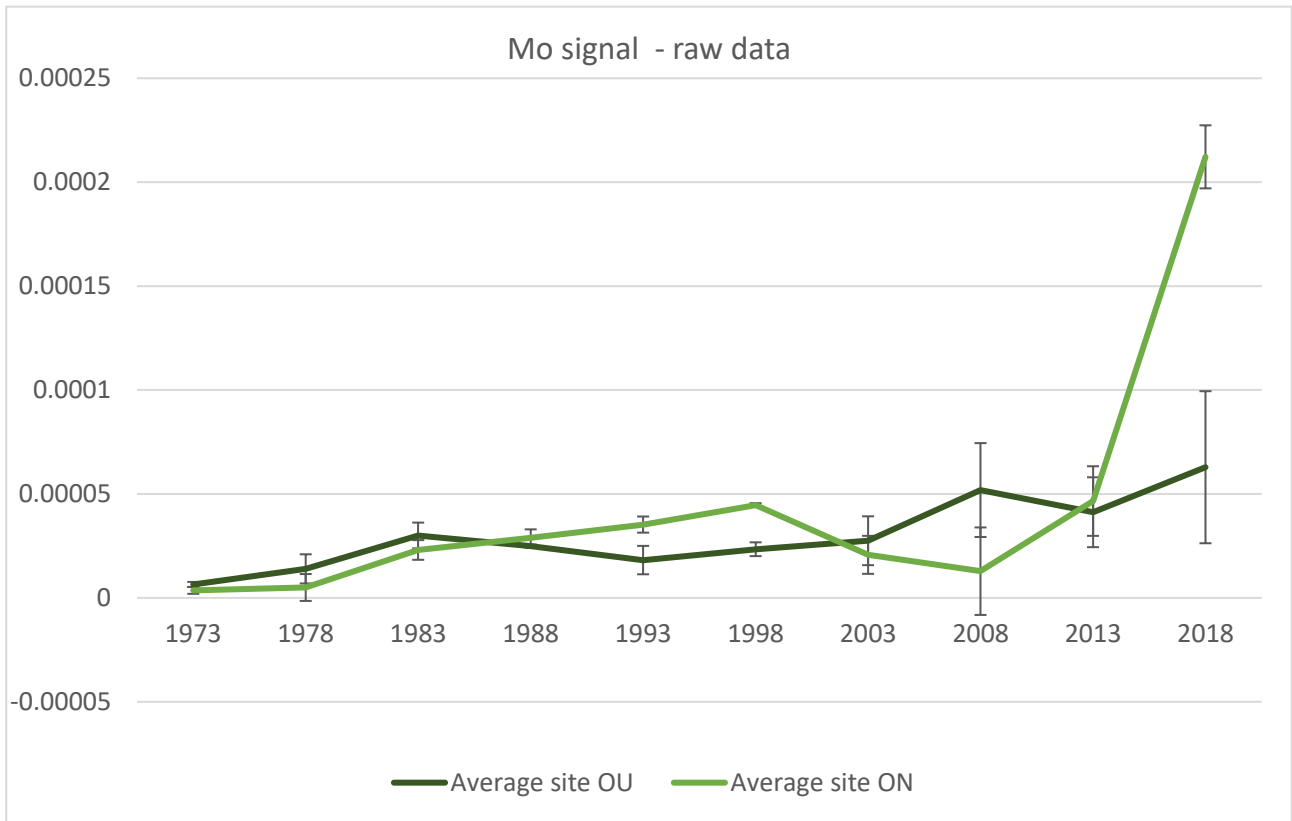


Figure 36: Raw average signal per site for the element Mo ($\pm SE$).

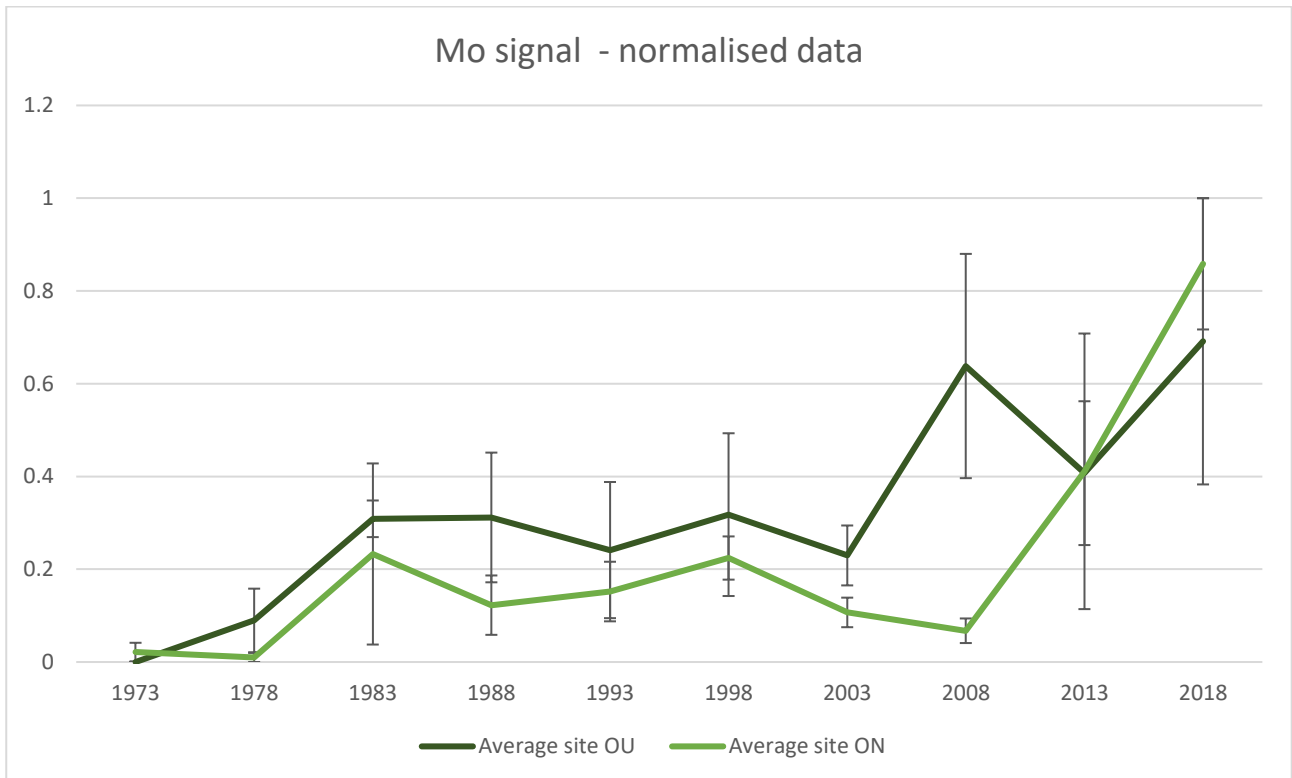


Figure 37: Normalised average signal per site for the element Mo ($\pm SE$).

Appendix

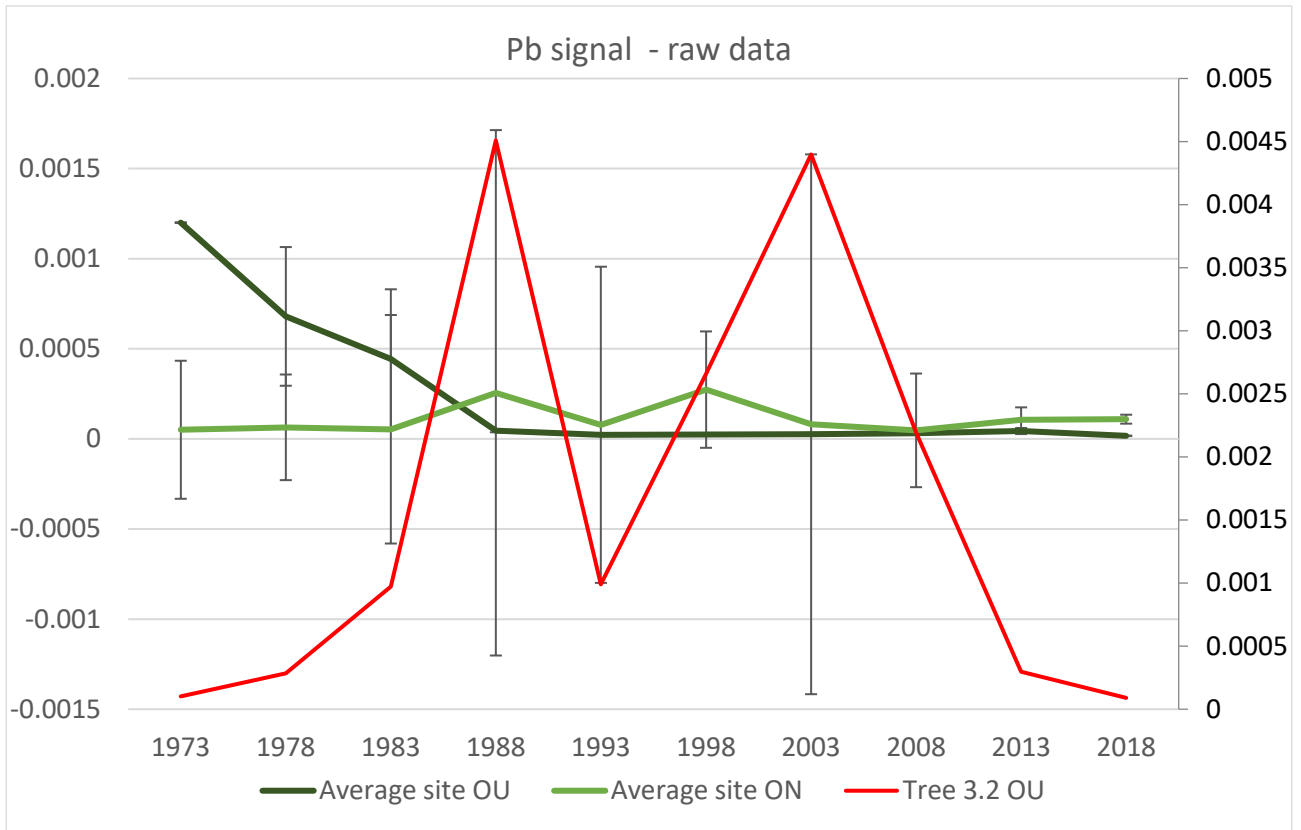


Figure 38: Raw average signal per site for the element Pb ($\pm SE$), with the concentration of tree 3.2 OU on the secondary y-axis.

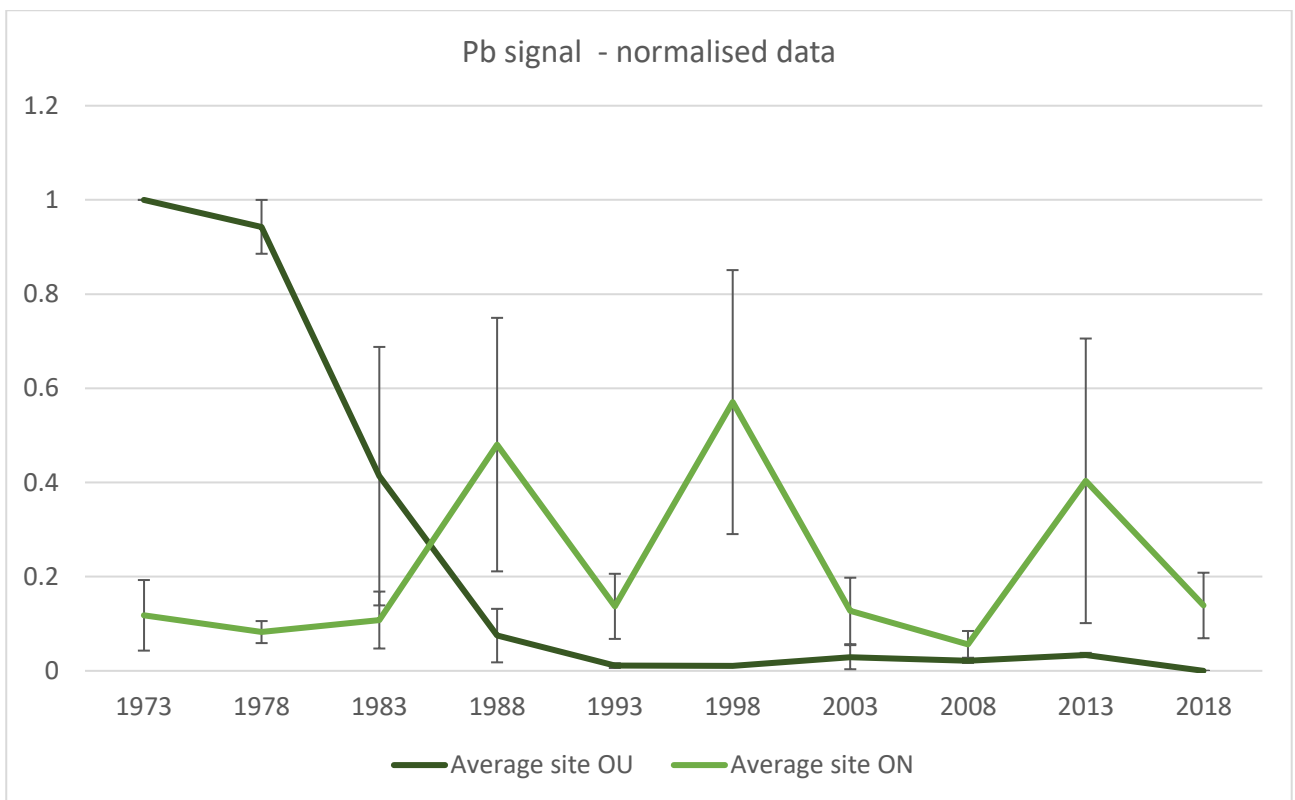


Figure 39: Normalised average signal per site for the element Pb ($\pm SE$).

Appendix

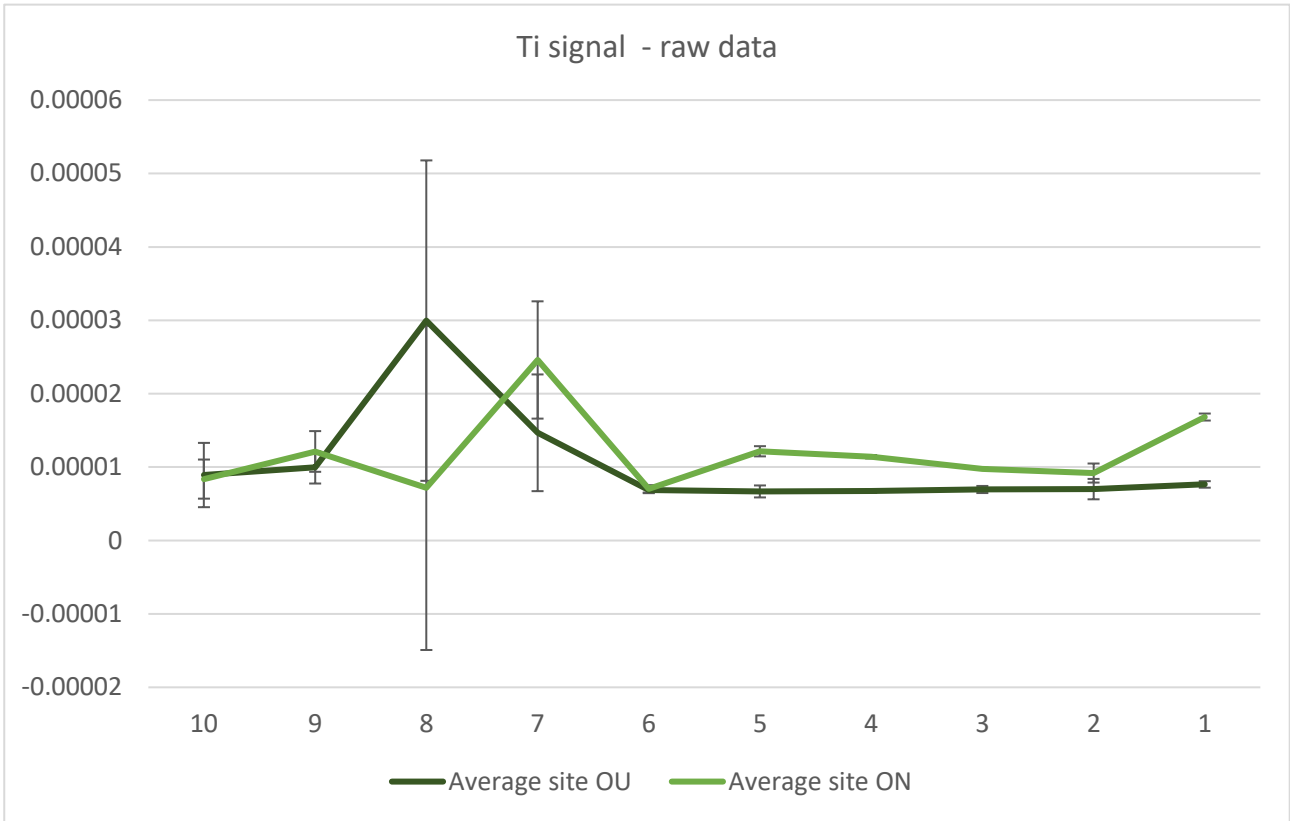


Figure 40: Raw average signal per site for the element Ti ($\pm SE$).

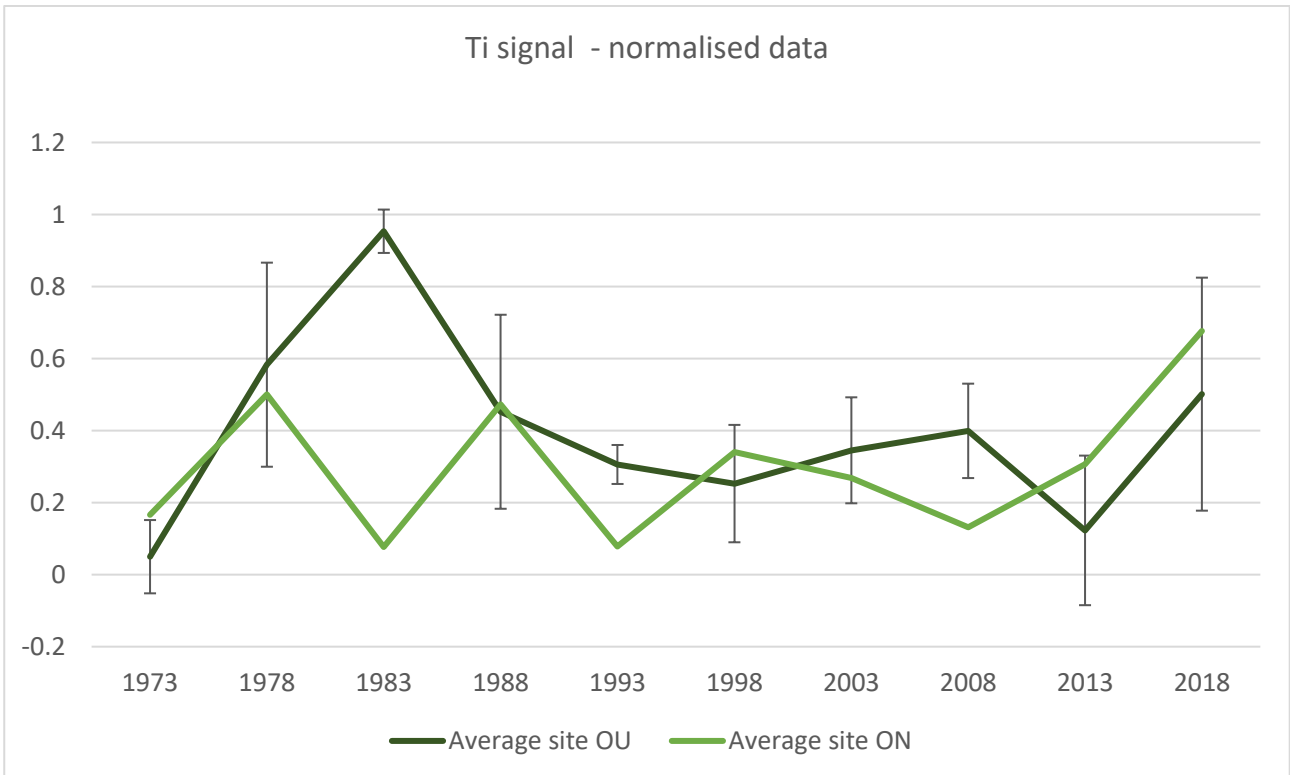


Figure 41: Normalised average signal per site for the element Ti ($\pm SE$).

Appendix

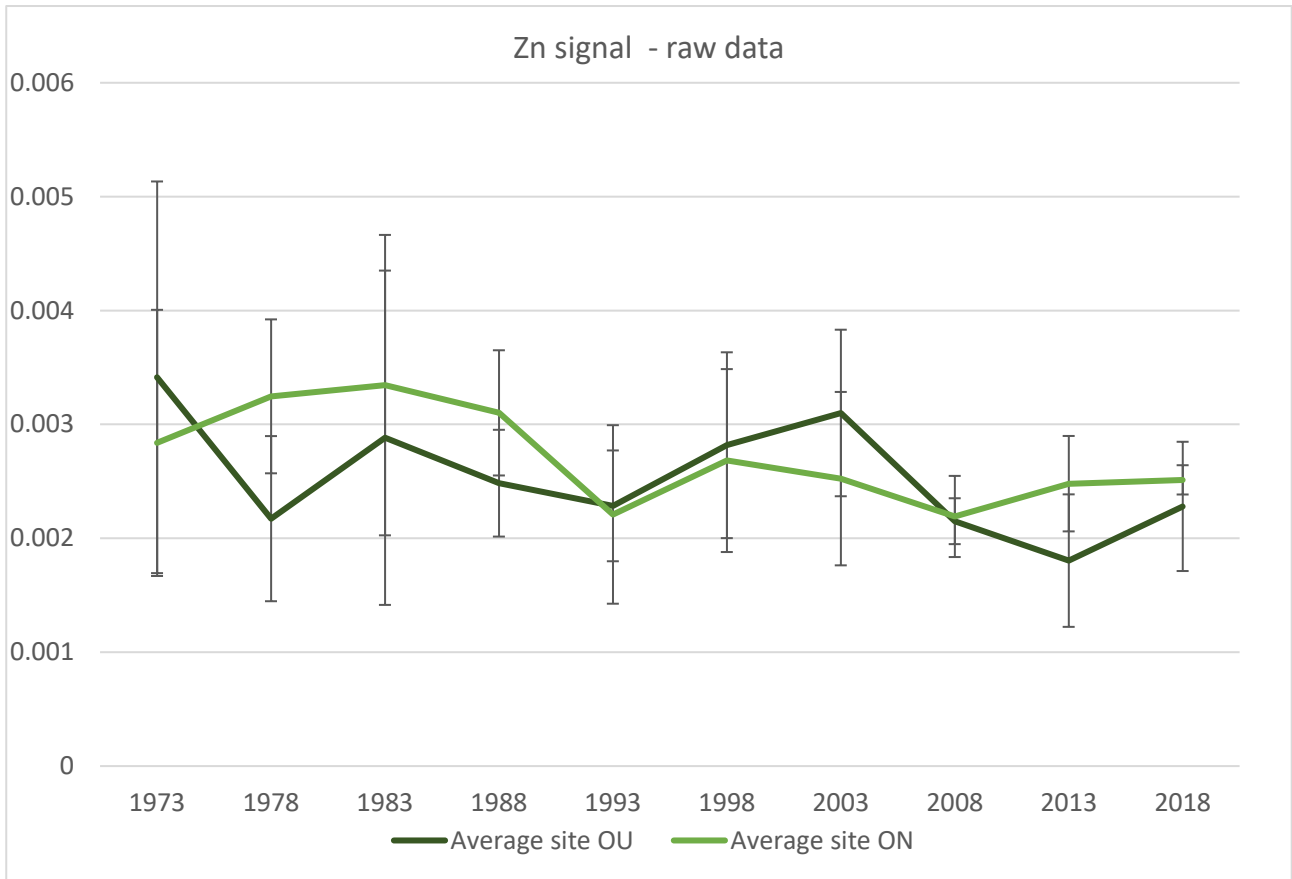


Figure 42: Raw average signal per site for the element Zn (\pm SE).

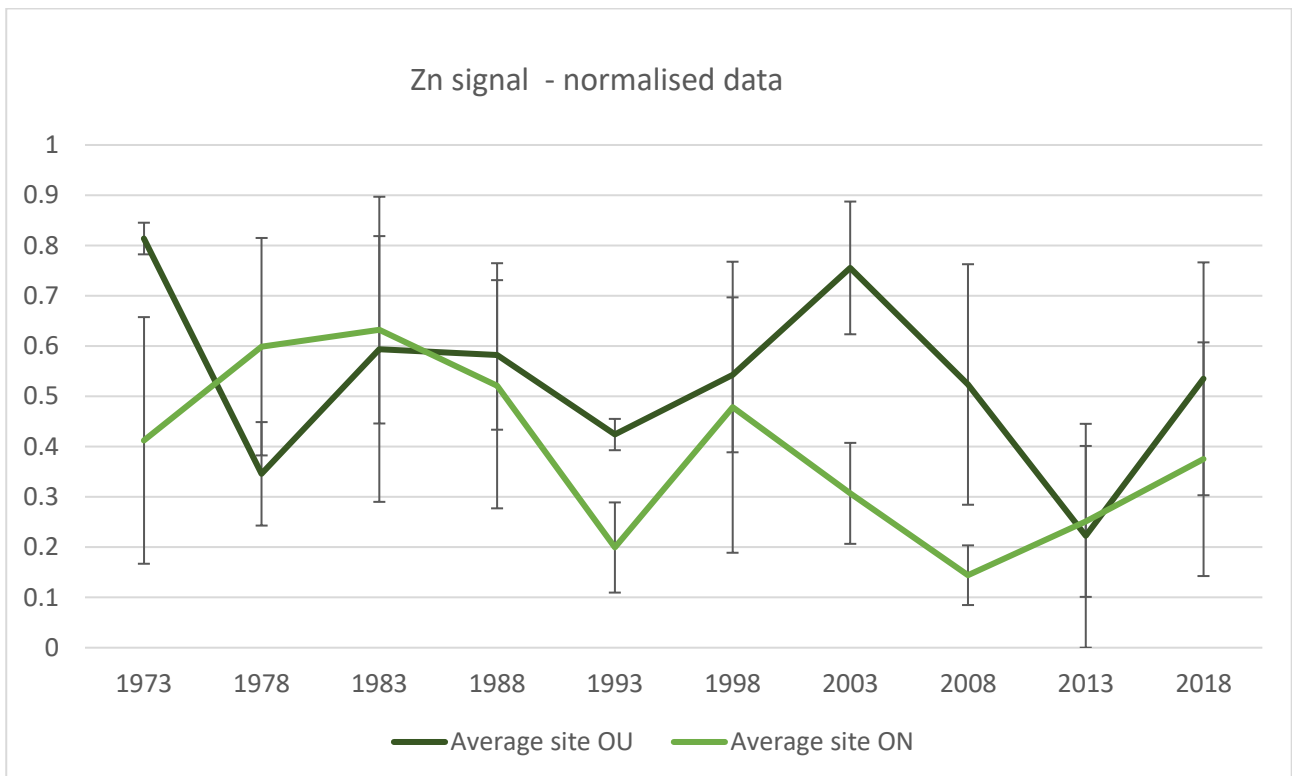


Figure 43: Normalised average signal per site for the element Zn (\pm SE).

Personal Declaration

I hereby declare that the submitted Thesis is the result of my own, independent work. All external sources are explicitly acknowledged in the Thesis.

Davide Bernasconi:

A handwritten signature in blue ink, appearing to read 'Bernasconi', written over a dotted line.

Zürich, 30.09.2021